



Norwegian University of  
Science and Technology

# Self-regulating oil based heat storage

**Christian Bogsnes**  
**Even Ersdal Hansen**

Master of Science in Mechanical Engineering

Submission date: June 2018

Supervisor: Ole Jørgen Nydal, EPT

Co-supervisor: Erling Næss, EPT

Norwegian University of Science and Technology  
Department of Energy and Process Engineering



EPT-M-2018-10  
EPT-M-2018-37**MASTER THESIS**

for

Christian Boggsnes and Even Ersdal Hansen

Spring 2018

English title

Self-regulating oil based heat storage

*Norwegian title**Selvregulerende oljebasert varmelager***Background and objective**

Oil can be used as heat transfer fluid, as well as heat storage medium for solar heat storage systems. Energy storage units are useful devices in solar energy systems. The intermittent solar energy can then be stored for continuous use either as electrical power (electrical batteries) or as heat. We are in particular interested in heat storage for cooking applications, which requires temperatures typically in the range 150-250 degrees C. This is an acceptable temperature range for thermal oils as heat storage media, as well as for many edible oils.

A thermal control system is needed in order to obtain a heat storage at a desired temperature. A new design for an oil based cooking plate is also needed, taking into account that many cooking pots can have thin and bulky walls.

A passive, expansion driven concept shall be tested and a cooking application shall be made. The work builds on a previous student project work and is related to a collaboration project with several African universities. The heating system, a heat storage and the application are parts of a complete test setup. The aim is to introduce the system for field tests together with the African universities.

**The following tasks are to be considered:**

- 1 A short literature review of solar cooking methods with heat storage
- 2 Design and testing of a heat control system and a cooking application
- 3 Considerations for upscaling to larger systems
- 4 Reporting

Within 14 days of receiving the written text on the master thesis, the candidate shall submit a research plan for his project to the department.

When the thesis is evaluated, emphasis is put on processing of the results, and that they are presented in tabular and/or graphic form in a clear manner, and that they are analyzed carefully.

The thesis should be formulated as a research report with summary both in English and Norwegian, conclusion, literature references, table of contents etc. During the preparation of the text, the candidate should make an effort to produce a well-structured and easily readable report. In order to ease the evaluation of the thesis, it is important that the cross-references are correct. In the making of the report, strong emphasis should be placed on both a thorough discussion of the results and an orderly presentation.

The candidate is requested to initiate and keep close contact with his/her academic supervisor(s) throughout the working period. The candidate must follow the rules and regulations of NTNU as well as passive directions given by the Department of Energy and Process Engineering.

Risk assessment of the candidate's work shall be carried out according to the department's procedures. The risk assessment must be documented and included as part of the final report. Events related to the candidate's work adversely affecting the health, safety or security, must be documented and included as part of the final report. If the documentation on risk assessment represents a large number of pages, the full version is to be submitted electronically to the supervisor and an excerpt is included in the report.

Pursuant to “Regulations concerning the supplementary provisions to the technology study program/Master of Science” at NTNU §20, the Department reserves the permission to utilize all the results and data for teaching and research purposes as well as in future publications.

The final report is to be submitted digitally in DAIM. An executive summary of the thesis including title, student's name, supervisor's name, year, department name, and NTNU's logo and name, shall be submitted to the department as a separate pdf file. Based on an agreement with the supervisor, the final report and other material and documents may be given to the supervisor in digital format.

- Work to be done in lab (Water power lab, Fluids engineering lab, Thermal engineering lab)  
 Field work

Department of Energy and Process Engineering, 15. January 2018



NN

Academic Supervisor Ole Jorgen Nydal

Co-Supervisor: Erling Næss

## Preface

This thesis is an extension of the project work "Passive Temperature Control of Heat Based Storage" which was written in the autumn of 2017. The first three chapters of the project work and this thesis involve overlapping information in order to make it possible for them to be read separately. It is written as a part of the project "Capacity building in Renewable Energy Education and Research" at the Norwegian University of Science and Technology, which is a collaboration project with the following universities: Mekelle (Ethiopia), Dar Es Salaam (Tanzania), Makerere (Uganda) and Eduardo Mondlane (Mozambique). The project is part of the EnPe programme, funded by the Norwegian Agency for Development Cooperation. EnPe is the Norwegian Programme for Capacity Development in Higher Education and Research for Development within the fields of Energy and Petroleum.

This thesis was conducted in collaboration with another thesis, "Mechanical Temperature Control of Oil Based Heat Storage", written by Alexander Bjåen Steen and Oskar Stadaas Sjøgren.

Trondheim, Norway

June 12, 2018



Christian Bogsnes



Even Ersdal Hansen

---

## Acknowledgements

First of all, the authors gratefully acknowledge the help of our supervisor, Ole Jørgen Nydal, and co-supervisor, Erling Næss. With their knowledge and guidance, we were able to improve the system throughout the work with this thesis.

Further, we would like to thank the technicians, and especially Benjamin Foss Hansen, for their help in the laboratory. In addition, a special thanks to Arild Sæther and Kristian Linderud Sandmo, for CNC milling. Without their help and skills, it would be impossible to realise our ideas and build the system.

We would also like to thank Karidewa Nyeinga. The field trip to Makerere University would not have been possible without his support.

Finally, we would like to thank Ayan "Alem" Mohamed Abdi for her contribution regarding the cooking of the injera bread. The contribution during the test, as well as her valuable feedback, was of great help.

---

## Abstract

This paper has investigated the possibility of storing excess energy from solar systems as heat, using sunflower oil as the heat storage medium and heat transfer fluid. Three subsystems were designed to heat, store and utilise the hot oil for cooking purposes. The system was primarily aimed for use in developing countries. Also, it was examined if the system could be built locally and if it would be useful. As resources and equipment may be scarce in many of these countries, it was desirable to make the system as simple and robust as possible. This paper covers the subsystems for heating and cooking, while the storage system was covered in a separate paper.

A self-regulating heating system was designed to heat the sunflower oil. It was shown that the heating system could be gravity-driven by utilising the density differences that occur when sunflower oil heated. A requirement for the storage to be successful was that it had to be filled with oil at a constant temperature. This was achieved by maintaining a certain oil level in the heating system. The heated oil was directed into the storage once it had expanded by the desired amount. A custom made fill valve controlled the inlet flow and the oil level in the heating system. The fill valve was designed based on results from previous work.

Two cooking applications intended for frying were designed and produced. The purpose of the first design was to create a simple application that could be produced using basic workshop tools. This criterion was met with an idea of acquiring frying pans of different dimensions and welding them together. Hot oil filled the middle pan, and a smaller one was lowered into it and was used for cooking. A third and larger pan collected the residual oil.

The second application was designed for cooking the traditional Ethiopian flatbread, injera. Therefore, it was inspired by griddles that are commonly used for this purpose. The application was made from aluminium because of its high thermal conductivity. Heat was transferred to the griddle by letting hot sunflower oil flow through a spiral-shaped channel, which was created using a CNC machine. Besides the inlet and the outlet, this application is completely closed, and thus it is safer to use than the other design.

It has been shown that it is possible to create a self-regulating heating system which is simple and robust, purely driven by gravitational forces. Tests showed that the output temperature could be kept within a 15°C range for nearly three hours, where the highest temperature was 263°C. A field trip to Uganda showed that it was possible to produce this system using local materials and machinery. The cooking applications were only partly successful, but the second design was promising. It was shown that the entire griddle could be kept at a temperature of above 110°C for nearly 30 minutes, which is the temperature required to cook injera. The feedback from a local Ethiopian was that the design had great potential. With a few modifications, it would be accepted by local communities and be a useful device.

---

## Sammendrag

Denne oppgaven har undersøkt muligheten for å lagre overskuddsenergi fra solenergisystemer som varme, ved å bruke solsikkeolje som medium for både varmelagring og varmetransport. Tre undersystemer ble designet for å kunne varme opp, lagre og utnytte oljen til matlaging. Systemet var hovedsakelig rettet mot bruk i utviklingsland. Det ble også undersøkt om det var mulig å bygge systemet lokalt, og om det ville være til nytte. Siden det kan være mangel på ressurser og utstyr i mange av disse landene var det viktig å lage systemet så enkelt som mulig. Denne oppgaven dekker undersystemene for oppvarming og matlaging, mens varmelageret er dekket i en annen oppgave.

Et selvregulerende oppvarmingssystem ble designet for å varme solsikkeoljen. Det ble vist at oppvarmingssystemet kunne være drevet av tyngdekraften ved å utnytte tetthetsforskjellene som oppstår når solsikkeolje blir varmet opp. Et krav for at varmelageret skulle fungere var at oljen måtte leveres ved en konstant temperatur. Dette ble oppnådd ved å holde et bestemt oljenivå i oppvarmingssystemet. Den varme oljen ble sendt til varmelageret når den nådde en ønsket ekspansjon. En skreddersydd flottørventil regulerte oljetilførselen til systemet, samt nivået. Flottørventilen ble designet på bakgrunn av tidligere arbeid.

To matlagingsapplikasjoner ment for steking ble designet og produsert. Målet med det første designet var å lage en enkel løsning som kunne bli laget ved hjelp av enkle verktøy. Dette kriteriet ble oppfylt ved å skaffe stekepanner i forskjellige dimensjoner for så å sveise dem sammen. Varm olje fylte den midterste pannen, og en mindre panne som ble brukt til steking ble nedsenket i oljebadet. En tredje panne ble brukt til å samle restoljen.

Den andre applikasjonen var designet for å kunne lage flatbrødet injera, som har sin opprinnelse i Etiopia. Derfor var designet inspirert av steketakker som brukes til dette. Applikasjonen ble laget av aluminium på grunn av metallens høye termiske konduktivitet. Varme ble overført til steketakken ved å la varm solsikkeolje renne gjennom en spiralformet kanal, som ble frest ut. Foruten om innløpet og utløpet var denne applikasjonen helt lukket og var derfor tryggere å bruke enn det andre designet.

Det har blitt vist at det er mulig å lage et enkelt, robust og selvregulerende oppvarmingssystem som kun er drevet av tyngdekraften. Testene viste at systemet kunne levere olje med en temperatur som kun varierte med 15°C over et tidsintervall på tre timer. Den høyeste temperaturen i disse testene var 263°C. En ekskursjon til Uganda viste at det var mulig å lage systemet med de materialene og det utstyret de hadde der. Matlagingsapplikasjonene var bare delvis vellykket, men det siste designet var lovende. Det ble vist at steketakken kunne holde en temperatur høyere enn 110°C, som er kravet for å kunne steke injera, i nesten 30 minutter. Tilbakemeldingen fra en lokal etiopier var at designet hadde stort potensial. Med noen få modifikasjoner ville det kunne bli akseptert av lokalbefolkningen og være nyttig for dem.



# Contents

|   |            |
|---|------------|
| <b>Acknowledgements</b>                               | <b>i</b>   |
| <b>Abstract</b>                                       | <b>ii</b>  |
| <b>Sammendrag</b>                                     | <b>iii</b> |
| <b>List of Figures</b>                                | <b>vii</b> |
| <b>List of Tables</b>                                 | <b>x</b>   |
| <b>Nomenclature</b>                                   | <b>xi</b>  |
| <b>1 Introduction</b>                                 | <b>1</b>   |
| 1.1 Background . . . . .                              | 1          |
| 1.2 Project Description . . . . .                     | 1          |
| <b>2 Theory</b>                                       | <b>3</b>   |
| 2.1 Solar Cooking Methods with Heat Storage . . . . . | 3          |
| 2.1.1 Solar Energy Collection . . . . .               | 3          |
| 2.1.2 Thermal Energy Storage . . . . .                | 6          |
| 2.2 Ohm's Law . . . . .                               | 9          |
| 2.3 Physical Properties of Sunflower Oil . . . . .    | 9          |
| 2.3.1 Specific Heat Capacity . . . . .                | 9          |
| 2.3.2 Density . . . . .                               | 10         |
| 2.3.3 Thermal Expansion Coefficient . . . . .         | 10         |

## CONTENTS

---

|          |   |           |
|----------|---|-----------|
| 2.4      | Pressure Loss . . . . .                                   | 11        |
| 2.5      | Heat Transfer in Laminar Flow in Pipes . . . . .          | 11        |
| 2.6      | Heat Transfer from Flat Horizontal Plate . . . . .        | 13        |
| 2.6.1    | Free Convection . . . . .                                 | 13        |
| 2.6.2    | Radiation . . . . .                                       | 14        |
| <b>3</b> | <b>Methodology</b>  | <b>16</b> |
| 3.1      | System Concept and Design . . . . .                       | 16        |
| 3.2      | System Improvements . . . . .                             | 18        |
| 3.2.1    | Inlet and Drain Valve . . . . .                           | 18        |
| 3.2.2    | Cold Section Tank . . . . .                               | 18        |
| 3.2.3    | Data Collection . . . . .                                 | 19        |
| 3.3      | Fill Valves . . . . .                                     | 21        |
| 3.3.1    | Fill Valve Workshop . . . . .                             | 22        |
| 3.3.2    | Custom Made Fill Valve . . . . .                          | 24        |
| 3.3.3    | Aquarium Fill Valve . . . . .                             | 29        |
| 3.4      | Cooking Application . . . . .                             | 31        |
| 3.4.1    | Open Cooking Application . . . . .                        | 32        |
| 3.4.2    | Closed Cooking Application . . . . .                      | 35        |
| 3.5      | Heat Storage Reversal . . . . .                           | 41        |
| <b>4</b> | <b>Field Work at Makerere University, Kampala, Uganda</b> | <b>43</b> |
| 4.1      | Motivation . . . . .                                      | 43        |
| 4.2      | System Components and Equipment . . . . .                 | 44        |
| 4.3      | Methodology . . . . .                                     | 47        |
| 4.4      | Test and Results . . . . .                                | 51        |
| 4.5      | Discussion . . . . .                                      | 53        |
| <b>5</b> | <b>Results</b>  | <b>54</b> |
| 5.1      | Fill Valve Test, 14.03.18 . . . . .                       | 54        |
| 5.2      | Fill Valve Test, 20.03.18 . . . . .                       | 55        |

## CONTENTS

---

|          |   |           |
|----------|---|-----------|
| 5.3      | Fill Valve Test, 21.03.18 . . . . .                     | 57        |
| 5.4      | Open Cooking Application Test, 03.04.18 . . . . .       | 57        |
| 5.5      | Open Cooking Application Test, 24.04.18 . . . . .       | 61        |
| 5.6      | Closed Cooking Application Test, 14.05.18 . . . . .     | 62        |
| 5.7      | Closed Cooking Application Test, 15.05.18 . . . . .     | 67        |
| 5.8      | Closed Cooking Application Test, 16.05.18 . . . . .     | 69        |
| <b>6</b> | <b>Discussion</b>                                       | <b>72</b> |
| 6.1      | System Setup and Considerations for Upscaling . . . . . | 72        |
| 6.2      | Fill Valves . . . . .                                   | 74        |
| 6.3      | Open Cooking Application . . . . .                      | 75        |
| 6.4      | Closed Cooking Application . . . . .                    | 75        |
| <b>7</b> | <b>Conclusion</b>                                       | <b>77</b> |
| 7.1      | Recommendations for Further Work . . . . .              | 78        |
|          | <b>Appendices</b>                                       | <b>83</b> |
| <b>A</b> | <b>Laminar Flow in Conduits</b>                         | <b>83</b> |
| <b>B</b> | <b>Risk Assessment Report</b>                           | <b>85</b> |

# List of Figures

|      |  |    |
|------|--|----|
| 2.1  | Illustration of different solar cookers [9]  | 4  |
| 2.2  | Hot box cooker using engine oil [11]   | 4  |
| 2.3  | Different indirect solar cookers [8]   | 5  |
| 2.4  | Correlations between temperature and supplied heat during heating and phase change[19] | 8  |
| 2.5  | Latent Heat Storage used by Sharma et al.[20]  | 8  |
| 2.6  | Specific heat capacity of sunflower oil  | 10 |
| 2.7  | Density of sunflower oil   | 10 |
| 3.1  | Initial sketch of the system   | 16 |
| 3.2  | 3D-model of the heating system   | 17 |
| 3.3  | Drain valve  | 18 |
| 3.4  | Inlet control valve  | 18 |
| 3.5  | Cold section modifications   | 19 |
| 3.6  | Cold level measurement   | 19 |
| 3.7  | Thermocouple rod   | 20 |
| 3.8  | Position of thermocouples  | 20 |
| 3.9  | Measurement of the mass flow rate  | 20 |
| 3.10 | FLIR E60 thermal camera  | 21 |
| 3.11 | Geberit Fill Valve   | 22 |
| 3.12 | Piston Fill Valve  | 22 |
| 3.13 | Sketch of a proposed fill valve  | 22 |
| 3.14 | Sketch of the produced fill valve  | 23 |
| 3.15 | 3D-model of the produced fill valve  | 23 |
| 3.16 | Fill valve in an open position   | 24 |
| 3.17 | Fill valve in a closed position  | 24 |
| 3.18 | Silver soldering   | 24 |
| 3.19 | Lathing with a reamer bit  | 24 |
| 3.20 | Fill valve piston  | 25 |
| 3.21 | Reaming the "T" manually   | 26 |
| 3.22 | 3D-printing of the floating device   | 26 |
| 3.23 | 3D-printed floating device   | 26 |
| 3.24 | Floating device made of ebazell 260  | 27 |
| 3.25 | Threading the inlet pipe of the "T"  | 27 |
| 3.26 | Creating fine-threaded nuts  | 27 |
| 3.27 | Fill valve test with water   | 28 |
| 3.28 | Volume flow rate test  | 29 |

## LIST OF FIGURES

---

|      |   |    |
|------|---|----|
| 3.29 | Aquarium fill valve test . . . . .  | 29 |
| 3.30 | Aquarium fill valve test results . . . . .  | 30 |
| 3.31 | Modified aquarium fill valve test setup . . . . .                                     | 31 |
| 3.32 | Open cooking design idea[7] . . . . .   | 32 |
| 3.33 | Sketch of a proposed frying application . . . . .                                     | 33 |
| 3.34 | Muurikka paella pan, $\varnothing$ 50 cm . . . . .                                    | 33 |
| 3.35 | Open cooking application . . . . .  | 34 |
| 3.36 | Open cooking application detail . . . . .   | 34 |
| 3.37 | Nuts to elevate the inner pan . . . . .   | 35 |
| 3.38 | 3D-model of a proposed closed application design . . . . .                            | 35 |
| 3.39 | Bottom view of transient simulation of the closed design at $t=180s$ . . . . .        | 37 |
| 3.40 | Simulated temperatures at the centre and outer edge of the plate . . . . .            | 37 |
| 3.41 | 3D-model of griddle, bottom . . . . .   | 40 |
| 3.42 | 3D-model of griddle, top . . . . .  | 40 |
| 3.43 | CNC milled griddle parts . . . . .  | 40 |
| 3.44 | Insulated and anodised griddle set up for cooking . . . . .                           | 41 |
| 3.45 | Heat storage ready for reversal . . . . .   | 42 |
|      |   |    |
| 4.1  | Cold oil container . . . . .  | 45 |
| 4.2  | Residual oil container . . . . .  | 45 |
| 4.3  | Bent metal sheets . . . . .   | 45 |
| 4.4  | Heating element with oblong bottom piece . . . . .                                    | 46 |
| 4.5  | Sunny sunflower oil . . . . .   | 46 |
| 4.6  | Pots for cooking application . . . . .  | 46 |
| 4.7  | Welding at the workshop . . . . .   | 47 |
| 4.8  | Fill valve inside the cold section . . . . .  | 48 |
| 4.9  | Silicon sealant . . . . .   | 48 |
| 4.10 | Portable heating element [43] . . . . .   | 48 |
| 4.11 | Complete test system . . . . .  | 49 |
| 4.12 | Insulated heating system . . . . .  | 49 |
| 4.13 | Heating element inside hot section . . . . .  | 50 |
| 4.14 | Heating element contacts . . . . .  | 50 |
| 4.15 | Recipe to manufacture the fill valve . . . . .  | 50 |
| 4.16 | System setup Test 1 . . . . .   | 51 |
| 4.17 | Heating element and thermocouples . . . . .   | 51 |
| 4.18 | Temperature graph from Test 1 . . . . .   | 51 |
| 4.19 | Melted heating element . . . . .  | 52 |
|      |   |    |
| 5.1  | Fill Valve Test Results, 14.03.18 . . . . .   | 55 |
| 5.2  | Fill Valve Test Results, 20.03.18 . . . . .   | 56 |
| 5.3  | Fill Valve Test Results, 21.03.18 . . . . .   | 57 |
| 5.4  | Temperatures in the hot section when charging heat storage, 03.04.18 . . . . .        | 58 |
| 5.5  | Oil temperature in the cooking application when testing the paella pan . . . . .      | 58 |
| 5.6  | First frying attempt . . . . .  | 59 |
| 5.7  | Wetted area of the paella pan . . . . .   | 59 |
| 5.8  | Oil temperature in the cooking application when testing the custom made pan . . . . . | 60 |
| 5.9  | Pancake made using the custom made pan . . . . .                                      | 60 |
| 5.10 | Oil temperatures in the cooking application during frying . . . . .                   | 61 |
| 5.11 | Making pancakes on open cooking application . . . . .                                 | 62 |

## LIST OF FIGURES

---

|      |   |    |
|------|---|----|
| 5.12 | Correlation between supply container level, cold section level and output temperature . . . . . | 63 |
| 5.13 | Temperature in the heat storage during charging . . . . .                                       | 64 |
| 5.14 | Heat storage reversal 14.05 . . . . .   | 64 |
| 5.15 | Application temperatures 14.05 . . . . .  | 64 |
| 5.16 | Griddle at $t \approx 60$ s . . . . .   | 65 |
| 5.17 | Griddle at $t \approx 300$ s . . . . .  | 65 |
| 5.18 | Pancake during frying . . . . .   | 66 |
| 5.19 | Griddle at $t \approx 700$ s . . . . .  | 66 |
| 5.20 | Griddle at $t \approx 1300$ s . . . . .   | 66 |
| 5.21 | Heat storage reversal, 15.05 . . . . .  | 67 |
| 5.22 | Application temperatures, 15.05 . . . . .   | 67 |
| 5.23 | Temperature development on surface of griddle . . . . .   | 68 |
| 5.24 | Charging and discharging of rock bed during test . . . . .                                      | 70 |
| 5.25 | Injera during cooking . . . . .   | 71 |
| 5.26 | IR photo of injera . . . . .  | 71 |
| 5.27 | Cooking application with lid . . . . .  | 71 |
| 5.28 | Picture of a successful injera bread . . . . .  | 71 |

# List of Tables

|     |  |    |
|-----|--|----|
| 3.1 | Description of the parts in the heating system . . . . .               | 17 |
| 3.2 | Volume flow rate test results . . . . .                                | 28 |
| 3.3 | Physical properties of sunflower oil at 145°C . . . . .                | 38 |
| 3.4 | Pressure drop calculations . . . . .                                   | 39 |
| 3.5 | Heat transfer calculations . . . . .                                   | 39 |
| 4.1 | Dimensions of the tanks in the system at Makerere University . . . . . | 47 |
| 5.1 | Flow rate test 24.04 . . . . .   | 62 |
| 5.2 | Important temperatures and surface area of griddle . . . . .           | 68 |
| 5.3 | Heat transfer from radiation . . . . .                                 | 69 |
| 5.4 | Thermophysical properties of air at 349 K . . . . .                    | 69 |
| 5.5 | Heat transfer from convection . . . . .                                | 69 |

# Nomenclature

Averaged conditions are denoted by an overbar in the text

|               |   |
|---------------|---|
| $\dot{m}$     | Mass flow rate, $\frac{kg}{s}$                          |
| $\theta$      | Angle, $^{\circ}$                                       |
| $\alpha$      | Angle, $^{\circ}$                                       |
| $\beta$       | Coefficient of thermal expansion, $\frac{1}{K}$         |
| $\varnothing$ | Outer pipe diameter                                     |
| $\epsilon$    | Emissivity  |
| $\mu$         | Dynamic viscosity, $\frac{kg \cdot m}{s}$               |
| $\nu$         | Kinematic viscosity, $\frac{m^2}{s}$                    |
| $\rho$        | Density, $\frac{kg}{m^3}$                               |
| $\sigma$      | Stefan-Boltzmann constant, $\frac{W}{m^2 K^4}$          |
| $A_c$         | Cross sectional area, $m^2$                             |
| $A_s$         | Surface area, $m^2$                                     |
| $C_f$         | Friction coefficient                                    |
| $c_p$         | Specific heat capacity, $\frac{J}{kgK}$                 |
| $c_{f,app}$   | Length-averaged apparent friction coefficient           |
| $D_h$         | Hydraulic diameter, m                                   |
| $g$           | Acceleration of gravity, $\frac{m}{s^2}$                |
| Gr            | Grashof number  |
| Gz            | Graetz number   |
| $h$           | Height, m; Heat transfer coefficient, $\frac{W}{m^2 K}$ |
| I             | Electric current, A                                     |
| $k$           | Thermal conductivity, $\frac{W}{mK}$                    |



|              |  |
|--------------|--|
| L            | Length, m  |
| LMTD         | Logarithmic Mean Temperature Difference, K           |
| Nu           | Nusselt number                                       |
| p            | Pressure, $\frac{N}{m^2}$                            |
| Pr           | Prandtl number                                       |
| Q            | Energy, J; Volumetric flow rate, $\frac{litre}{min}$ |
| q            | Heat transfer rate, W                                |
| $q_{conv}$   | Convection heat transfer rate, W                     |
| $q_{rad}$    | Radiation heat transfer rate, W                      |
| R            | Resistance, $\Omega$                                 |
| r            | Radius, m  |
| Ra           | Rayleigh   |
| Re           | Reynolds number                                      |
| T            | Temperature, K                                       |
| t            | Wall thickness, m                                    |
| $T_{\infty}$ | Surrounding temperature, K                           |
| $T_f$        | Film temperature, K                                  |
| $T_s$        | Surface temperature, K                               |
| U            | Electric potential, V; Velocity, $\frac{m}{s}$       |
| V            | Volume, $m^3$  |
| x            | Characteristic dimension, m                          |
| $x_{fd,h}$   | Hydrodynamic entry length, m                         |
| $x_{fd,t}$   | Thermal entry length, m                              |

# Chapter 1

## Introduction

### 1.1 Background

Nearly 600 million people in sub-Saharan Africa live without access to electricity, and the electrification rate is particularly low in the rural areas[1]. Most of the rural households in this region are under-lit and use flame-based lighting with a weak light output which has several adverse impacts on both health and the environment. For their cooking purposes, many use traditional biomass, such as firewood, and some use kerosene as well[2]. Using such inefficient fuels results in a high level of indoor air pollution that causes many premature deaths[3]. The use of firewood is not ideal as there is a rising concern regarding deforestation in the world today. Another negative aspect of the traditional methods is that they require frequent purchases of fuel and as a result, they have a high operating cost during their lifetime[2]. Among others, a photovoltaic (PV) system or a wind turbine can replace these methods with a safe and clean source of energy. If the consumers in these areas can overcome the relatively high initial cost, a small-scale system with a few light bulbs, a phone charger, and even a small TV can make a significant impact on their lives[4]. There is a great potential for renewable energy throughout Africa, but in most places, they remain unexploited. All of the sub-Saharan African countries have many hours of sunlight all year around. Within the coastal areas there are also large wind resources, and in the East African valley hydro and geothermal resources can be found[5].

### 1.2 Project Description

This report will look into how the excess energy from solar systems can be captured and utilised for cooking at a later point. The idea is that a regular family should not have to use their battery as the primary source for cooking in the evening. If the excess energy is stored and utilised for cooking after nightfall, the family would still have enough energy in their battery to provide sufficient lighting and to charge their phones. It is also important that the cooking application makes it possible to prepare traditional dishes since cooking is an important part of the culture in many countries. This has to be considered when designing a cooking application if it is to be accepted and adopted by local communities[6]. To be able to use heat for cooking purposes, it has to be stored at high temperatures. Therefore, the storage medium needs to have a high boiling point. Because of its low boiling point, water is not suitable as a storage medium in this system. On the other hand, most oils have a higher boiling point. Therefore, they are suitable as a heat transfer fluid and storage media for solar heat storage systems. During the project

work, different types of oil were tested, and it was decided to continue with sunflower oil as the heat storage medium and heat transfer fluid in this thesis. Sunflower oil was found to fulfil essential criteria regarding accessibility and affordability in sub-Saharan Africa. Also, it was found to withstand temperatures in the range between 150-250°C, which is needed for cooking purposes.

A complete system, which can be divided into three smaller subsystems, will be built and tested. The system has to be simple and robust so that it is easy to use and requires little maintenance. For those reasons, it will operate without a pump and a thermostat. In addition, the parts of the system should be created without using advanced tools or machinery. This is because the main goal is for similar systems to be built in developing countries where such tools or machinery may not be available.

For heating sunflower oil to the required temperatures, a heating system will be designed. Except for a heating element which will be connected to a power source, no electronic devices should be used. The system will be driven by the thermal expansion and density differences that occur when the oil is heated. It will be designed so that an adjustable expansion volume determines the outlet temperature of the system. This can be obtained by controlling the oil level. A mechanical fill valve will be used to control the level and inlet flow rate of cold oil. From the project work it was found that its ability to maintain a certain level is directly related to the stability of the output temperatures. How this stability can be achieved will be looked into since a constant temperature is required for the heat storage to function as intended.

The other subsystem is a heat storage. It will utilise the concept of stratification, which is why a constant inlet temperature is important. This system was designed by Sjøgren and Steen[7].

Finally, a cooking application for frying will be designed. The design should fulfil two important criteria; ease of manufacturing and meet cultural needs. Two designs were discussed in the project work and will be looked further into.

This report is structured as follows:

**Chapter 2:** A brief introduction to solar cooking methods using heat storage will be given. In addition, theory which is relevant for designing and analysing the systems will be presented.

**Chapter 3:** Presentation of the system and how it functions. Details about the design, production and testing processes of individual components.

**Chapter 4:** A summary of the production and testing of a complete system during the field trip to Makerere University in Uganda.

**Chapter 5:** Results from a selection of the tests performed during this project. The performance of a fill valve and two cooking applications were tested.

**Chapter 6:** Evaluation of the design and production process, test results and the performance of the system.

**Chapter 7:** Presentation of the most important findings and recommendations for further work.

# Chapter 2

## Theory

This chapter will present relevant theory regarding topics which were important when designing, producing and testing the system. It contains information on solar cooking methods, heat storage and solar radiation collectors, as well as Ohm's law and electrical power. Further, the physical properties of sunflower oil are presented. Finally, theory on pressure loss along pipes, as well as heat transfer in pipes and from flat horizontal plates are presented because it is relevant regarding the design of the cooking application.

### 2.1 Solar Cooking Methods with Heat Storage

Solar cookers are devices that enable the use of solar energy for cooking purposes. They can be divided into two main categories; solar cookers without storage and solar cookers with storage. There are several types of solar cookers within each of these two categories. Those who do not use storage may only be used during the day when the sun is shining. Solar cookers with heat storage allow the user to utilise the solar energy after sunset, or during periods when solar radiation is low. Because the supply of solar energy is usually high during the day, and since there is still a demand for cooking in the evening, this is a useful concept. Another advantage when using heat storage is that it enables indoor cooking[8]. This section will look into solar cookers with storage. Different ways of collecting solar energy, types of storage and cooking applications will be discussed.

#### 2.1.1 Solar Energy Collection

There are several ways to collect energy from solar radiation. One of the most common is by using PV panels, where solar radiation is made into electricity. Another way to utilise solar energy is to concentrate the solar radiation and exploit the heat produced. With a direct solar cooker, the solar radiation is concentrated directly at the cooking vessel. This involves a certain risk for the user as one needs to be located nearby the concentrated heat beam when cooking. Also, direct solar cookers imply no storage possibilities. Therefore, these types of cookers are not considered relevant for this paper. An indirect solar cooker, on the other hand, uses a heat transfer medium to transfer the heat away from the solar focus point. Thus, the cooking area can be situated some distance away from the receiver. In addition, an indirect solar cooker gives opportunities for storage.

Commercially available solar cookers where storage is possible are hot box cooker, flat plate collector, evacuated tube collector and concentrating type collectors [8].

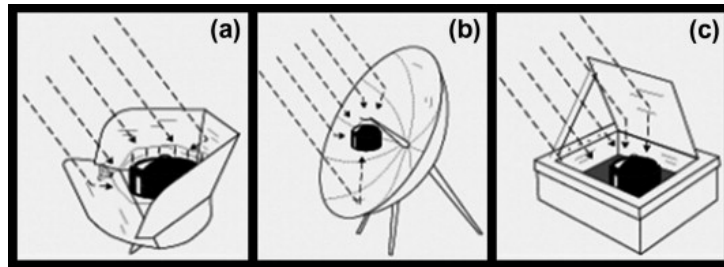


Figure 2.1: Illustration of different solar cookers [9]

Figure 2.1 illustrates how a flat panel solar cooker (a), a solar parabolic cooker (b) and a solar box cooker (c) reflects the solar radiation towards a cooking vessel. In this figure, direct solar cookers are illustrated. However, the same concepts apply for solar cookers with storage or a heat transfer fluid.

The most common solar cooker for personal use is the solar box cooker [10]. It consists of an enclosed inner box covered with clear glass or plastic, a reflector and insulation. The reflector is not concentrating, which leads to slow and steady cooking. The flat panel solar cooker consists of flat reflective panels that focus the solar radiation towards the cooking vessel or heat storage. This alternative is the cheapest and easiest to put together, but its performance is fragile to windy and cloudy weather. The parabolic cooker concentrates a lot of solar energy on the vessel, which reaches high temperatures. The cooking goes faster, but it requires more precision to focus the solar radiation to the right place. Also, because of the concentrated solar beam, the user needs to be careful not to burn itself or the food.

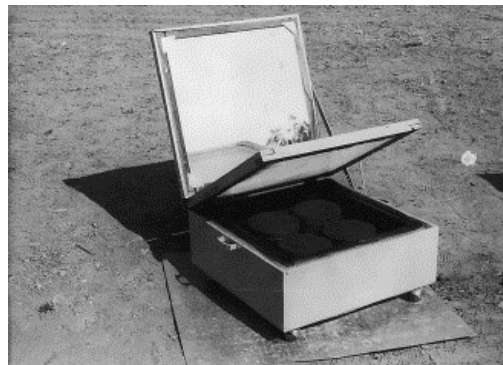


Figure 2.2: Hot box cooker using engine oil [11]

Figure 2.2 shows a hot box using engine oil as storage medium, made by Nahar [11]. The device consists of a double-walled box. The space between the inner trays is filled with 5 kg of used engine oil and is completely sealed. The space outside the inner trays is filled with glass wool insulation. The tilt of the reflector can be varied from a closed position, at  $0^\circ$ , to  $120^\circ$ . Inside the cooker, four cooking pots of 200 mm diameter can be kept to cook four dishes at the same time. During the day, the stagnation temperature inside the cooking chambers was the

same as if the solar box cooker did not have storage. After sunset, the temperature inside the box cooker with storage was  $23^{\circ}\text{C}$  higher than for a box cooker without storage. This resulted in Nahar managing to cook rice and mung beans perfectly in the evening, something that would not be possible without storage.

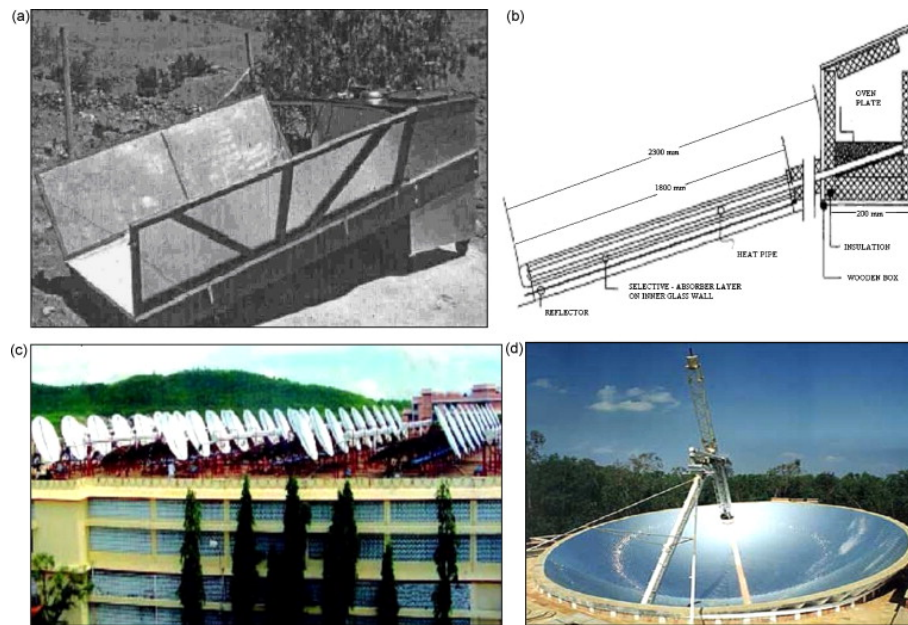


Figure 2.3: Different indirect solar cookers [8]

The solar cooker in picture (a) in Figure 2.3 is a flat plate collector type developed by Schwarzer and Silva[12]. The system consists of two flat plate collectors, two non-removable cooking pots and a storage tank. Vegetable oil is used as both storage medium and heat transfer fluid in the system. The oil is heated inside the flat plate collectors and flows naturally to either the cooking unit or storage. This is controlled manually by valves.

A sketch of a solar cooker using vacuum-tube collectors with integrated heat pipes is shown in picture (b) in Figure 2.3. The reason for integrating the heat pipes is due to their extremely high thermal conductivity which ensures that the heat is transported from the collectors to the cooking plate without noticeably decreased temperature. Balzar et al.[13] modified the collector in their workshop, which is made up of six evacuated double-wall tubes mounted on a concentrating aluminium reflector. They managed to obtain a cooking temperature of up to  $250^{\circ}\text{C}$ , as well as a short heat-up time with water as the working fluid.

In picture (c) and (d) in Figure 2.3, parabolic concentrators and a spherical reflector are shown, respectively. Both these systems are situated in India and are commercially successful steam cooking systems[8]. The 106 parabolic concentrators in picture (c) can cook 30 000 meals per day, and is the world's largest system.

Parabolic concentrators are popular due to their ability to concentrate solar radiation, and because its beam is sharper than for a spherical concentrator. A downside with both concepts is that they are susceptible to the sun changing its position. As the beams from a parabolic concentrator are sharper than the beams from a spherical concentrator, it also means that it is more sensible to a change in the position of the sun. Therefore, as opposed to the evacuated tube solar cooker, they need constant tracking. Usually, they are tracking the sun in one or two

axis using a tracking device.

## 2.1.2 Thermal Energy Storage

Thermal Energy Storage (TES) is a great way to accommodate the mismatch between when energy is supplied and when energy is needed. In a solar system, the TES can be charged during the day and discharged in the evening. There are three main categories of TES; sensible-, latent- and thermochemical heat storage[14]. Sensible heat is the energy released or absorbed by a material as its temperature is reduced or increased, respectively. Latent heat, on the other hand, is associated with the phase change of a material. The third type, thermochemical heat storage, utilises reversible endothermic chemical reactions. More detailed information on the three storage alternatives will be looked further into later in this section.

Before deciding on which TES system and type of heat storage medium (HSM) that is the best alternative, one need to consider several factors. One should choose an HSM based on parameters like preferred temperature range, medium characteristics, and which cooking application that is to be used.

Gill et al.[14] made a list of important things to consider when designing a TES system:

- The energy density of the HSM. This is to keep the storage capacity as high as possible without having to increase the storage volume too much.
- Good heat transfer between the HSM and the heat transfer fluid (HTF) to achieve good efficiency. This is if the HSM is not the same as the HTF. In this project, the HTF is also a part of the HTM in a dual system that will be explained in more detail in Section 2.1.2.1. It is also important that there is compatibility between the HSM and the HTF to ensure safety.
- Complete reversibility of a number of charging/discharging cycles, as well as the mechanical and chemical stability of the storage medium so that it can withstand all these cycles. This is to increase the lifetime of the system.
- Low thermal losses.
- Ease of control.

### 2.1.2.1 Sensible Heat Storage

A sensible heat storage (SHS) utilises the fact that when the temperature of a material change, energy is either released or absorbed. This energy is called sensible heat[14]. It is an easy concept and a well-developed technology, but it is considered to be the least efficient of the mentioned types of TES because it requires a large volume of storage medium per unit of energy stored[15].

$$Q = V \int_{T_1}^{T_2} \rho c_p dT \quad (2.1)$$

Equation 2.1 shows how sensible heat (Q) is related to volume, (V), density, ( $\rho$ ) and heat capacity ( $c_p$ ) of a material as the temperature changes. In many cases, a heat storage has to deliver temperatures above a certain level which is determined by the requirements of the load. Since the temperature drops when energy is released, the storage must be heated to a temperature above this requirement. A higher temperature means that the heat loss through the surface

of the storage tank will increase. The effect of this heat loss can be reduced by increasing the volume of the tank relative to its surface area. Another issue is that when the temperature drops during discharge, the delivered heat flux is reduced. This means that cooking will be less effective while discharging. On the positive side, the charging and discharging process of an SHS is completely reversible over the course of its life time[16].

The storage media used in SHS can be either liquid or solid, such as water, heat transfer oil, metals or rocks. When a solid material is used as the storage medium, the heat can be collected by sending a fluid flow through the solid. By using a liquid storage medium, one can obtain what is known as thermal stratification. Buoyancy forces make sure that a layer of hot oil lies on top of a colder layer. This can be achieved if mixing during charging is eliminated. As a result, the surface area of the storage containing hot liquid is kept at a minimum and heat loss is reduced. However, since heat is transferred from the oil to the surface of the tank, the oil near its wall will be colder. This can ruin the layers because it may create natural convection currents between them. Therefore, it is very important to insulate such a tank. If the oil is extracted above the cold layer in the storage, the temperature of the hot layer can be kept at a temperature closer to the required temperature of the load. Therefore, the mean temperature in a stratified storage may be lower than in a conventional SHS, which means that the overall heat loss is reduced[17].

Schwarzer and Silva[12] developed a solar cooker which can be made of any size depending on the purpose. The heat transfer medium is usually a type of vegetable oil. It can be used directly or led into a heat storage tank with pebbles. The hot oil transfers a part of its sensible heat to the food through a double-walled pot. The storage system in this thesis used a similar concept. It was an SHS using both liquid and solid storage media. More specifically, sunflower oil and pebbles were used in an oil based rock bed. This is a dual system, where a solid and liquid is used as heat storage medium, and where the liquid also works as the heat transfer fluid. The concept of stratification was applied. When the storage was charged, the heat could be used in a cooking application through a reversal procedure which will be explained in Section 3.5.

### **2.1.2.2 Latent Heat Storage**

When a material changes its phase, energy is either released or absorbed without the temperature changing. This energy is called latent heat, and as shown in Figure 2.4 it can occur during the transition from solid to liquid or liquid to gas. Materials expand a lot more when transitioning from liquid to gas than it does when transitioning from solid to liquid. Since it requires a smaller storage volume, the most frequently used phase change is from solid to liquid, which typically expands around 10 per cent. Latent heat storage (LHS) is regarded to be an efficient way to store heat because of its compactness and because it supplies heat at a constant temperature[8][16]. Faninger[18] states that the latent heat of fusion equals around 80-100 times the sensible heat required to heat a material by 1 K. They illustrated this by showing that the energy required to transform 1 kg of ice to 1 kg of water is equivalent to the energy required to heat 1 kg of water at 0°C to 80°C.

For a cooking application using an LHS to work successfully, the phase changing material (PCM) should have a melting point which is close to the desired temperature[17]. Sharma et al.[20] found that food cooked with solar cookers usually have a temperature around 95°C to 97°C. A PCM with a melting point of 82°C was used because they could not find a suitable material within the desired range of 95°C to 105°C.



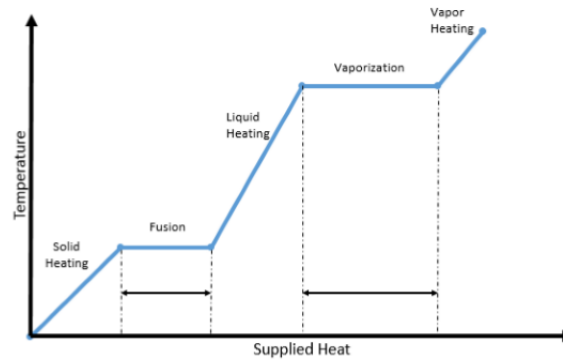


Figure 2.4: Correlations between temperature and supplied heat during heating and phase change[19]

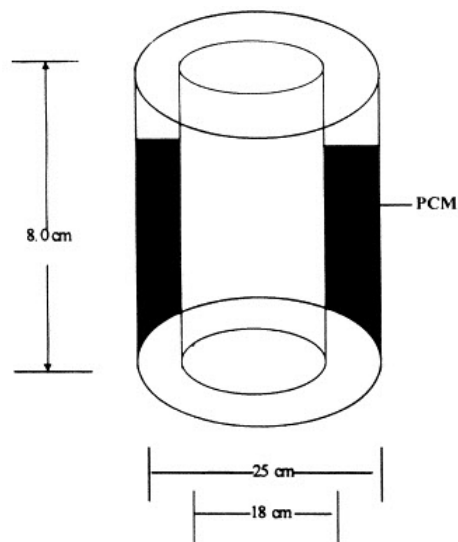


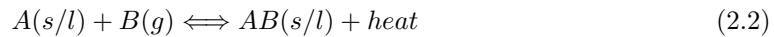
Figure 2.5: Latent Heat Storage used by Sharma et al.[20]

Figure 2.5 shows the design of their LHS. A cooking vessel can be lowered into the LHS. Fins were placed along the inner wall to increase heat transfer from the PCM to the cooking vessel. Experiments showed that two batches of food could be cooked during winter and three batches of food during summer. The possibility of evening cooking by the use of an LHS was also proved.

### 2.1.2.3 Thermochemical Heat Storage

As mentioned previously, a thermochemical heat storage (THS) utilises reversible endothermic chemical reactions. Chemical products are dissociated by heat added from solar radiation and stored separately. Mixing the separated products will reverse the process, and almost all of the heat will be released[14]. The principal of a reversible endothermic chemical reaction is illustrated

in Equation 2.2 where A and B are two separate molecules.



Silica gel, Zeolite and  $\text{CaCl}_2 \cdot \text{H}_2\text{O}$  are the most promising materials for THS. They have 8-10 times higher storage density than SHS materials and approximately two times higher storage density than LHS materials[21]. This means that a THS requires a significantly smaller storage volume than SHS and LHS. Another advantage with a THS is that it can be charged at lower temperatures. This means that it can be stored without insulation at room temperature for a long time without losing a significant amount of energy. THS technology is still in the early stages of development[22], but because of its high potential, many research studies are currently ongoing.

## 2.2 Ohm's Law

Ohm's law states that the current between two points through a conductor is proportional to the potential difference across the conductor[23]. Introducing the constant of proportionality, called the resistance, Ohm's law is shown in Equation 2.3.

$$I = \frac{U}{R} \quad (2.3)$$

For the rest of this section, all definitions are retrieved from the Engineering ToolBox[24]. In Equation 2.3, I is the current in units of amperes (A). One ampere is the current which one volt can send through a resistance of one ohm. U is the electric potential in units of volts (V). One volt is the potential required to send one ampere of current through one ohm of resistance. R is the resistance in units of ohms ( $\Omega$ ). One ohm is the resistance offered to the passage of one ampere when impelled by one volt.

## 2.3 Physical Properties of Sunflower Oil

The physical properties of sunflower oil change significantly with temperature. These changes are important to consider both in the calculations for how to design the heating system and to interpret results from the tests. Heat capacity and density affect the mass flow rate, and the thermal expansion coefficient affects the change in volume when oil is heated. These physical properties are therefore presented in this section.

### 2.3.1 Specific Heat Capacity

Specific heat capacity is a measure of the energy required to increase the temperature of a unit of mass for a substance. Fasina et al.[25] experimentally tested the specific heat capacity of twelve vegetable oils in the temperature range of 35 to 180°C, including sunflower oil. They used a differential scanning calorimeter to estimate the specific heat capacity and found that it increased linearly with increasing temperature.

Since the variation of temperature in their experiment only ranges from 35 to 180°C, it was decided to extrapolate the specific heat capacity for the oil to cover the temperature range in this project. Because the specific heat capacity and temperature are linearly dependent, the values found for 25 and 250°C are considered exact enough. The values for specific heat capacity are plotted in Figure 2.6.

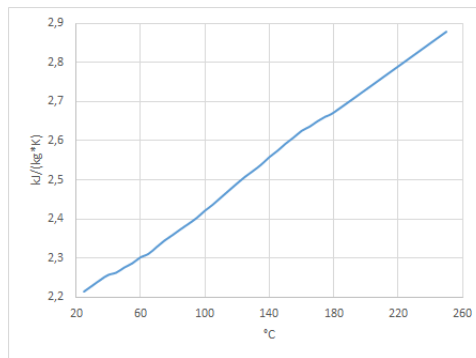


Figure 2.6: Specific heat capacity of sunflower oil

### 2.3.2 Density

Density is a measure of the mass per unit of volume for a substance. Esteban et al.[26] tested the temperature dependence of the density of vegetable oils for use as fuel in diesel engines. They tested several vegetable oils, including sunflower oil. They state that it is an accepted fact that vegetable oil density decreases linearly with increasing temperature. A set of calibrated hydrometers were used to measure the density. The density change was tested in the range from 10 to 140°C, and the values are plotted in Figure 2.7. The value for 25°C are interpolated between 20 and 30°C, and the value for 250°C are extrapolated from the values between 10 and 140°C.

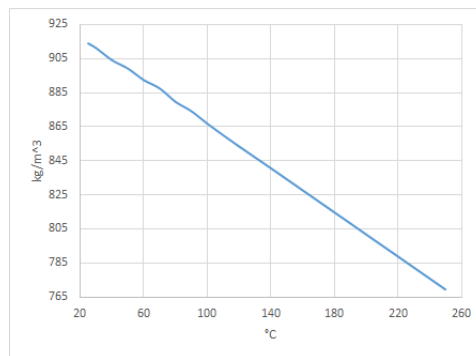


Figure 2.7: Density of sunflower oil

### 2.3.3 Thermal Expansion Coefficient

As shown in Section 2.3.2, the density of the oil depends on the temperature. This means that the volume a certain amount of oil occupies changes as the temperature changes. This change in volume per change in temperature is called the thermal expansion coefficient. Since the density changes linearly for sunflower oil, this means that the thermal expansion coefficient is constant.

For general calculations,  $0.07 \frac{\%}{\text{C}}$  is an acceptable approximate value when calculating the thermal expansion coefficient for vegetable oils. While for sunflower oil explicit, the thermal expansion coefficient is  $0.0746 \frac{\%}{\text{C}}$  [27].

## 2.4 Pressure Loss

The system consists of many pipes and channels. It is important to design it so that the pressure drop is insignificant to ensure that the desired mass flow rate through them can be obtained. One of the cooking application ideas involves relatively narrow channels, and that causes a higher pressure drop than for channels with a larger cross sectional area.

$$p = \rho gh \quad (2.4)$$

Equation 2.4 shows how to determine the hydrostatic pressure between the outlet of the heat storage and the inlet of the cooking application given the density ( $\rho$ ) of the fluid, the acceleration of gravity ( $g$ ) and the height difference ( $h$ ). This pressure, minus the pressure loss in the supply pipe, needs to be larger than the pressure loss in the application.

The total pressure drop for flow in a pipe or duct of a given length ( $L$ ), hydraulic diameter ( $D_h$ ), density ( $\rho$ ) and velocity ( $U$ ) can be calculated using Equation 2.5.

$$\Delta p = 4 \cdot c_{f,app} \frac{L}{D_h} \frac{\rho U^2}{2} \quad (2.5)$$

$c_{f,app}$  is the length-averaged apparent friction coefficient, which includes both viscous friction and flow acceleration. Equation 2.6 is an empirical formula which can be used to determine this coefficient, and it usually has an error margin of +2% compared to the full Navier-Stokes equation for several channel geometries.

$$c_{f,app} \cdot Re = \frac{3.44}{\sqrt{\zeta}} + \frac{c_{f,p} \cdot Re + \frac{K_\infty}{4 \cdot \zeta} - \frac{3.44}{\sqrt{\zeta}}}{1 + \frac{c}{\zeta^2}} \quad (2.6)$$

In Equation 2.6,  $\zeta = \frac{L/D_h}{Re}$ ,  $Re = \frac{\rho \cdot U \cdot D_h}{\mu}$  and  $D_h = 4 \cdot \frac{A_c}{P}$ . Values for  $c_{f,p} \cdot Re$ ,  $K_\infty$  and  $c$  are tabulated for different channel geometries, see Appendix A. Equation 2.5 and 2.6, as well as the definitions, are retrieved from the same Appendix.[28].

## 2.5 Heat Transfer in Laminar Flow in Pipes

As mentioned in the previous section, one of the proposed designs for a cooking application involves narrow ducts. To estimate the amount of heat that can be transferred from the hot oil to the cooking application, the convection coefficient must be found. All of the information in this section is taken from the book *Fundamentals of Heat and Mass Transfer, 7th Edition* by Bergman et al.[29].

Flow inside pipes is called internal flow. When flow enters a pipe, viscous effects between the flow and the surface will create a boundary layer that develops as the flow moves further into the pipe. At one point the boundary layers will merge, and the velocity profile will no longer change and becomes what is known as fully developed. The length from the inlet to this point is called the hydrodynamic entry length,  $x_{fd,h}$ .

$$\frac{x_{fd,h}}{D_h} \approx 0.05 \cdot Re \quad (2.7)$$

Equation 2.7 is valid for laminar flow, meaning  $Re \leq 2300$ , which is what the flows examined in this report will be. It also assumes a nearly uniform velocity profile at the inlet.

If the flow enters a pipe with constant surface temperature, a thermal boundary layer will start to develop and eventually reach a thermally fully developed condition due to convective heat transfer. The length from the inlet until the position where the flow reaches this condition is called the thermal entry length.

$$\frac{x_{fd,t}}{D_h} \approx 0.05 \cdot Re \cdot Pr \quad (2.8)$$

Equation 2.8 is also only valid for laminar flow. By comparing Equation 2.7 and 2.8, it can be seen that it is the Prandtl number that determines which layer will develop faster.

$$Pr = \frac{\text{Momentum Diffusivity}}{\text{Thermal Diffusivity}} = \frac{\mu \cdot c_p}{k} \quad (2.9)$$

For gases, the Prandtl number is generally low, and the hydrodynamic entry length will be longer than the thermal entry length. For oils which generally have higher Prandtl numbers, the opposite is true.

If either or both of these profiles are not fully developed in the entire region where one wants to determine the average heat transfer coefficient, it must be calculated by using different correlations.

$$\overline{Nu}_{pipe} = 3.66 + \frac{0.0668 \cdot Gz_D}{1 + 0.04 \cdot Gz_D^{2/3}} \quad (2.10)$$

The Nusselt number is a dimensionless number which provides a measure of the convective heat transfer at the surface. Equation 2.10 is applicable whenever the surface temperature is constant or  $Pr \geq 5$ .

$Gz_D$  is the Graetz number, which is a dimensionless number that characterises laminar flow.

$$Gz_D \equiv (D/L) \cdot Re \cdot Pr \quad (2.11)$$

By combining Equation 2.10 and 2.11, the average Nusselt number ( $\overline{Nu}_{pipe}$ ) for a pipe of a given length (L) can be determined. Since it is only valid for pipes, it cannot be used in the case of a duct. Therefore, an approximation was made by looking at the ratio between the calculated  $\overline{Nu}_{pipe}$  and the known case when the flow is fully developed along the entire length of the pipe. Further, it was assumed that the same ratio would apply for the case with a duct as shown in Equation 2.12.

$$\frac{\overline{Nu}_{pipe}}{\overline{Nu}_{pipe,lam}} = \frac{\overline{Nu}_{duct}}{\overline{Nu}_{duct,lam}} \quad (2.12)$$

For uniform surface temperature,  $\overline{Nu}_{pipe,lam}$  is equal to 3.66 and  $\overline{Nu}_{duct,lam}$  depends on the width/height ratio of the duct.

$$\overline{Nu}_{duct} \equiv \frac{\bar{h} \cdot D_h}{k} \quad (2.13)$$

The overall averaged heat transfer coefficient ( $\bar{h}$ ) can then be determined by using Equation 2.13.

$$q = \bar{h} \cdot A_s \cdot LMTD \quad (2.14)$$

Finally, Equation 2.14 can be used to determine the rate at which heat is transferred from the oil to the cooking application given a certain inlet, outlet and griddle temperature. The area ( $A_s$ ) in this equation is the entire surface area of the given channel.

$$LMTD = \frac{\Delta T_A - \Delta T_B}{\ln \Delta T_A - \ln \Delta T_B} \quad (2.15)$$

The Logarithmic Mean Temperature Difference (LMTD) is a commonly used parameter in heat exchangers. A higher value means that a larger amount of heat will be transferred. Here,  $\Delta T_A$  and  $\Delta T_B$  are the temperature difference between the desired griddle temperature and the inlet and outlet temperature, respectively. In other words, it is assumed that the entire griddle is of uniform temperature. This assumption was deemed reasonable since aluminium has a high conductivity compared to the free convection coefficient of air.

## 2.6 Heat Transfer from Flat Horizontal Plate

It is of interest to calculate the amount of energy from the heated oil that can be utilised for cooking purposes. As the griddle surface is heated, energy is transferred to the surroundings in the form of heat. There are three modes of heat transfer: conduction, convection and radiation. In this thesis, the energy from the cooking application was measured while no food was prepared on the griddle. Therefore, the heat was transferred from the griddle by free convection and radiation, only. All equations in this section are taken from *Heat Transfer, 10th edition* by J.P. Holman[30].

### 2.6.1 Free Convection

Free convection is observed as a result of the motion of air due to changes in density. When the air above the heated surface gets heated, the density of the air decreases and the air rises. New air with lower density fills the gap before it also gets heated and rises. In this way, natural circulation occurs, and it is therefore called free convection.

Equation 2.16 displays how to find the heat transfer from convection using an overall averaged heat transfer coefficient.

$$q_{conv} = h \cdot A_s \cdot (T_s - T_\infty) \quad (2.16)$$

The overall averaged heat transfer coefficient can be found from the relation for the average Nusselt number in Equation 2.17.

$$\overline{Nu} = \frac{\bar{h}x}{k} \quad (2.17)$$

For free convection, the average Nusselt number can be determined by using Equation 2.18 for a variety of circumstances, including heat transfer from a horizontal flat plate.

$$\overline{Nu}_f = C(Gr_f Pr_f)^m \quad (2.18)$$

Here, the subscript f indicates that the properties in the dimensionless groups shall be evaluated at the film temperature, which is given by Equation 2.19

$$T_f = \frac{T_s + T_\infty}{2} \quad (2.19)$$

In Equation 2.18, Gr is the Grashof number and Pr is the Prandtl number; two dimensionless numbers displayed in Equation 2.20 and Equation 2.9, respectively. C and m are correlation constants, and values for these are provided for different geometries in Table 7-1 in Chapter 7 in *Heat Transfer, 10th Edition*.

$$Gr = \frac{g \cdot \beta \cdot (T_s - T_\infty) \cdot x^3}{\nu^2} \quad (2.20)$$

Here,  $\beta$  is the coefficient of thermal expansion. Assuming that air behaves as an ideal gas, it is given by Equation 2.21.

$$\beta = \frac{1}{T_f} \quad (2.21)$$

The product of the Grashof and Prandtl number is called the Rayleigh number, and is displayed in Equation 2.23. This can be found by using Equation 2.20 and 2.9, as well as the correlation between the dynamic and kinematic viscosity from Equation 2.22.

$$\nu = \frac{\mu}{\rho} \quad (2.22)$$

$$Ra = \frac{g \cdot \beta \cdot (T_s - T_\infty) \cdot x^3 \cdot \rho^2 \cdot c_p}{\mu \cdot k} \quad (2.23)$$

In Equation 2.23, x is the characteristic dimension, which depends on the geometry of the problem. For free convection from a horizontal plate, the correlation is

$$x = \frac{A_s}{P} \quad (2.24)$$

In Equation 2.24,  $A_s$  is the surface area and P is the perimeter of the plate.

## 2.6.2 Radiation

As opposed to convection heat transfer, where energy is transferred through a medium such as air, heat can also be transferred through a vacuum by radiation. If there is a temperature difference that causes this heat transfer, it is called thermal radiation. The relationship between thermal radiation and this temperature difference is given in Equation 2.25.

$$q_{rad} = \sigma \cdot \epsilon \cdot (T_s^4 - T_\infty^4) \cdot A_s \quad (2.25)$$

Here,  $\epsilon$  is the emissivity, which is a materials effectiveness in emitting energy as thermal radiation. The emissivity of a material depends on its surface temperature and the finish of the surface.



# Chapter 3

## Methodology

This chapter will look into the concept of the system and how it was designed. Changes and improvements that were made, based on the results and recommendations for further work in the project work, will be explained. It will also contain information about how and why components such as a fill valve and frying applications were designed and produced.

### 3.1 System Concept and Design

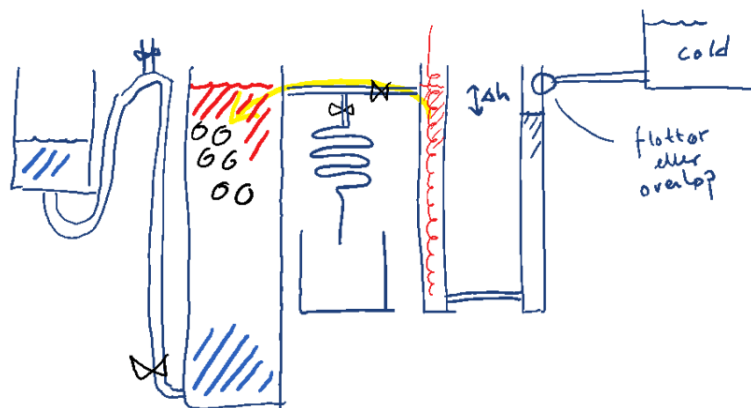


Figure 3.1: Initial sketch of the system

Figure 3.1 shows the sketch which the system is based on. The purpose is to deliver oil at a certain temperature to a heat storage which is an oil based rock bed. A layer of hot oil should be created through stratification. Initially, the rock bed will be filled with cold oil that will drain into a container as hot oil enters. The goal is to obtain hot oil at around 225°C in the rock bed so that it can be used for cooking.

The project work focused on how oil can be delivered at a certain temperature without using a pump or a thermostat. This was obtained by creating a heating system consisting of two

vertical cylinders connected by a small pipe. A heating element was placed in one of the cylinders, henceforth referred to as the hot section. In the other cylinder, henceforth referred to as the cold section, a fill valve was placed to control the oil level. Initially, the oil is cold in both sections, and both levels will be the same. Since there is no heating in the cold section, this level will remain at this initial level. The oil in the hot section expands until it reaches the outlet to the rock bed. The connecting pipe was slightly tilted to prevent heated oil going from the hot section to the cold section. When the hot oil starts to flow into the rock bed, the level in the cold section decreases. The fill valve should then open to maintain the initial level. Since the expansion of sunflower oil and its temperature are linearly dependent, the distance between the outlet and the initial level determines the output temperature.

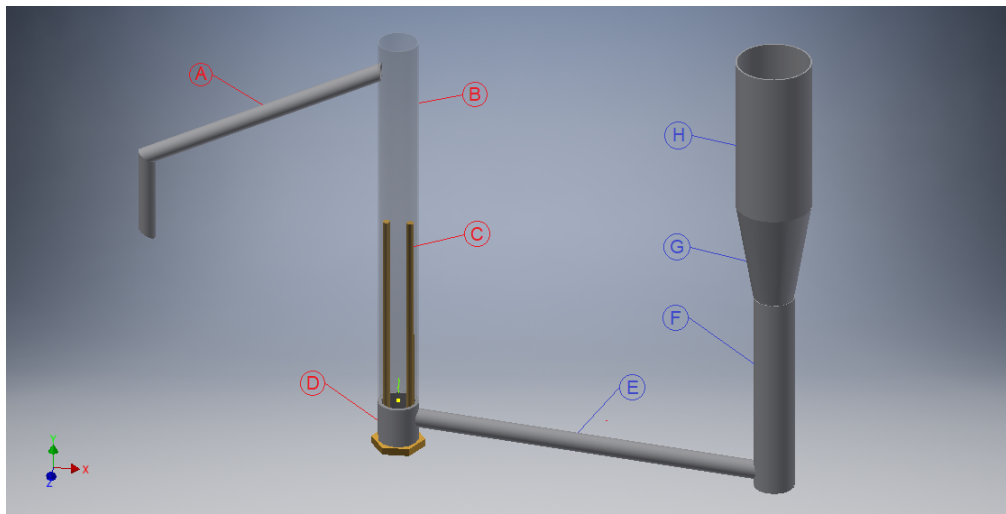


Figure 3.2: 3D-model of the heating system

| Label | Description                     | Specifications   |
|-------|---------------------------------|--|
| A     | Pipe supplying rock bed         | $\varnothing$ : 22 mm, L: 330 mm + 150 mm, t: 1 mm         |
| B     | Hot oil cylinder                | $\varnothing$ : 48.3 mm, L: 470 mm, t: 2 mm                |
| C     | Heating element                 | P: 500W, L: 270 mm, V: 48 mL                               |
| D     | Coupling muff                   | $\varnothing$ : 48.3 mm, L: 48 mm, t: 2 mm                 |
| E     | Pipe supplying cold oil         | $\varnothing$ : 22 mm, L: 400 mm, t: 1 mm, $\alpha$ : 6.5° |
| F     | Lower part of cold oil cylinder | $\varnothing$ : 48.3 mm, L: 244 mm, t: 2 mm                |
| G     | Cone                            | $\varnothing$ : 48.3 mm to 88.9 mm, L: 121 mm, t: 2 mm     |
| H     | Upper part of cold oil cylinder | $\varnothing$ : 88.9 mm, L: 186 mm, t: 2 mm                |

Table 3.1: Description of the parts in the heating system

Figure 3.2 shows the model which the system was based on. This 3D-model, along with all other 3D-models in this thesis, are drawn using Autodesk Inventor®[31] unless stated otherwise. A and E are made of low-alloy steel, while the remaining parts are made of stainless steel. Their specifications are described in Table 3.1.

## 3.2 System Improvements

During the project work, it became clear that there was room for improvements in the heating system. These were made to make it easier to perform tests and to collect more accurate data.

### 3.2.1 Inlet and Drain Valve



Figure 3.3: Drain valve



Figure 3.4: Inlet control valve

In many situations, it was found necessary to drain oil from the system because the level was higher than what was desired. This happened when performing tests on the fill valve or if the system was flooded. As an option to the cumbersome method of syphoning oil through a hose, the drain valve shown in Figure 3.3 was installed at the lowest point of the heating system. It is easier to make adjustments to the fill valve if oil is not continuously entering the cold section. Therefore, a valve was attached to the hose between the storage tank and the fill valve as shown in Figure 3.4.

### 3.2.2 Cold Section Tank

The original cold section consisted of two stainless steel pipes of different dimensions, which were connected using a cone. It was designed that way to reduce the amount of oil in the system. While this could be a way to reduce material costs, it had a couple of drawbacks. Firstly, the inner diameter of the pipe containing the fill valve was 84.9 mm. This restricts the possible size of a fill valve. If the fill valve or its floating device occupies a large part of the volume, a relatively small amount of oil entering the system will result in a significant level difference. This will cause the fill valve to be unstable. Secondly, since the cold section was made out of stainless steel, observations had to be made from above. Although flashlights and ladders were available, measurements of the oil level were inaccurate.

To address these issues a part of the pipe above the cone in the cold section was cut off. 2 cm was left to leave room to mount a custom made fill valve as shown in Figure 3.5. A stainless steel plate with a thickness of 0.75 mm and an 80 mm diameter hole in the middle was glued on top using a silicone based sealant called Tec7[32]. The inlet of the fill valve, which will be



Figure 3.5: Cold section modifications

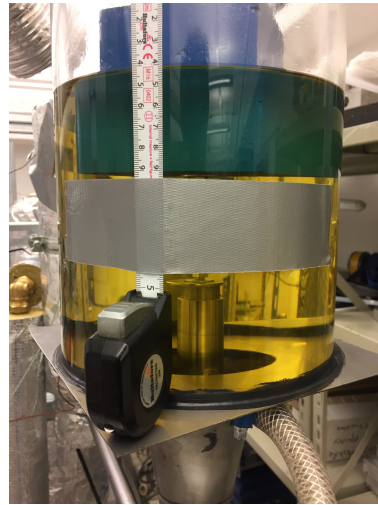


Figure 3.6: Cold level measurement

discussed later, can be seen below this plate. In the background, a transparent plexiglass pipe with a length of 20 cm and 20 cm diameter with Tec7 around its edge can be seen. This was later mounted on top of the plate to replace the part of the pipe which was cut off. When testing, it was found that the lowest level the fill valve could keep in this setup was too high. Therefore, 10 cm of the pipe below the cone was removed using a pipe cutter as shown in Figure 3.5. Because of this adjustment, the plexiglass pipe was no longer long enough. Therefore, it had to be replaced with a similar plexiglass pipe with a length of 30 cm. The transparency of the plexiglass enabled the level to be more accurately measured, using a measuring tape as shown in Figure 3.6. The fill valve and floating device could also be observed through the sunflower oil, which was of great importance when trying to optimise its performance.

### 3.2.3 Data Collection

Thermocouples were placed to monitor and record the temperature in points of interest in the hot section. They provide information about when the desired output temperature is reached and if the temperatures become too high. During the project work, three thermocouples were lowered into the hot section, and one was placed in the pipe from the cold section as indicated by the red numbers in Figure 3.8. While they served the purpose mentioned above, no data was collected along the heating element. Also, since they were not mounted to a fixed position, there was a possibility that they could move slightly between tests. To address these issues, seven thermocouples were attached to a threaded rod using nuts as shown in Figure 3.7. The five lowest thermocouples were placed with a 6 cm distance between them, with the fifth being just above the heating element as the yellow numbers in Figure 3.8 indicate. In addition, two more thermocouples were placed in the hot section, where one was positioned near the outlet. An eight thermocouple was placed in the pipe supplying the rock bed to get more precise data from the oil right before it entered the rock bed. All of the thermocouples were connected to a computer through a Thermocouple Data Logger from Pico Technology[33]. Before placing the thermocouples, they were tested in boiling water. This test showed that they were all within  $2^{\circ}\text{C}$ , which means that there are some measurement uncertainties.

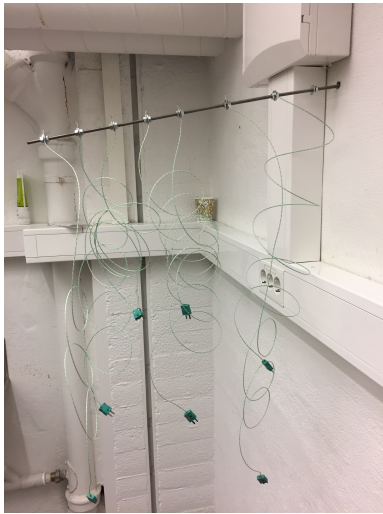


Figure 3.7: Thermocouple rod

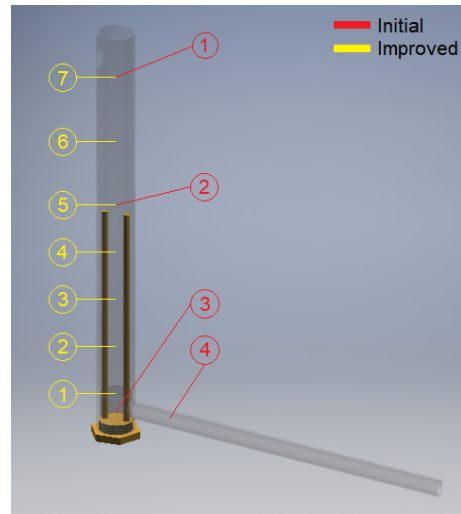


Figure 3.8: Position of thermocouples

It was desirable to collect data regarding the mass flow rate because the surface temperature of the cooking application depends on it. A higher flow rate results in higher surface temperature, as long as the temperature of oil entering is the same. All mass flow rates in this thesis were measured manually. A cylindrical flask was used to collect the oil, as seen in Figure 3.9. By recording the time it took to fill a certain volume, the mass flow rate could be calculated by using the density at the given temperature. Volume flow rate is used in some functionality tests of the fill valves where the temperature is constant.



Figure 3.9: Measurement of the mass flow rate

All infrared photos in this thesis are taken with the thermal camera in Figure 3.10, a FLIR E60 model. Because both of the cooking applications were mounted inside the system rig, it was not ideal to take the photos from straight above. The photos are therefore taken from a slight angle. It was discovered that for high temperatures this angle led to a 5°C temperature difference compared to a photo taken from directly above. All temperatures in this thesis that are taken with the thermal camera are therefore 5 °C lower than the actual temperature if not stated otherwise. Also, the thermal camera that was used is not capable of measuring temperatures above 150°C. Therefore, when 150°C is used in this thesis, it equals 150°C or higher.



Figure 3.10: FLIR E60 thermal camera

### 3.3 Fill Valves

The most decisive component of the heating system is the fill valve. A slight change of the level in the cold section will result in a change in the output temperature. An important criterion is that it should operate manually. Therefore, the level has to change somewhat for the fill valve to open since it works as a feedback control system. A feedforward control system which could account for the level change before it occurs would be preferable, but this would be more advanced and is beyond the scope of this system. This section will describe challenges with the previously tested fill valves and how they were solved.

The two fill valves that were tested during the project work, shown in Figure 3.11 and 3.12, had three main issues in common that made them perform inadequately;

1. As the level in the cold storage decreased, a lower pressure was exerted on their similar closing mechanisms. Therefore, the buoyancy force required by the floating device to close the valve was reduced. This resulted in a lower level in the cold section and higher output temperatures.



Figure 3.11: Geberit Fill Valve



Figure 3.12: Piston Fill Valve

2. Leaving the fill valves exposed to air caused the oil to make them sticky over time. This increased the static friction and made it more difficult for them to open and close.
3. Even after the fill valves closed, there was oil between their outlet and the level in the cold section. This caused the level in the cold section to rise even after the valves were closed. This effect possibly enhanced the oscillating output temperature that was observed.

### 3.3.1 Fill Valve Workshop

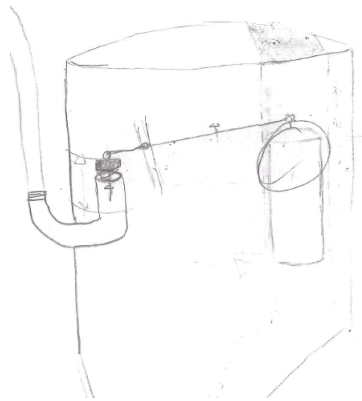


Figure 3.13: Sketch of a proposed fill valve

With the above mentioned issues in mind, an effort was made to find a different type of fill valve. Unfortunately, most fill valves are designed for water and constant inlet pressure. Therefore, a brainstorming process for a custom made design was initiated. This was an iterative

process where several technicians and professors were consulted. Figure 3.13 shows a rough sketch of one of the first ideas. The inlet can be seen to the left, and it was to be below the cold oil level to address the two latter issues. A rod with a conic silicone plug attached on one side and a floating device on the other should function as the closing mechanism. It was believed that by placing the centre of rotation close to the silicone plug, the effect of a varying inlet pressure could be neglected. However, if placed too close, a significant drop in the oil level would be required for it to open. Another drawback with this idea is that it would be difficult to adjust the level after being mounted. For those reasons, the design was rejected.

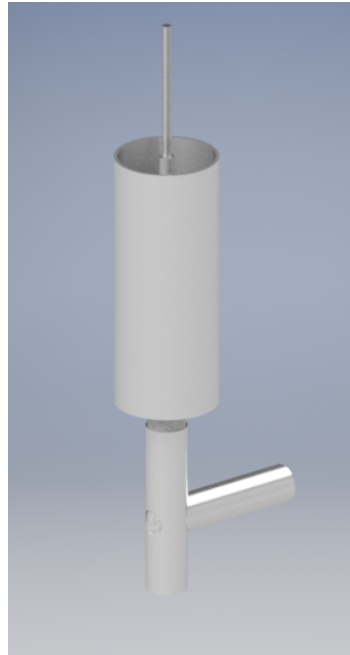
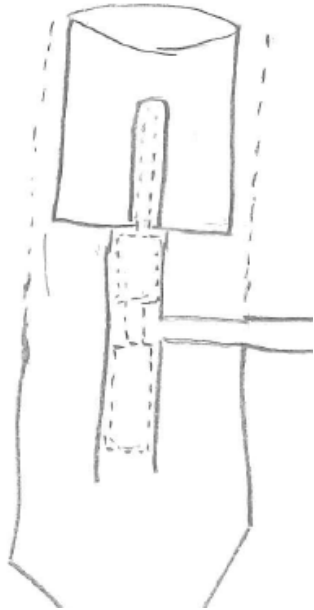


Figure 3.14: Sketch of the produced fill valve Figure 3.15: 3D-model of the produced fill valve

Figure 3.14 shows a sketch of another design. It consists of three separate parts. The first part is a hollow "T"-shaped pipe, that functions both as an inlet and an outlet. The second part is a piston which can move smoothly inside the "T" in order to open and close the fill valve. The dashed lines illustrate this piston. As the "T" was to be mounted beneath the oil level, it would not be exposed to air. In addition, the oil level would not increase after it was closed. The third part of the design is a floating device that moves the piston depending on the oil level. The fill valve would remain fully open until the buoyancy force of the floating device was strong enough to lift the piston into a closing position. It differentiates from the other fill valves because the closing mechanism is driven by the vertical buoyancy force of the floating device, and is unaffected by the horizontal pressure force exerted by the inlet flow. This was believed to make it independent of the level in the cold storage tank. Since this design addressed all of the issues mentioned above, it was decided to produce it. A 3D-model was drawn and is shown in Figure 3.15.

Figure 3.16 and 3.17 are section views of the 3D-model and they illustrate the closing mechanism. The "T" is in a fixed position, while the piston and the floating device are connected and move as one. The function of the upper part of the piston is to increase its stability.



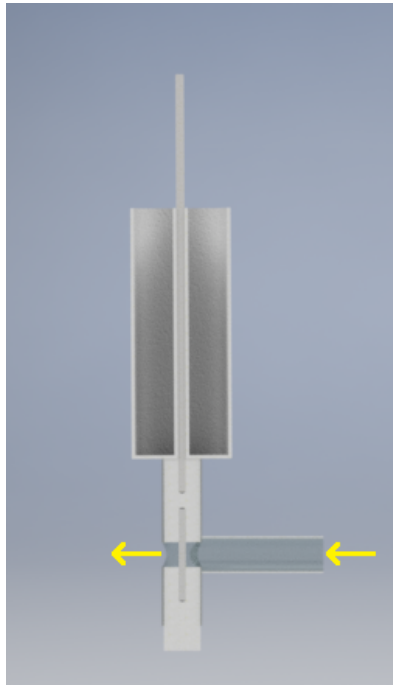


Figure 3.16: Fill valve in an open position

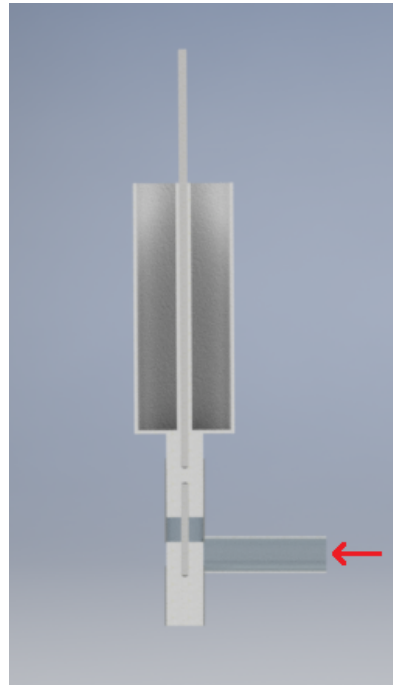


Figure 3.17: Fill valve in a closed position

### 3.3.2 Custom Made Fill Valve

To make it possible for the piston to move smoothly inside the "T" as well as keeping the fill valve leak-proof when closed, the parts were created using high precision machines in the laboratory.

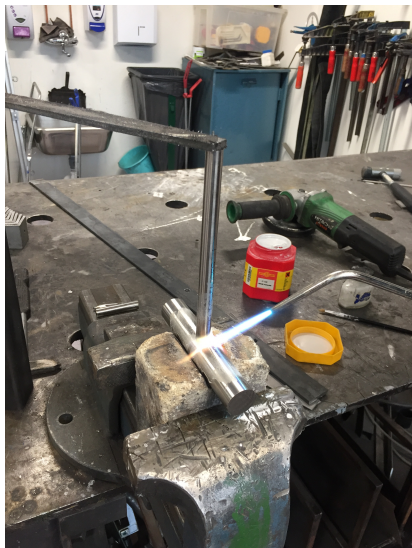


Figure 3.18: Silver soldering

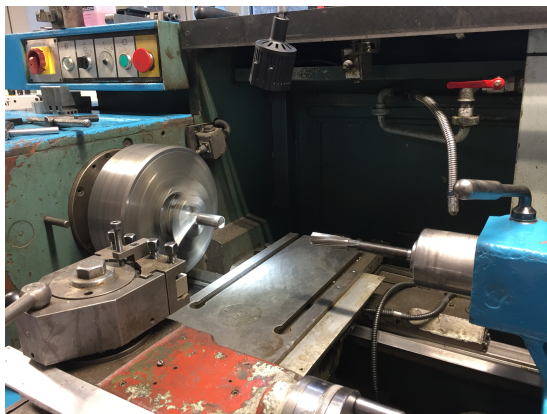


Figure 3.19: Lathing with a reamer bit

The "T" was made in collaboration with the technicians in the laboratory. It consisted of two separate pieces. One piece was made from a stainless steel type 316 axle rod. This piece is where the piston was to be placed. The inlet pipe was made from the same material, with an outer diameter of 10 mm and a 1 mm wall thickness. They were joined together by silver soldering as shown in Figure 3.18. Since the axle had a high thermal mass, it was difficult to heat it up to the same temperature as the inlet pipe and as a result, the two parts did not join very well. Therefore, a hole was drilled in the axial direction of the axle before soldering once again. When joined, an 8 mm diameter hole was drilled through the inlet pipe and the axle creating the outlet. To make sure that the piston could move smoothly, a 20 mm reamer bit was used as shown in Figure 3.19.



Figure 3.20: Fill valve piston

To create the piston shown in Figure 3.20, a stainless steel type 303 axle rod with a diameter of 20 mm was used. According to the technicians, this type of stainless steel was chosen because it is easy to machine. The 3D-models show that the two larger parts were to be connected using a threaded rod, but making it as a single piece was believed to increase its stability. The diameter in the middle part of the piston, which is 41 mm long, was reduced to 7 mm in order to let flow through as explained earlier. The diameter of the top and bottom part remained untouched and are 22 mm and 29 mm long, respectively. Figure 3.20 also shows that the bottom part is hollow. This was done to reduce its weight. At the top of the piston, a 20 mm deep hole was then drilled and threaded so that a threaded M5 rod could be attached. A nut on this rod makes it possible to adjust the oil level at which the floating device lifts the piston into a closed position. A disk was placed on the top of the piston to prevent it from falling through the "T" if the system was to be drained.

When the piston was led through the "T", it was found to be too tight for it to move smoothly. Therefore, the hole in the "T" was slightly expanded by hand, using the same 20 mm reamer bit, as shown in Figure 3.21. After the expansion, the piston was still tight, but it could now move smoothly.



Figure 3.21: Reaming the "T" manually

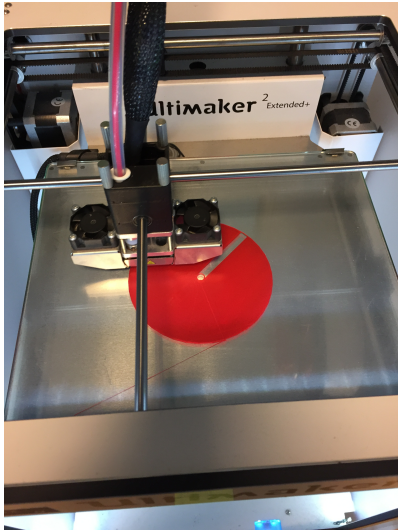


Figure 3.22: 3D-printing of the floating device

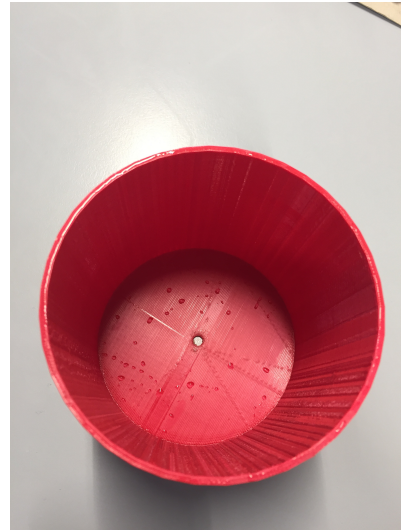


Figure 3.23: 3D-printed floating device

The final part of the fill valve was the floating device. Preferably, it should be as light as possible and at the same time occupy a large volume in order to have a strong buoyancy force. A 10 cm high cup with an outer diameter of 10 cm and 2 mm thick walls was 3D-printed in PLA, which is a light plastic material. Figure 3.22 shows the base being printed and Figure 3.23 shows the final product. The 3D-printer that was used required a lot of time to print this model in high quality. Therefore, the quality was set so that it could be printed in less than 8 hours. As a result, the connection between the base and a small cylinder which was to contain the M5 rod was weak, and it fell off. The walls were also leaking when it was tested with water.

Realising that 3D-printing the floating device was only overcomplicating the issue, the floating device shown in Figure 3.24 was made. It is a 10 cm cube made from a foam board called

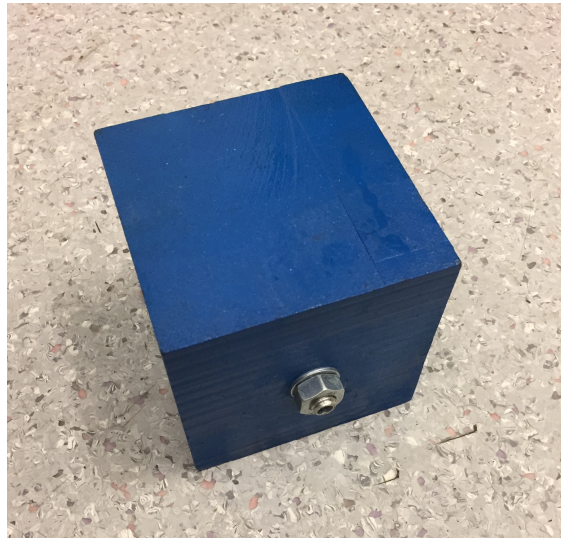


Figure 3.24: Floating device made of ebazell 260

ebazell 260[34]. With a density of approximately  $0.25 \frac{kg}{m^3}$ , it provides a decent buoyancy force in sunflower oil at 23°C. It was lacquered to prevent it from contaminating the oil. A pipe was placed through the centre so that the threaded rod attached to the piston could be led through without damaging it.

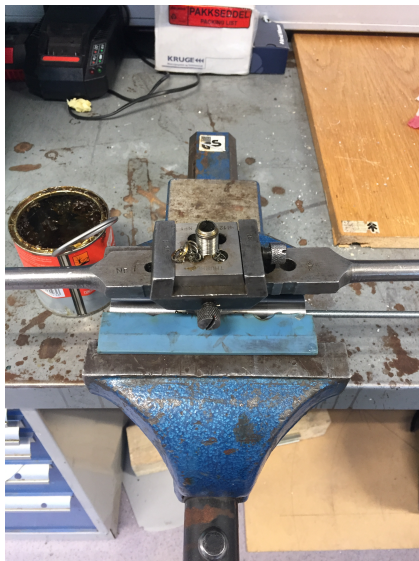


Figure 3.25: Threading the inlet pipe of the "T"

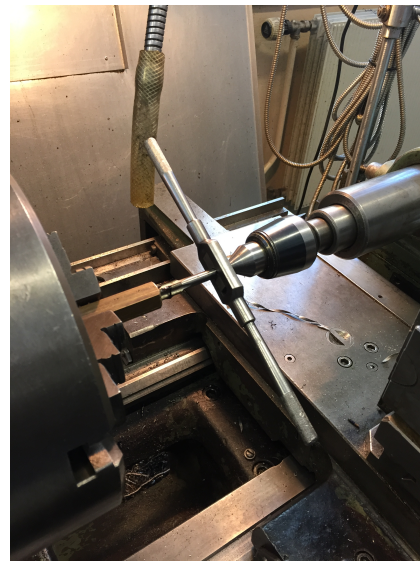


Figure 3.26: Creating fine-threaded nuts

Finally, the outer side of the inlet of the "T" was threaded as shown in Figure 3.25. Since the wall thickness of the inlet pipe was relatively small, a standard M10 thread die could not be used. Therefore, a finer thread die had to be used. Nuts that fitted were created as shown in Figure 3.26 since they were not of standard size. Also, a fine-threaded hose nipple was made,

and the fill valve was ready to be mounted to the cold section. Tec7 was used to prevent leakage through the threads.



Figure 3.27: Fill valve test with water

Once all of the parts had been manufactured, the fill valve was set up and tested with water as shown in Figure 3.27. It was aligned so that the piston was as close to vertical as possible. Thus, the entire buoyancy force of the floating device could be utilised to lift the piston without rubbing into the "T". This test successfully showed that it was able to close once a certain water level was reached. Applying a higher water pressure after it was closed caused leakages through the threads and around the hose nipple. Therefore, a hose clamp was attached, and more Tec7 was applied.

After it was clear that the fill valve would close at a certain level, it was mounted to the test rig as shown in Figure 3.28. As mentioned, merely being able to close is not adequate for a fill valve in this system. It also has to be able to keep a constant level. Therefore, a flow rate test using sunflower oil was initiated. Starting with an empty cold section, oil was let into the system through the "T". The level where the fill valve closed was used as a reference level in this test.

| Test        | $Q, \frac{\text{litre}}{\text{min}}$ | $\Delta h, \text{mm}$ |
|-------------|--------------------------------------|-----------------------|
| Single hose | 0.055                                | 1-3                   |
| Two hoses   | 0.157                                | 3-5                   |
| 500 W       | 0.078                                | 2-4                   |

Table 3.2: Volume flow rate test results

The volume flow rate test was conducted to determine the accuracy of the fill valve. All of the flow rates in Table 3.2 are measured with oil at room temperature which is approximately 23°C, following the procedure described in Section 3.2.3. Two tests were conducted by syphoning oil



Figure 3.28: Volume flow rate test

from the heating system without any effect on the heating element. First, one hose was used, and in the second test two hoses were used. For the test with 500 W applied to the heating element, the flow rate was found by measuring the cold oil displaced from the heat storage.  $\Delta h$  is the observed level drop compared to the reference level. All three tests showed that the level is not kept constant and that it deviates from the reference level. However, the largest level differences were observed as soon as a test was started. Within less than a minute they stabilised in a slightly narrower range. The effect of these oscillations are still notable and they are reflected in the test results that will be presented in Chapter 5.

### 3.3.3 Aquarium Fill Valve



Figure 3.29: Aquarium fill valve test

At the same time as the custom made fill valve was designed and produced, a relatively cheap and simple fill valve intended for use in aquariums was purchased. The level can be adjusted by loosening a nut and adjust the angle of the floating device. Once mounted to a fixed position, this function enables the level to be changed within a range of approximately 4 cm.

Figure 3.29 shows how the fill valve was mounted to do an initial test of its closing mechanism. It was connected to the cold storage which was placed approximately 1 m above it. The pot has a diameter of 20 cm, and the level was measured manually using a measuring tape.

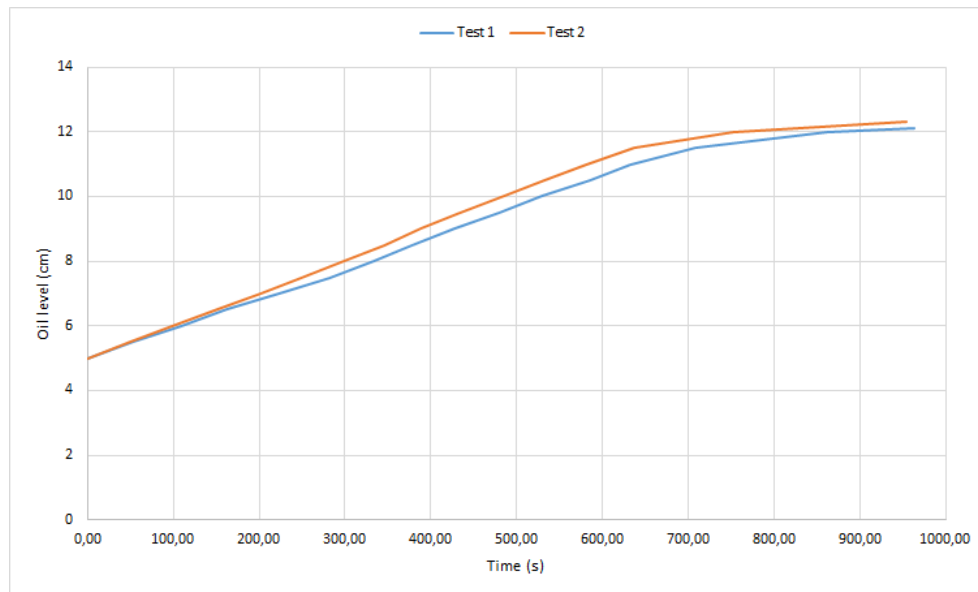


Figure 3.30: Aquarium fill valve test results

By measuring the time of every 5 mm level increase until the fill valve closed, an idea of its performance was obtained. Two tests were conducted, and the results are presented in Figure 3.30. The initial height difference from the cold storage level to the outlet was 1.1 m and 1.2 m for Test 1 and 2, respectively. For Test 1, a slight increase in the flow rate can be seen at a level of around 8 cm. At that point, 2 litres of oil was added to the cold storage to check if its level had an effect. The oil reached the floating device at approximately 11.1 cm, and as seen from the plot, the flow was reduced. However, the fill valve did not close before the level reached 12.1 cm and 12.3 cm around 400 s later. In other words, it takes a long time for it to close completely. A higher inlet pressure can be seen to result in a higher final level. To summarise, it was quite clear that the level in the cold storage affected the fill valve.

A third test was initiated to test the volume flow rate as shown in Figure 3.31. However, at a level of about 8.5 cm, a substantial decrease of the flow rate was observed. Therefore, the fill valve was disassembled, and a small fibreglass thread which blocked the inlet was found. It came from one of the thermocouples in either the hot section or the rock bed. Since the oil in the system is reused many times, such small contaminating particles should be expected. For that reason, the hole in the fill valve was expanded. Also, the floating device from the custom made fill valve was attached to increase the buoyancy and thus decrease the level change required to close it.



Figure 3.31: Modified aquarium fill valve test setup

Shortly after this test, a successful test with the custom made fill valve was conducted. Therefore, this fill valve was shelved and not examined any further.

### 3.4 Cooking Application

While it is important for the system to be able to deliver constant oil temperatures, the ultimate goal of the project is that the system can be used for cooking purposes. While Sjøgren and Steen[35] focus on an application for boiling, this report will focus on an application for frying. However, through a joint effort, two types of design that could apply for both boiling and frying were found. The first design is an open system which will be discussed in Section 3.4.1. This design was produced for both boiling and frying through cooperation. Because it was a simple design which was relatively easy to manufacture, it was built first. The second design is a more advanced closed system and will be discussed in Section 3.4.2. Early simulations and calculations for this design were also conducted as collaborative work.

The frying applications were designed so that they could be used to make the traditional Ethiopian sourdough flatbread, injera. Therefore, the diameter had to be larger than for a regular frying pan, and more similar to a griddle. It seems like there is no agreement about what temperature the griddle should have when making injera. WASS Electronics is the producer of a 1000 W electric griddle with adjustable temperature control. Its diameter is 40 cm, and they recommend to set it to somewhere between 110°C and 150°C when cooking injera[36]. On the other hand, Tesfay et al. [37] claims that injera requires a temperature of between 180°C and 220°C to be well baked. In this system, the temperature of the frying application is limited by



the temperature in the heat storage. Approximately 10 litres of oil with a mean temperature of 170°C is available from the heat storage when fully charged[7]. Therefore, the design needs to prevent heat losses and maximise the amount of energy that can be transferred from the hot oil to the frying pan in order to achieve the lowest temperature range mentioned above.

### 3.4.1 Open Cooking Application

The idea for the design of the open cooking application was to put three frying pans with different diameter inside each other. The inner pan is where the injera bread is to be cooked. The pan in the middle is where the heated oil will enter, and the outer pan is where the used oil is collected before it leaves the cooking application and goes into the residual oil tank. Figure 3.32 illustrates the concept using pots. The heated oil enters the space between the middle and the inner pot (illustrated by red arrows). As more oil enters, it spreads out and transfers heat to the inner pot, before draining over the edge of the middle pot and into the outer pot before it exits the application (illustrated by yellow arrows).

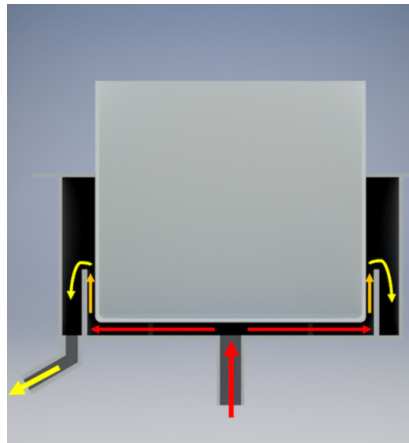


Figure 3.32: Open cooking design idea[7]

Using this idea as a starting point, the search for suitable frying pans started. Since the injera bread is traditionally at least 40 cm in diameter, the inner pan had to be at least as wide. A paella pan from Muurikka with a diameter of 50 cm was found and used to develop the cooking application. 50 cm is the diameter of the upper ring, and because of the slope of the walls, the diameter of the actual frying surface is only 44 cm. Because of the tilted walls, it was found that it was possible to use two identical pans as the inner and middle pan. Creating a 5 mm gap between the two pans would make space for the oil. Further, by cutting off the top of the middle pan, the oil could drain over the edge. As mentioned, the initial idea was to have three pans, where the outer pan was supposed to collect the oil after it drained over the edge of the middle one. However, a new design was proposed to avoid buying a third pan. The new design suggested having two cylinders with different diameters that were to be closed with a metal ring attached at the bottom. These cylinders would function as a substitute for the outer pan, as they would collect the residual oil. The sketch of this idea is shown in Figure 3.33, and it was delivered to the workshop at NTNU.

Unfortunately, manufacturing the two cylinders and weld everything together would be very time-consuming. Also, there was no guarantee that the product would be leak proof because welding thin metal sheets are difficult.

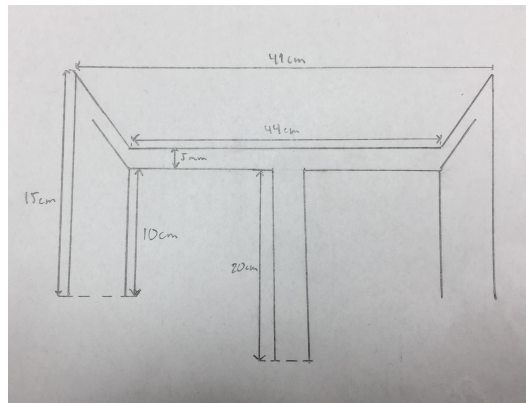


Figure 3.33: Sketch of a proposed frying application

Therefore, a new brainstorming process was initiated. At this point, the two 50 cm diameter paella pans were already acquired. One of them is shown in Figure 3.34. The handles of one of the pans were removed, and its height was reduced using a grinder. The solution that was decided upon was to use the two 50 cm diameter paella pans as the middle and outer pans. In addition, a 40 cm diameter paella pan was acquired. This would serve as the inner pan where the injera was to be baked. The diameter of the cooking surface area of this pan was 35 cm. Even though this was slightly smaller than the initial demand, it was considered to be good enough because the main priority at that moment was to come up with a functional prototype.



Figure 3.34: Muurikka paella pan,  $\varnothing$ 50 cm

Because of a heavy workload at the workshop at NTNU, it was decided to produce the cooking application externally. Trøndelag Isolering AS were contacted since they could assemble

the application as well as insulate it. The three pans were delivered to their workshop along with detailed instructions on how to produce the application.

To assemble the two 50 cm diameter pans, a hole was drilled through the centre of both of them. Further, the supply pipe was mounted using a modified nut. The size of the nut was reduced using a file to reduce the distance from the inner pan to the middle pan. This was done to avoid a large volume of oil to accumulate between them. Further, a box made of two-layered metal sheets was made to cover the paella pans. Insulation was put between the two layers. Pyrogel®XT-E was used as insulation material. Two layers of 10 mm was placed beneath, around the sides and partially on top of the application. It is suitable for high temperature applications as it has extremely good insulation capability at high temperatures. In addition, it has good water repellent properties[38]. This is especially positive in an application like this one, where oil spills may occur.

To the right in Figure 3.35, the completed version of the open cooking application can be seen. The bottom pipe is the supply pipe, and the upper one is where the oil is leaving the application. Figure 3.36 shows a detail from the cooking application where the edge of the middle pan has been bent using a special tool. In this photo, it can also be seen that the insulation is hanging freely. This was later fixed upon request in order to limit the chances of the insulation getting in contact with the oil.



Figure 3.35: Open cooking application

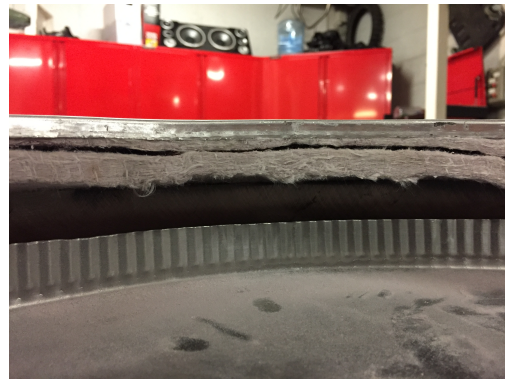


Figure 3.36: Open cooking application detail

Initially, the idea was that the 40 cm diameter paella pan should rest on the inner edge of the application, so that a 5 mm layer of oil could flow underneath it. To the left in Figure 3.35 is a custom made pan that was made by Trøndelag Isolering AS. They made it because one of their workers had misunderstood the instructions and drilled a hole in the 40 cm diameter paella pan. Therefore, the cooking application was designed to be used with the custom made pan. After it was brought back to the lab at NTNU, it was discovered that it was slightly oversized and did not fit inside the cooking application. Therefore, the outer diameter was reduced using a belt sander. Another 40 cm diameter paella pan was also acquired.

To ensure that the pans did not block the oil supply, three nuts were used, as shown in Figure 3.37. As these nuts were higher than the nut in the middle, the pans would always be above the inlet.

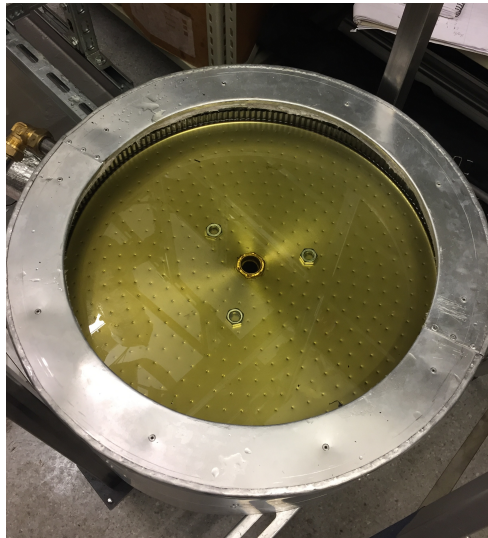


Figure 3.37: Nuts to elevate the inner pan

### 3.4.2 Closed Cooking Application

A major drawback with the open design is that it is not entirely closed. It is indeed practical to be able to remove the pan for cleaning. However, if undesired water comes in contact with the hot oil, it could be dangerous for the user. Also, it is impractical to cook injera when the pan has high edges. To overcome these issues, it was desirable to create a closed griddle.

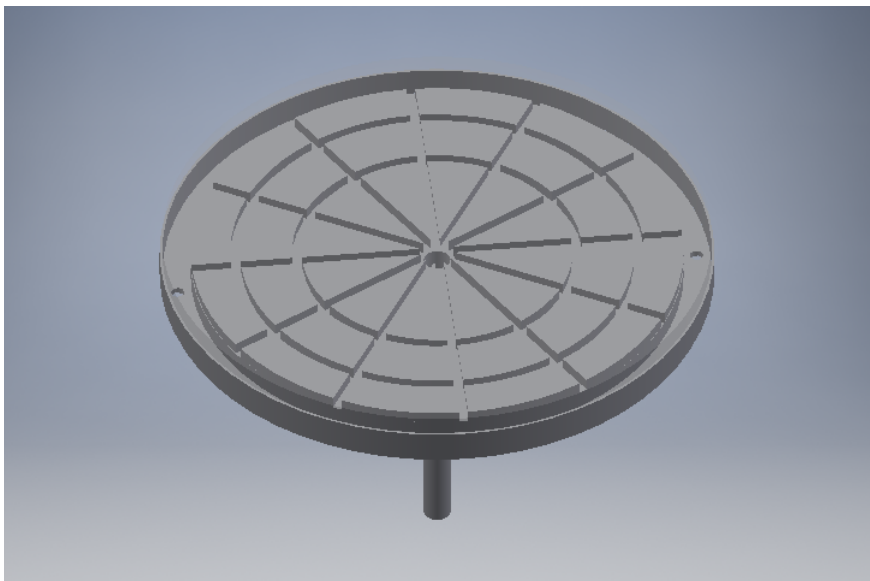


Figure 3.38: 3D-model of a proposed closed application design

The first idea was to mill channels in a highly conductive material as shown in Figure 3.38. On top of this milled part, a pan was to be welded to make sure no foreign substances could

contaminate the oil. By placing the application below the outlet of the heat storage, the pressure difference makes the flow enter at the bottom and distribute both in the radial and angular direction. A channel was placed at the edge to collect the used oil and guide it to a residual container. If this application is slightly tilted, it is likely that it would have difficulties distributing oil through all of the channels and thus creating an unevenly heated griddle. Another issue was that it is difficult to calculate pressure loss and heat transfer for such a geometry. Since the material and production cost related to this application is quite high, it is important to have as accurate estimates of its performance as possible. For those reasons, it was decided to look into other designs for a closed cooking application.

Although it is desirable to have a level surface when making injera, it should not be expected that the griddle will be perfectly level. By having a single inlet and a single outlet, one can make sure that the entire channel is filled with oil. Besides, given a constant cross sectional area, the pressure loss and heat transfer can be determined using the expressions in Section 2.4 and 2.5.

In order to distribute the heat to all parts of the plate, it was suggested to shape the channel as a spiral. When designing the geometry of the spiral-shaped channel, the following factors were considered:

- Determine the number of revolutions required to reach an even temperature distribution.
- Make sure the length and cross sectional area of the spiral is such that the pressure loss in the channel is lower than the pressure difference between the storage and the inlet of the application.
- Consult with technicians to make sure that the design could be realised with the available tools and machinery.

Since the surface temperature of the griddle should be minimum  $110^{\circ}\text{C}$ , it was assumed that it should have an output temperature of around  $120^{\circ}\text{C}$  to prevent heat from being extracted from the griddle to the oil.

To get a better understanding of how the heat would be distributed using the spiral-shaped design, a simplified model was made in COMSOL Multiphysics®. This is a software for modelling and simulating engineering problems [39]. A 20 mm thick aluminium plate with 15 ring-shaped channels were drawn. The distance between each channel is equivalent to the width of each channel. Its diameter is 20 cm, and the boundary condition of the top was set to extract 500 W. The boundary condition for the surface area of the inner channel was set to a temperature of  $170^{\circ}\text{C}$ . For the remaining rings, the temperature was set at a linearly decreasing temperature with the outer channel having a temperature of  $120^{\circ}\text{C}$ . All channels use an average heat transfer coefficient of  $98\text{ W}/\text{m}^2\text{K}$  which was calculated using a channel width of 3 mm and height 15 mm.

A transient simulation was run to see how long it would take for the temperature in the plate to stabilise, and how high temperatures that could be expected. Figure 3.39 shows the model and the result at  $t=180\text{ s}$ , which is where it stabilised. The mean temperature at this point was approximately  $125^{\circ}\text{C}$ . The temperature distribution on the top of the plate was identical. Figure 3.40 shows how the temperature at the centre and the outer edge of the plate changed over time.

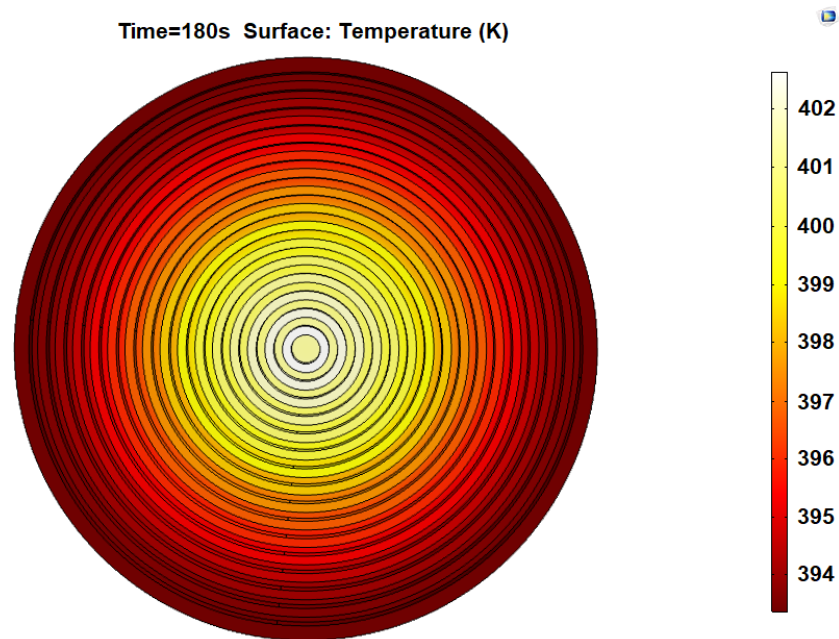


Figure 3.39: Bottom view of transient simulation of the closed design at  $t=180s$

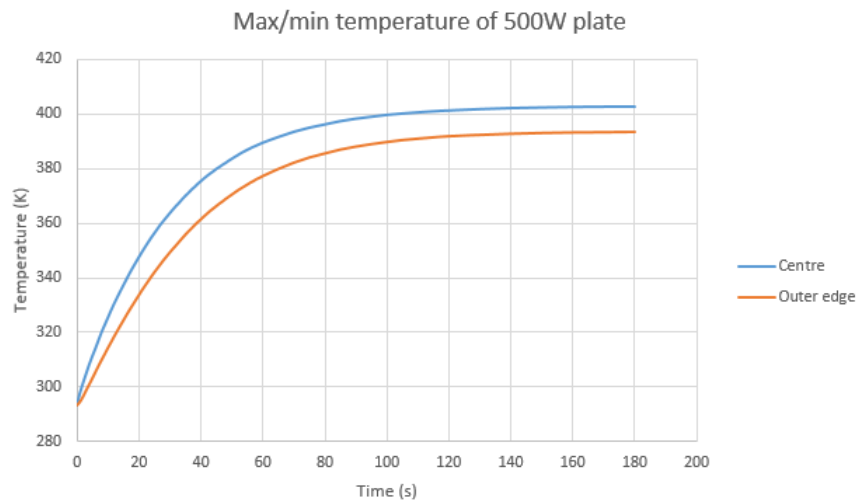


Figure 3.40: Simulated temperatures at the centre and outer edge of the plate

Rings replaced the spiral, and there is an insulating boundary condition at the bottom and sides of the plate. Nevertheless, this simplified simulation shows that the spiral-shaped design will be able to create a relatively uniform temperature distribution with an acceptable magnitude given the available heat. However, lower temperatures should be expected since it does not account for heat losses.

| Property | Value at 145°C           |
|----------|--------------------------|
| $\rho$   | 837.6 kg/m <sup>3</sup>  |
| $\mu$    | 0.00475 kg/m s           |
| $c_p$    | 2574 J/kg K              |
| k[40]    | 0.166 W/m <sup>2</sup> K |
| Pr       | 73.7                     |

Table 3.3: Physical properties of sunflower oil at 145°C

The previously mentioned cooking application from WASS Electronics has a size which is decent for cooking injera. Therefore, it was decided to design the griddle to have a similar effect and size. Physical properties of sunflower oil at the mean temperature of 145°C are shown in Table 3.3. These values were used when calculating pressure loss and the rate of heat transferred for different cross sectional geometries.

$$P = \dot{m}c_p\Delta T \quad (3.1)$$

By solving Equation 3.1 with respect to  $\dot{m}$ , an estimate of the required mass flow rate was obtained. It gives a mass flow rate of 0.00777 kg/s, which means a cooking time of approximately 18 minutes with the current heat storage. This flow rate was used in the expressions from Section 2.4 and 2.5 in attempt to find the cross sectional geometry which optimised both pressure loss and heat transfer.

The inlet of the cooking application will be placed approximately 1 m below the outlet of the heat storage. The hydrostatic pressure created by this height difference was found to be 8217 Pa by using Equation 2.4.

A 20 mm thick aluminium plate that was available at the laboratory could be used to make the griddle. Since the channels were to be milled, two plates had to be used in order to make it a closed system. As a result, the final thickness of the application was 40 mm. The initial idea was to have a thinner plate to reduce the amount of energy required to heat it up. However, the plate will cool down when injera batter is poured onto it, especially towards the edges. Therefore, it needs to have a certain thickness in order to maintain a high temperature when cooking.

Circular, triangular, square and rectangular cross sectional geometries for the spiral-shaped channel were discussed. After consulting with the technicians, it became clear that it had to be either square or rectangular. From Equation 2.14 it can be seen that in order to extract as much heat as possible, the surface area of the channel should be maximised. As mentioned in Section 2.4, the pressure loss depends on several constants which are tabulated in Appendix A. For the chosen rectangular geometry, they are given by their width/height ratio. Since this table is far from linear, it was decided to avoid interpolation. Therefore, only two ratios, 0.2 and 0.5, were considered. It was also decided to keep a similar amount of rings as the COMSOL simulation. In other words, letting the width of each channel be equal to the distance between them. This corresponds to an Archimedean spiral, which means that the distance between a ring and the next is constant.

$$r = a + b\theta \quad (3.2)$$

The radius of a spiral at any point, in polar coordinates, is given by Equation 3.2[41]. Here,  $a$  is the start point of the spiral and  $b$  determines the length between each ring. The constant  $b$  can be found by setting  $2\pi b = c$ , where  $c$  is the desired distance between each ring. For a spiral-shaped channel of width  $w$ ,  $c$  should be set to  $2w$  in order to make the separating material of equal width.

$$L = \int_0^{n2\pi} \sqrt{r^2 + \left(\frac{dr}{d\theta}\right)^2} d\theta \quad (3.3)$$

Equation 3.3 shows how to determine the arc length of a curve in polar coordinates. Here,  $n$  is the number of turns and the term  $\frac{dr}{d\theta}$  is equal to  $b$  in Equation 3.2[41].

After performing pressure loss and heat transfer calculations using the two width/height ratios with different lengths, the relation of 0.2 turned out to be the best option. Satisfactory results were obtained using a width of 5 mm and a height of 25 mm and are presented in Table 3.4 and 3.5, respectively. The expressions from Section 2.4 and 2.5 were used in these calculations.

| Property             | Value                  |
|----------------------|------------------------|
| L                    | 11.92 m                |
| $A_c$                | $0.000125 \text{ m}^2$ |
| $A_s$                | $0.715 \text{ m}^2$    |
| $D_h$                | 0.0083 m               |
| Re                   | 109.1                  |
| $C_{f,p} \cdot Re$   | 19.07                  |
| $c$                  | 0.000076               |
| $K_\infty$           | 0.931                  |
| $\zeta$              | 13.11                  |
| $C_{f,app} \cdot Re$ | 20.04                  |
| $p_{hydrostatic}$    | 8217 Pa                |
| $\Delta p$           | 2424 Pa                |

Table 3.4: Pressure drop calculations

| Property        | Value                           |
|-----------------|---------------------------------|
| L               | 11.92 m                         |
| $A_c$           | $0.000125 \text{ m}^2$          |
| $A_s$           | $0.715 \text{ m}^2$             |
| $D_h$           | 0.0083 m                        |
| Re              | 109.1                           |
| Pr              | 85.5                            |
| $x_{fd,h}$      | 0.045 m                         |
| $x_{fd,t}$      | 3.885 m                         |
| $Gz_D$          | 6.52                            |
| $Nu_{pipe}$     | 4.042                           |
| $Nu_{duct,lam}$ | 2.98                            |
| $Nu_{duct}$     | 5.334                           |
| $h$             | $95.54 \text{ W/m}^2 \text{ K}$ |
| LMTD            | 27.91 K                         |
| q               | 1126 W                          |

Table 3.5: Heat transfer calculations

The calculated effect of the plate shown in 3.5 is slightly higher than 1000 W. To have a physically viable solution, they should be equal. However; there are a lot of uncertainties involved in the calculations. The empirical formulas, the simplification of a ratio between laminar flow in pipes and ducts, assumed temperature and sunflower physical properties should not be expected to be entirely accurate. Moreover, no considerations were made regarding heat loss through the sides and bottom of the griddle. Also, the mass flow rate can be reduced to increase the cooking time. The result of this would be that the outlet temperature would drop, and thus the area which is suitable for cooking would be reduced. Although it would not be ideal, smaller injeras could be made for testing. For those reasons, it was decided to produce the griddle with the specifications above.



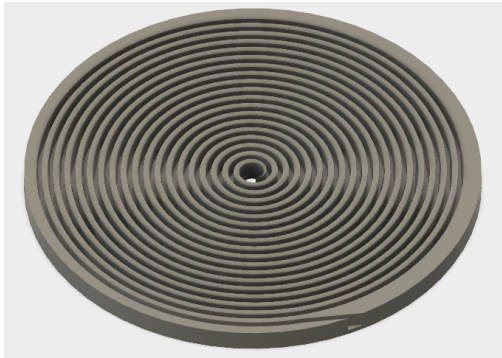


Figure 3.41: 3D-model of griddle, bottom

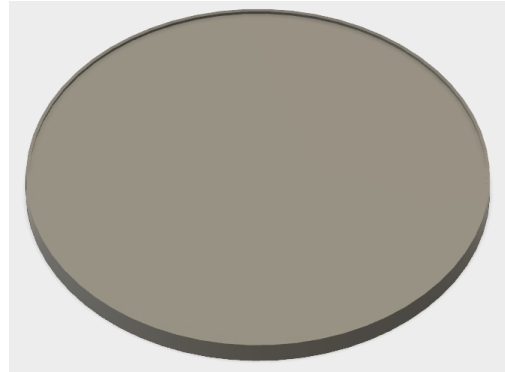


Figure 3.42: 3D-model of griddle, top

The griddle was modelled as two different parts in Autodesk Fusion 360<sup>TM</sup>[42]. They are shown in Figure 3.41 and 3.42. According to the technicians, milling deep and narrow channels can be problematic. This is because it is challenging for the machine to remove shavings, and the bit can easily break. Therefore, it was decided to mill channels in both parts. The spiral in the bottom part is 15 mm deep, while the spiral in the top part is 10 mm deep. A larger thickness between the channel and the top surface was believed to reduce the temperature drop caused by pouring injera batter on it. In addition, a 3 mm high and 3 mm wide edge was made on the top part to prevent the batter from spilling. The CAD files were sent to the technicians, who added two holes near the edge for guiding bolts that would be used when putting them together.



Figure 3.43: CNC milled griddle parts

Figure 3.43 shows the two parts after being realised through CNC milling. The spirals are mirrored, and by putting bolts in the holes, they connect perfectly. They were then welded together, and inlet and outlet pipes were attached. Further, it was decided to anodise the griddle to make it more durable and corrosion-resistant.



Figure 3.44: Insulated and anodised griddle set up for cooking

The anodising process caused the griddle to get the black colour seen in Figure 3.44. To ensure that the entire channel was filled with oil when cooking, the outlet pipe was shaped as shown. The griddle was connected to the heat storage by multiple insulated copper pipes with an inner diameter of 20 mm and a total length of 2.5 m. Using the procedure described in Section 2.4, this gives a pressure loss of 107 Pa. In other words, the pressure loss in the supply pipe is not a concern.

Since there is no drainage valve in this application, cold oil would remain in the channels after use. This oil was removed between tests by using compressed air.

### 3.5 Heat Storage Reversal

The cooking applications that will be tested in this thesis will utilise the heated sunflower oil. Sjøgren and Steen[7] thoroughly explain this part of the system. This section will include brief information which is of importance to understand how tests were conducted in this report.

Figure 3.45 shows how the heat storage part of the system is set up when it is to be reversed. The insulated tank with red tapes is the heat storage tank which contains pebbles. Each horizontal red tape indicates the position of a thermocouple. At the top of the tank, the supply pipe from the heating system can be seen. The outlet from the storage to the cooking application is near the top of the heat storage, at the right-hand side. Two valves can be seen between the heat storage and the plastic container at the top left. The upper valve is used during the charging process. Its function is to maintain a certain level in the heat storage. The lowermost valve is used to control the flow rate into the cooking application. Here, it is at a closed position. When opened, the pressure difference created by the elevated plastic container will drive the flow into the cooking application.



Figure 3.45: Heat storage ready for reversal

## Chapter 4

# Field Work at Makerere University, Kampala, Uganda

In collaboration with Sjøgren and Steen[35], a week-long field trip was conducted to Makerere University in Kampala, Uganda, in April 2018. The goal was to see if it was possible to construct a complete self-regulating oil based heat storage system with a functioning cooking application with the materials and equipment available in Kampala.

This chapter will introduce the motivation for the field trip, before presenting components and equipment. Further, the process of setting up the system and a review of the tests are presented. At last, results from these tests will be discussed.

### 4.1 Motivation

The motivation for visiting the university in Kampala was:

- See if it was possible to build and test a complete system setup with the available resources in a developing country.
- Exchange knowledge and ideas with students and professors from another culture, but the same academic background.

Since the primary goal for this thesis was to design and build an oil-based heat storage system that was to be implemented in rural areas in Africa, it was important to see if it could be produced locally and at a low cost. Since Makerere University is one of the universities that are part of the collaboration project, and it is situated in a developing country with an abundance of sun, this was a good location.

Another reason for choosing Makerere University as the field trip destination was that several PhD- and master students at the university research topics that are relevant to this thesis. Some research on heat storage using a rock bed, others on how to supply a heat storage medium at a constant temperature using non-automatic devices. For that reason, some of the students at Makerere University were contributing in the process of building the system. Therefore, a complete review of the system was necessary to familiarise them with the concept.

## 4.2 System Components and Equipment

The components needed to make the system are listed below:

- Two containers; one supply container and one residual container
- Plastic hose to transfer the oil from the supply container to the fill valve
- Two hose clamps; one for connecting the hose to the cold oil tank and one for the fill valve
- Fill valve
- Sunflower oil, as heat transfer fluid and storage medium
- Pipes in different dimensions and lengths to construct the heating system. Also, small diameter pipes were needed to connect the cooking application to the heat storage
- Heating element
- Heat storage tank
- Ball valve to control the mass flow rate from the storage tank to the cooking application
- Three pots in different sizes to construct the cooking application.

Because the availability of the components listed above may be limited in remote areas, the system is relatively simple. Also, the system is designed so that it contains few components that require advanced manufacturing because high-technology machines can be difficult and expensive to get hold of.

The only component that was brought from NTNU was the fill valve. The reason is that manufacturing this component requires equipment such as a lathe and soldering equipment. This equipment was not necessarily available at Makerere University. Also, due to the duration of the field trip, it was important to spend the available time on the entire system instead of making the fill valve.

However, after visiting one of the workshops at Makerere University it was discovered that there were several lathes in good condition available. According to students at the university, equipment for soldering was also available. However, according to the people at the Department of Physics, the workers at the workshop were not very accurate at their work. As mentioned, high precision is needed to produce the fill valve. Therefore it was a good idea to bring the fill valve from NTNU.

The container for the supply oil, shown in Figure 4.1, was a standard plastic tank that was slightly transparent so that one could easily see the oil level in the tank. Along with it came a small ball valve which made it easy to stop the oil supply whenever needed. A standard transparent hose in soft plastic connecting the oil container to the fill valve can also be seen.

Figure 4.2 is a picture of the 25 litres pot that was used as the residual oil container. The reason for using a pot instead of a plastic tank is that the residual oil is over 100°C.



Figure 4.1: Cold oil container



Figure 4.2: Residual oil container

Getting hold of pipes in different dimensions to build a system similar to the one made at NTNU proved to be more difficult than initially assumed. Therefore, instead of pipes, a metal sheet was bought. Further, the metal sheet was cut and bent into containers in different sizes, as seen in Figure 4.3. The one on the right is where the heating element was to be placed, the one in the middle is for the fill valve, and the one to the left is the heat storage tank.



Figure 4.3: Bent metal sheets

To copy the system from NTNU, it was desired to obtain a similar heating element that could be mounted on the bottom of the hot section. Figure 4.4 shows the heating element that was acquired. This was a 4000 W 220 V heating element with an oblong bottom piece.

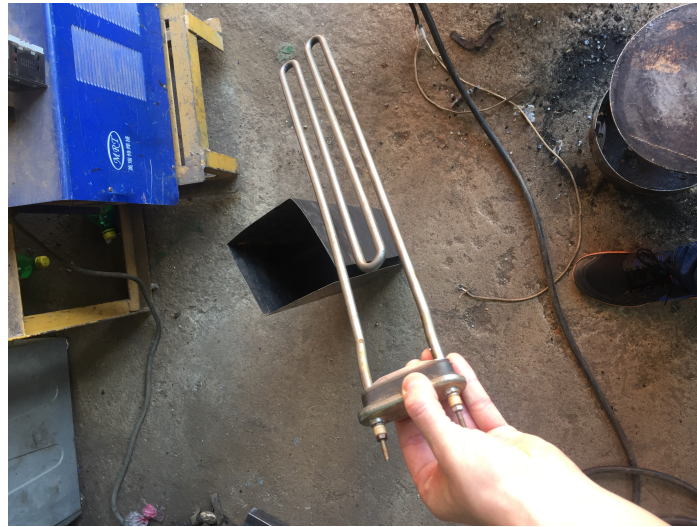


Figure 4.4: Heating element with oblong bottom piece

Sunflower oil was used as heat transfer fluid and storage medium. In Figure 4.5 one can see one of the sunflower oil types that were used. The other type was Sunseed. They are both refined sunflower oils.



Figure 4.5: Sunny sunflower oil



Figure 4.6: Pots for cooking application

For the cooking application, three steel pots in different sizes were acquired. They contain 3, 5 and 7 litres, respectively, and are pictured in Figure 4.6. The production of the cooking application from these pots, as well as the ball valve and pipes connecting the boiler to the heat storage tank, is covered by Sjøgren and Steen.

### 4.3 Methodology

When designing the heating system it was desirable to make something that was similar in size to the system made at NTNU. The specifications for the three different tanks in the system can be viewed in Table 4.1.

| Description                      | Cross sectional area | Height | Volume |
|----------------------------------|----------------------|--------|--------|
| Cold section for fill valve      | 20 cm x 20 cm        | 55 cm  | 22 L   |
| Heat section for heating element | 5 cm x 10 cm         | 50 cm  | 2,5 L  |
| Heat storage tank                | 20 cm x 20 cm        | 40 cm  | 16 L   |

Table 4.1: Dimensions of the tanks in the system at Makerere University

The cross sectional area of the cold section was set to 20 cm x 20 cm to make sure that there was enough space for oil around the floater so that the delivered temperature would not fluctuate as much. The cross sectional area of the hot section was set to 5 cm x 10 cm so that a heating element shown in Figure 4.4 would fit.

As seen in Figure 4.7, the bent metal sheets in Figure 4.3 was then welded in the workshop to create boxes. Further, one can see the pipe connecting the two boxes. It was a  $\varnothing 30$  mm pipe that was found in the lab. It was cut in two halves and connected with a muff so that the two boxes could be dissembled for transportation purposes; on request from the students at Makerere.



Figure 4.7: Welding at the workshop

Mounting the "T" had to be done in a slightly different way than what was planned. Because the tank was 20 cm x 20 cm, the inlet pipe was not long enough to go through the wall and at the same time allow the floating device to move freely. Therefore, the "T" was mounted using a rod as seen in Figure 4.8. In terms of performance, this modification would not influence the fill valve. The only thing that is different is that the supply hose is on the inside of the tank.



To make sure that the hole where the rod entered the tank was leak-proof, the silicone sealant in Figure 4.9 was used. Further, the entire system was filled with cold oil to check for weaknesses in the welds. Unfortunately, there were several leakages, and more silicone was applied to make the system leak-proof.



Figure 4.8: Fill valve inside the cold section



Figure 4.9: Silicon sealant



Figure 4.10: Portable heating element [43]

The heating element in Figure 4.4 was eight times as powerful as the one used at NTNU, but the volume of the hot section was similar. When this was discovered, it was decided to look for another option since it was not certain that the sunflower oil could handle that amount of power. There was a different type of heating element available in the laboratory, a portable heating element similar to the one shown in Figure 4.10. According to the students, this type of heating element is commonly used for heating water, and it had an effect of 1500 W. It had to be lowered into the hot section because it would short-circuit if it came in contact with the metal. Lowering it from the top had two disadvantages; the hot oil could melt the handle, and less heat could be utilised if its metal part was not completely submerged. Another complication was that the hot section was designed for the previously mentioned heating element which had a different cross sectional area; thus it did not fit. Therefore, the hot section was expanded by hammering a piece of wood into it to make the cross sectional area more circular.

The system was set up as shown in Figure 4.11. The supply tank was placed on top of a cupboard, the heating section and the storage tank was placed on a desk, the cooking application on a chair, and finally the residual container on the floor. As a result, the elevation difference required for the system to be driven by the gravitational force was obtained.



Figure 4.11: Complete test system



Figure 4.12: Insulated heating system

A test that will be described in Section 4.4 was conducted without insulation. After this test, the hot section and the pipe leading into the heat storage was insulated, as shown in Figure 4.12. Due to some complications during the first test, a new heating element similar to the one shown in Figure 4.4 was acquired. This heating element had an effect of 365 W and a voltage of 24 V, and it was mounted at the bottom of the heating section as shown in Figure 4.13.



Figure 4.13: Heating element inside hot section



Figure 4.14: Heating element contacts

As seen in Figure 4.14 the heating element did not have a cable with a plugin, so it had to be connected directly to a variac.

Unfortunately, the fill valve had to be brought back to NTNU for further testing because it was the only prototype. However, since it was found that the equipment required for making the fill valve was available at Makerere University, a recipe was made upon request from the students at Makerere. The recipe is depicted in Figure 4.15.

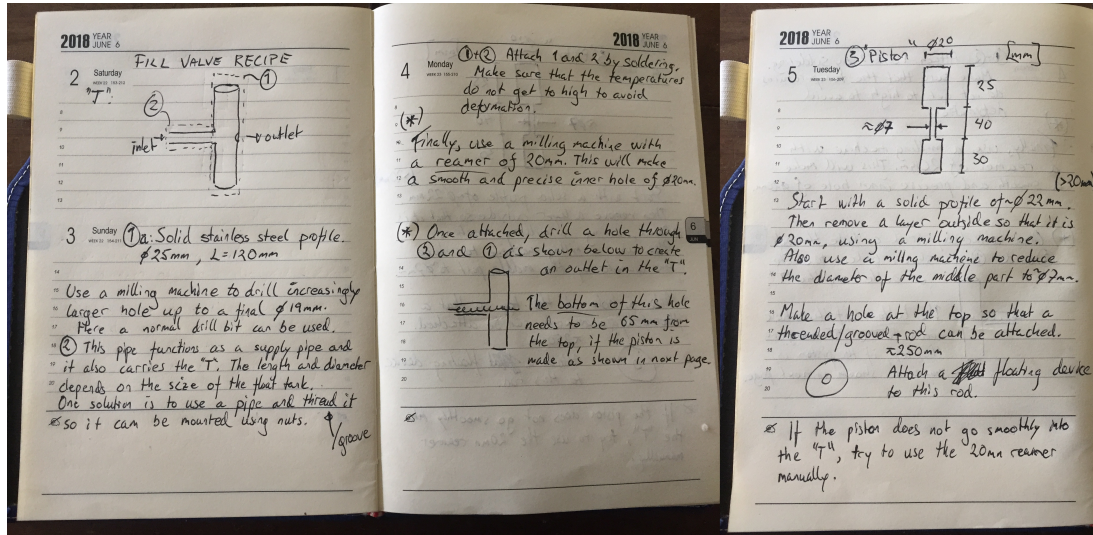


Figure 4.15: Recipe to manufacture the fill valve

Note: What is referred to as milling machine in the recipe, should have been a lathe machine.

## 4.4 Test and Results

Figure 4.16 shows the setup for Test 1. Since the heating element was 1500 W, three times more than the one used at NTNU, it was connected to a variac to provide more control during the test. As the heating element had to be lowered from the top, a wooden monopod was used to hold the cable of the heating element which was hanging freely inside the hot section. To monitor the temperature of the oil, a thermocouple data logger from Pico was used; the same type as at NTNU. Because of limited access to thermocouples, one was placed in the bottom of the storage tank and only two in the hot section. One of the thermocouples was placed near the heating element, and the other just below the outlet. One can see both the heating element and the two thermocouples in Figure 4.17.



Figure 4.16: System setup Test 1



Figure 4.17: Heating element and thermocouples

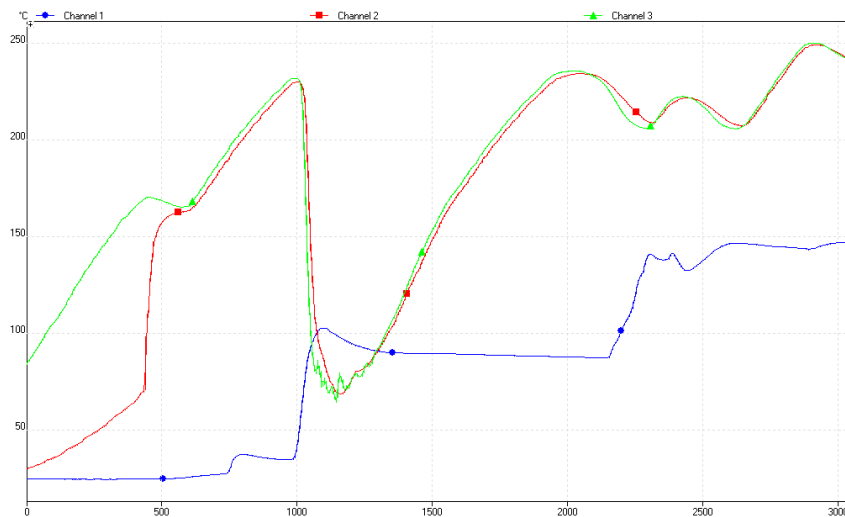


Figure 4.18: Temperature graph from Test 1

Figure 4.18 shows the temperatures from the first test. Channel 1 is the temperature in the heat storage, channel 2 is the temperature at the outlet of the hot section, and channel 3 is the temperature near the heating element.

The purpose of this test was mainly to figure out at which position the fill valve should maintain the initial oil level, to achieve a stable temperature around 230°C for the oil delivered to the heat storage. For this reason, the heated part of the heating system was not insulated in this test.

From the start of the test, the heating element was set to deliver the maximum power of 1500W. As seen from the plot, the temperature of the oil raised to 230°C after 1000 seconds. As the temperature gradient was so steep at this temperature level, cold oil was let into the system as the fill valve was adjusted. After 2000 seconds the temperature again reached 230°C, but this time it plateaued and oscillated down to temperatures around 210°C. As this was a bit low, the fill valve was slightly adjusted around 2600 seconds. At approximately 2900 seconds the temperatures reached 250°C before starting to decline again, which indicated that the temperature would have stabilised somewhere around 240°C. The fact that a slight adjustment of the fill valve caused a temperature rise of around 20°C was likely a result of the heating element being lowered from the top. This is because the volume of oil that is expanded is significantly less than if the heating element is mounted from the bottom. Unfortunately, the test had to be aborted just after 3000 seconds because the heating element started to melt, see Figure 4.19. The plastic components melted because it was hanging just above the oil level, and when the oil was heated the plastic could no longer withstand the heat.



Figure 4.19: Melted heating element

As mentioned in Section 4.3, a different heating element was mounted at the bottom of the hot section after the first test. However, when it was to be connected to the power supply, it was found that the variac could only withstand a current of 8 A. If this current is exceeded, the variac could potentially start burning. It was already known that the electric potential of the heating element was 24 V. The resistance was measured by an ohmmeter to be 1.6  $\Omega$ . By using Equation 2.3, the current was found to be 15 A. Therefore; it was unfortunately not possible to conduct a second test with the equipment available at the lab at that time.

## 4.5 Discussion

The overall impression from the field trip to Makerere University was that it was a success, at least considering the short duration of the stay. In the end, the main goal was to create a heating system that could deliver oil at a stable temperature and a cooking application that could boil water. Regarding the cooking application, Sjøgren and Steen[35] managed to boil 2 litres of water for a significant amount of time. They had to use a hotplate to heat oil for their experiment because of the incident with the heating element. However, the students at Makerere University were concerned regarding the price of the cooking application. If this type of cooking application were to be further developed, the most important aspect would be to find a cheaper way to produce it.

Regarding the heating system itself, it seems as if availability is the biggest issue. Getting hold of a suitable heating element was harder than expected. The easiest way to get one is through the second-hand market, but according to the students at Makerere, the specifications written on the package is often incorrect.

Further, pipes were not easy to get hold of either. However, the improvised solution of using metal sheets that were cut, bent and welded into boxes was partly successful. Firstly, the quality of the welding was not good enough. Leakages made the workspace very greasy, and with hot oil, it can potentially harm persons and objects nearby. If the workshop welds the boxes more precisely, they will be a decent substitute for the pipes. Another drawback of using a box instead of two pipes with different diameters in the cold section is that it increases the amount of oil in the system. As one of the students at Makerere suggested; one way to come around this disadvantage is to fill the tank with small rocks to reduce the volume of oil, and this way compensate for the oversized tank.

At last, it was positive to realise that it should be doable to make the fill valve locally in Kampala. Most of the necessary equipment was available at Makerere University, so hopefully, it will be manufactured successfully in the future. The challenge will be to find someone who can do the work precise enough.

Even though it was not enough time to put together a system where everything worked simultaneously, every part was successfully constructed and tested separately. In the end, representatives from both universities expressed their satisfaction with the work that was conducted during the week at Makerere University.

# Chapter 5

## Results

This chapter includes a selection of the tests that were conducted during this thesis. At first, testing the custom made fill valve was the main focus. Therefore, the first tests contain information about its performance. Parameters that are considered are the temperature of the delivered oil at different effects, as well as the temperature distribution in the oil along the heating element. The custom made fill valve was used in all of the tests presented in this chapter.

Results from the tests of the two different cooking applications will then be presented. Important parameters for these tests are the temperature of the oil entering and leaving the applications, as well as the temperature of the pans surface area. In some of the tests, the results from the charging and discharging of the rock bed are included. Even though the main goal was to make injera, most of the tests were carried out using pancake batter to get an indication of its cooking ability. In the final test, injera batter was used. In some of the tests, a thermal camera was used to measure the temperature of the griddle.

Temperatures recorded using thermocouples, are referred to in the text as TC and their respective channel number if not stated otherwise.

### 5.1 Fill Valve Test, 14.03.18

This section will present the results of the first test where the heat storage was charged. The goal was to examine the fill valve's ability to maintain a steady temperature, and how the output temperature would change when applying different effects to the heating element. Initially, it was set to 500 W.

This test was conducted before the solution with thermocouples attached to a rod was in place. Therefore, only data from the top of the heating element and above were recorded. The green thermocouple was placed just inside the pipe supplying the rock bed, and it shows a rapid increase at the point when the hot air from the oil entered the pipe. The sudden decline of its temperature at  $t \approx 700$  s was due to the exhaust being turned on. At  $t \approx 1500$  s, the temperature at the top of the hot section, indicated by the red graph, reached its maximum of 245°C. For the next 1000 s, it did not drop below 241°C. The temperature drop that can be observed at this point was a result of setting the effect to 250 W. For the next 3000 s the red thermocouple was kept within a range of 218-227°C, before the effect was set to 100 W at  $t \approx 5500$  s. The temperature drop caused by this reduction was less steep, and it took around 2500 s for it to stabilise at 203°C. Thereafter, the effect was again set to 500 W and the temperature quickly increased, and it peaked at 249°C.

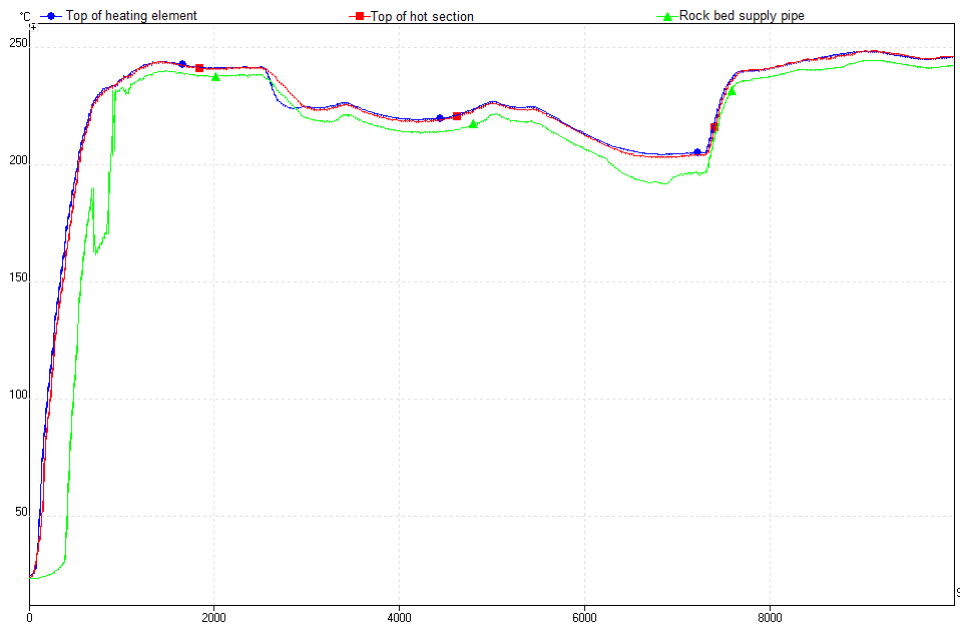


Figure 5.1: Fill Valve Test Results, 14.03.18

Although the temperature of the oil delivered to the heat storage changed within a range of around  $50^{\circ}\text{C}$  during this test, the stratification was satisfactory, and a successful boiling experiment was conducted.

## 5.2 Fill Valve Test, 20.03.18

This section will present the results of the first test using the thermocouple rod explained in Section 3.2.3. The remaining tests will use this rod, and the placement of the thermocouples can be seen in Figure 3.8. This gives a better understanding of the temperature distribution around the heating element. One goal of this test was to study this temperature distribution. The other goal was to perform a similar test as in Section 5.1, with an effect of 500W, 250W and 100W, to see if the fill valve was able to achieve similar results.

From the plot in Figure 5.2 one can see the temperature distribution of the oil during this test. For TC 1-4 the temperatures are rising the higher the thermocouples are located. TC 5-7 keeps approximately the same temperature during the entire test. It is important to notice that even though the temperature in TC 1-4 fluctuates significantly, the three thermocouples above the heating element records a relatively steady temperature, which indicates that the fill valve works as well as needed to deliver a steady temperature.



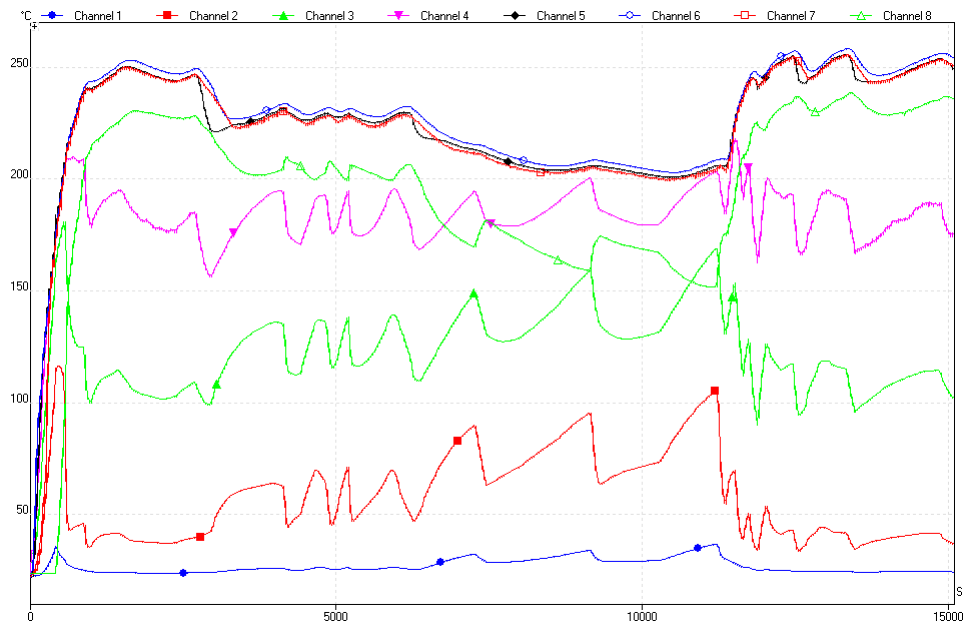


Figure 5.2: Fill Valve Test Results, 20.03.18

Compared to the test in Section 5.1, the temperatures are similar. At first, the effect was set to 500W and the temperature at the top of the hot section reached temperatures between 243 and 250°C, which is slightly higher than for the previous test. When the effect was reduced to 250W after 2700 s, the temperature declined into the range of 224-230°C, which again is slightly higher than then for the previous test. After 6100 s the effect was decreased again, to 100W, and the temperature stabilises between 200 and 206°C; approximately the same as for the previous test. After 11400 s, the effect was increased to 500W, and the temperature raised to a level fluctuating around 250°C.

Regarding the temperature in the pipe supplying the rock bed, it was noticeably lower during the entire test compared to the test results from Section 5.1. The reason is that the thermocouple was now placed further into the pipe to get a better insight in the actual temperature of the oil delivered to the rock bed, as supposed to the previous test where it was placed just inside the pipe. This temperature difference shows that there is a substantial heat loss in the pipe, and explains why the temperature delivered to the rock bed is 20 and 40 °C lower than TC 7 at 500W and 100W, respectively.

One thing worth mentioning is that TC 6 exceeds TC 7 during the entire test. This is the only test where this case occurred, and it is not easy to explain why. One reason can be that the thermocouple was in contact with the inside of the pipe, and for this reason reached a higher temperature than normal.

Given the similarities in the two tests, the overall performance of the fill valve was satisfactory.

### 5.3 Fill Valve Test, 21.03.18

After the temperatures at different effects had been examined, it was decided to test the fill valve's ability to maintain a constant temperature for a longer period. The results presented in this section are from a test where the effect was set to 500 W and remained unchanged.

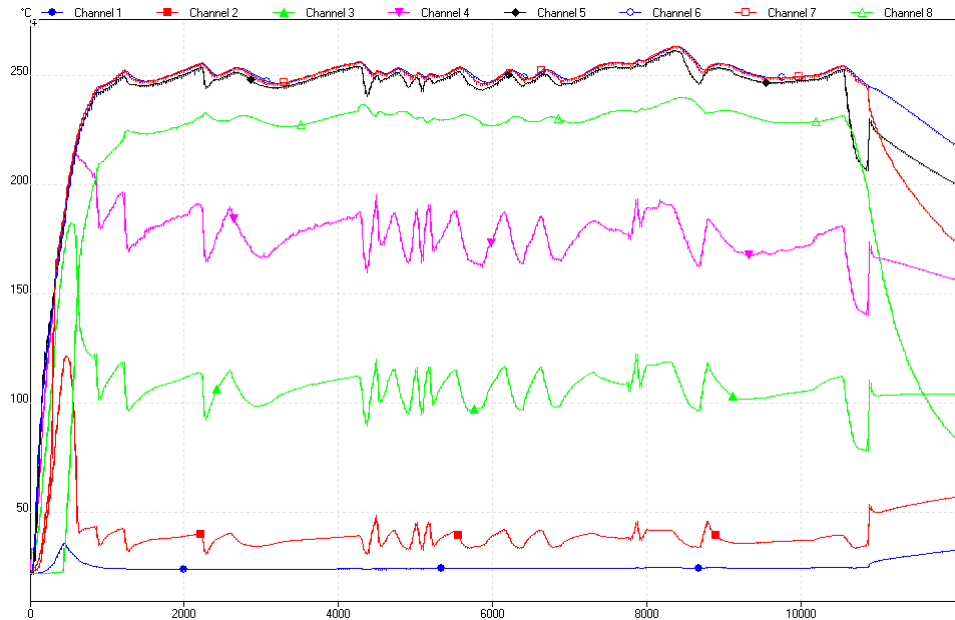


Figure 5.3: Fill Valve Test Results, 21.03.18

TC 7 reached its first local maximum at  $t \approx 1250$  s at a temperature of  $252^\circ\text{C}$ . From that point; it was kept within a range of  $245\text{--}263^\circ\text{C}$  for the remainder of the test. TC 8 shows that the temperature of the oil which is delivered to the rock bed is around  $20^\circ\text{C}$  lower. About  $10500$  s after the heating element was turned on, the TC in the bottom of the rock bed was at  $74^\circ\text{C}$  which means that the heat storage is fully charged and the power was turned off.

### 5.4 Open Cooking Application Test, 03.04.18

As mentioned in Section 3.4.1, two different pans were available for the open cooking application. The goal of this test was to figure out if the pans could become hot enough to fry pancakes.

Figure 5.4 illustrates how crucial it is to make sure that the supply container does not run out of oil. TC 7 was kept within a range of  $238\text{--}250^\circ\text{C}$  until the supply of cold oil stopped at  $t \approx 5700$  s. As a result, the temperature of the oil in the hot section kept increasing at a rapid rate. Even TC 2, which had been unaffected in the previous tests, had its temperature increased. This was not discovered before the person present, who was preparing for the frying test, looked at the computer. In other words; neither smell, sound or smoke warned about what was going on. The system was then flooded, resulting in a temperature drop for all TCs at  $t \approx 6400$  s before resuming to normal temperatures at  $t \approx 7700$  s.

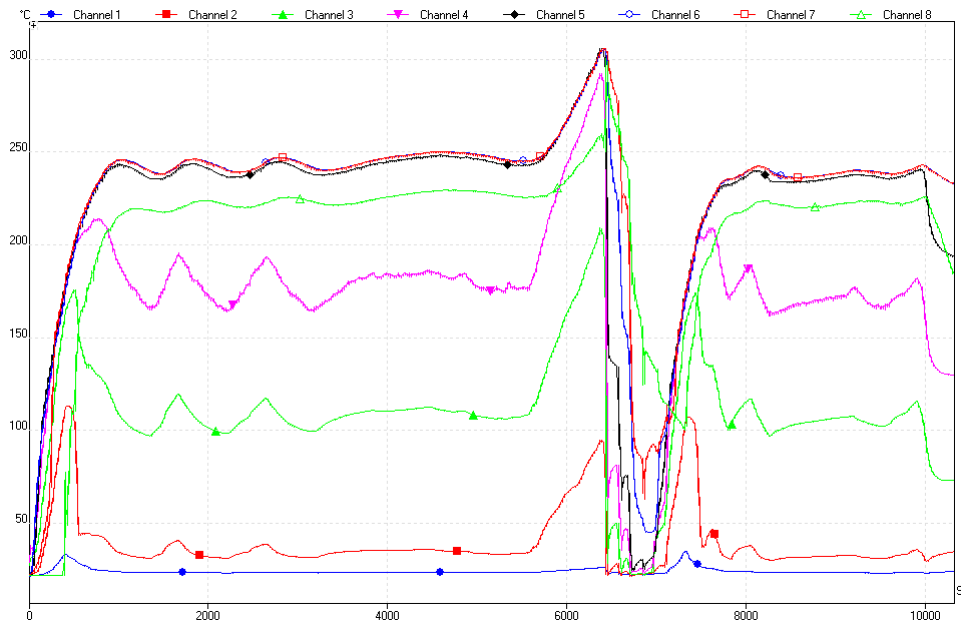


Figure 5.4: Temperatures in the hot section when charging heat storage, 03.04.18

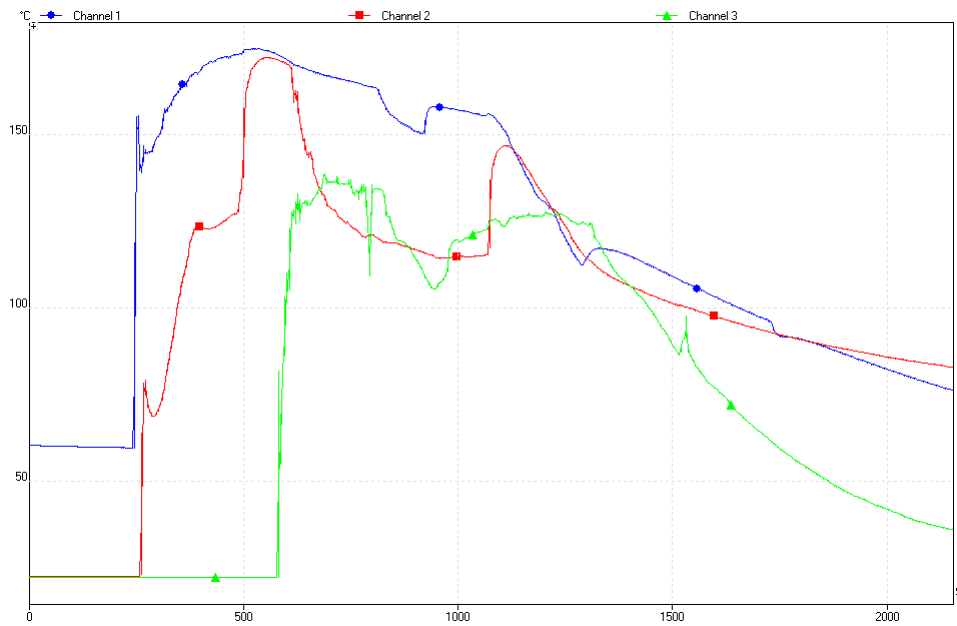


Figure 5.5: Oil temperature in the cooking application when testing the paella pan

In Figure 5.5, TC 1 is the temperature at the outlet of the heat storage, TC 2 is the inlet of the cooking application, and TC 3 is the outlet. Since no outlet flow had been observed after 250 s with the initial flow rate, it was decided to increase it at  $t \approx 500$  s. This had an immediate impact; TC 2 reached the magnitude of TC 1. Outlet flow was observed around 100 s later, and

the flow rate was reduced.

The gap between TC 1 and 2 two seemed to be largely dependent on the flow rate, where a small gap means a high flow rate and reduced heat loss in the pipe connecting the application with the rock bed. The difference between TC 2 and 3 indicates the amount of heat transferred to the pan. As seen in the plot, it is possible for  $TC\ 3 > TC\ 2 > TC\ 1$  at some points. This does not make physical sense but can occur when the mass flow rate is changed because of delay in the system.



Figure 5.6: First frying attempt

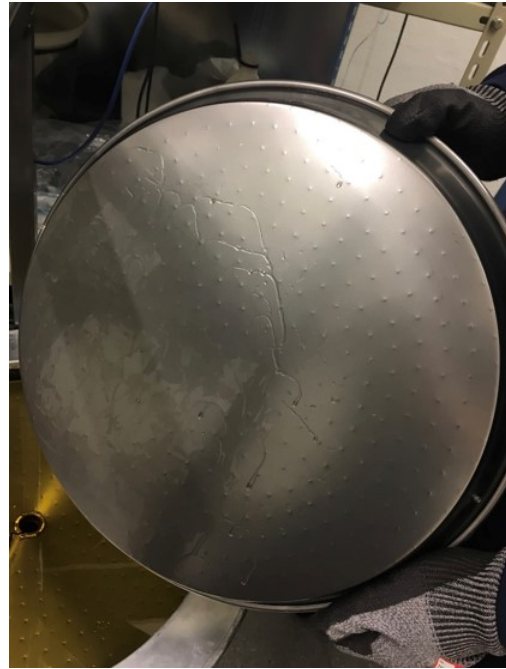


Figure 5.7: Wetted area of the paella pan

After  $t \approx 650$  s, the paella pan seemed to be warm enough since the butter was turning brown, and pancake batter was poured into it. It was decided to test the pan with a small pancake as the temperature was significantly higher in the centre of the griddle. After a few minutes, it became clear that the pan was not hot enough, and the test was aborted. Figure 5.6 shows the result of the pancake made in this test. Figure 5.7 shows the bottom of the pan after it was removed. Only a part of the pan was wet, suggesting that it was not going deep enough into the application. This explains why the pancake was far from cooked. As discussed in Section 3.4.1, the pan should be resting on the nuts to maximise the heat transferred.

Since the paella pan did not work as intended, it was decided to test the custom made pan using the remaining hot oil in the heat storage. At  $t \approx 350$  s in Figure 5.8, the flow rate was increased to raise the temperature of the pan, and frying was initiated. The pan has a large thermal mass. This is illustrated from  $t \approx 550$  s, where TC 3 is significantly higher than TC 2. This means that the pan is using some of its energy to heat the oil rather than the food.

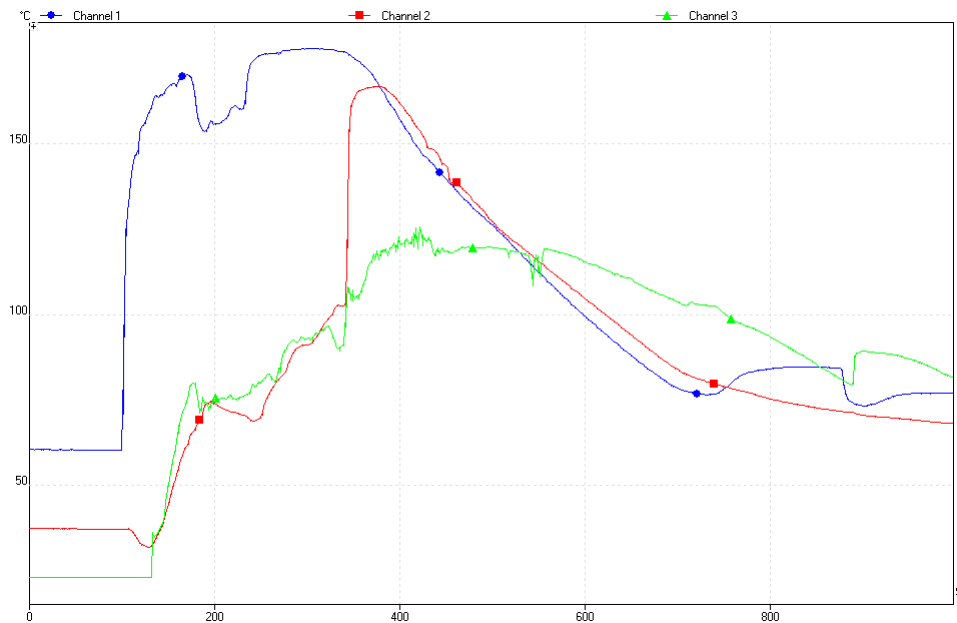


Figure 5.8: Oil temperature in the cooking application when testing the custom made pan

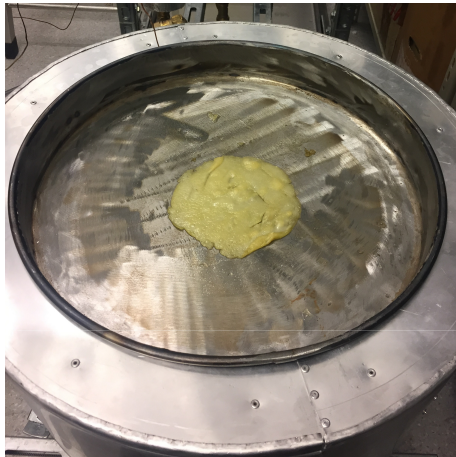


Figure 5.9: Pancake made using the custom made pan

Since the custom made pan was adequately submerged in the oil, it became warmer. Because of its thermal mass, it took some time to reach temperatures where the butter turned brown. The pancake showed in Figure 5.9 has some crust, but it cannot be characterised as sufficiently cooked. Perhaps a better result could have been obtained if this pan was used during the entire test. As the paella pan was tested first, the temperature of the storage medium was reduced when testing the custom made pan.

This test had a practical approach to discover weaknesses with the design and to try to find an efficient flow rate. It was clear that the paella pan had to be modified if it was to be used.

## 5.5 Open Cooking Application Test, 24.04.18

After the previous test, it was clear that the paella had to be modified before further tested. Therefore, the edge was cut off so that the entire pan would fit inside the cooking application and small metal pieces were welded onto the inside of the pan as handles. Also, it was noticed that the pan was floating on the oil instead of being adequately lowered in it. Therefore, as a temporary solution, a pipe and a wrench were taped to the handles to provide more weight.

The purpose of this test was to check if the modified paella pan was suitable for frying and to get a grasp of how different mass flow rates impact the temperatures of the oil and thereby the frying pan. Unfortunately, much corrosion had occurred on the surface of the custom made pan, and it was considered unusable for cooking purposes. At first, the rock bed was charged until it was fully loaded.

Figure 5.10 illustrates the temperatures of the oil from the heat storage and in the cooking application. The thermocouples are located at the same position as in the test from Section 5.4.

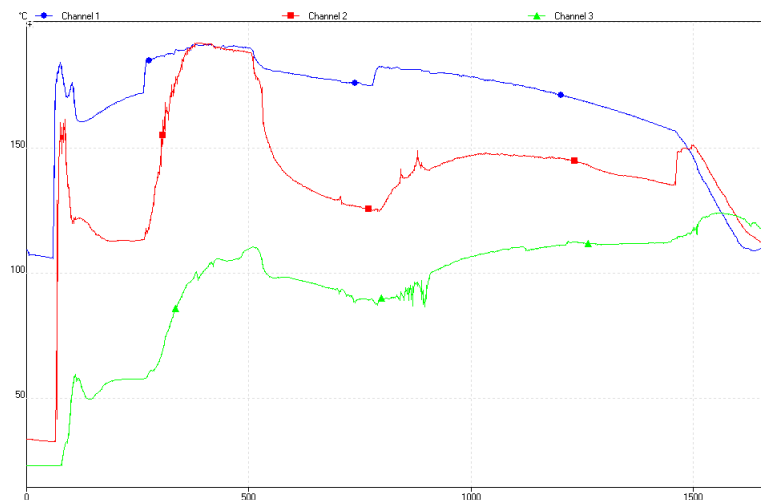


Figure 5.10: Oil temperatures in the cooking application during frying

The plan was to keep a high mass flow rate in the beginning, until the thermocouple at the outlet was affected. When this occurs, it is certain that the cold oil that was already in the application has been replaced with the heated oil. Shortly after the temperature in the outlet started to rise around 100 seconds, it was decided to reduce the mass flow rate. The reason for closing is to keep the oil in the system for a certain amount of time so that the pan can extract as much heat as possible before the oil exits. Unfortunately, this mass flow rate was not recorded. Because the temperature at the outlet started to plateau at only 60°C, it was once again decided to increase the mass flow rate after  $t \approx 270$  s. The mass flow rates for the rest of the experiment can be studied in Table 5.1. Soon after the mass flow rate was increased, TC 2 rises and reaches TC 1. Because of the high mass flow rate, heat losses do not affect the temperature in the oil from leaving the heat storage until it reaches the cooking application. This caused the exit temperature to reach approximately 110°C. As 110°C was considered warm enough the mass flow rate was once again reduced for the temperature to plateau. This was done 500 seconds into the test. Unfortunately, the ball valve controlling the mass flow rate is very sensitive, and the mass flow rate dropped from 0.0111 to 0.0017 kg per second which led to a 20°C temperature

drop in the outlet. For this reason, it was decided to increase the mass flow rate one more time, after  $t \approx 780$  s. This mass flow rate was maintained for the rest of the experiment.

| Time [s] | $\dot{m}$ [ $\frac{kg}{s}$ ] |
|----------|------------------------------|
| 270-500  | 0.0111                       |
| 500-780  | 0.0017                       |
| 780-     | 0.0085                       |

Table 5.1: Flow rate test 24.04

As for the frying of the pancake, the result can be inspected in Figure 5.11. Near the centre, the pancake was utterly done and achieved a nice, golden surface. At the edges, the pancake was cooked all the way through, but it did not obtain an appealing colour. In the end, the experiment was a success. It showed that it is possible to make pancakes on the cooking application, even though it is clear that the pan did not achieve a uniform temperature.

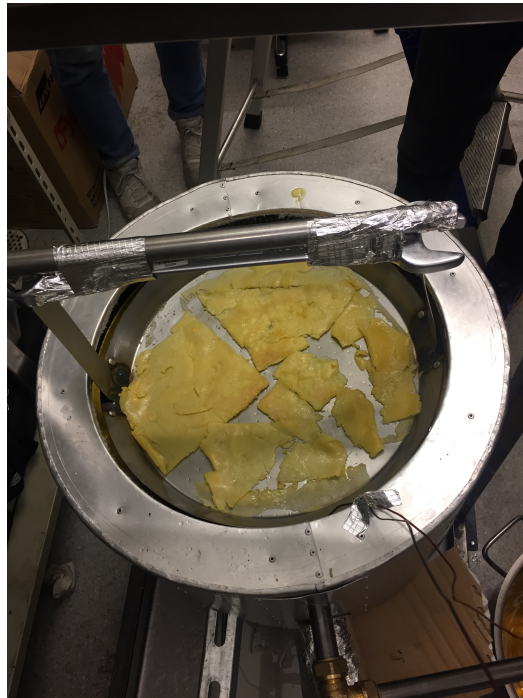


Figure 5.11: Making pancakes on open cooking application

## 5.6 Closed Cooking Application Test, 14.05.18

This section will cover the first test of the closed cooking application. In addition, it will look into how the output temperature of the heating system is affected by the level in the cold section. The fill valves dependency of the level in the supply container will also be carefully examined. Further, it was of interest to find out how much the valve should be opened to deliver the desired flow rate. Finally, it was also tested if this temperature was high enough to fry pancakes.

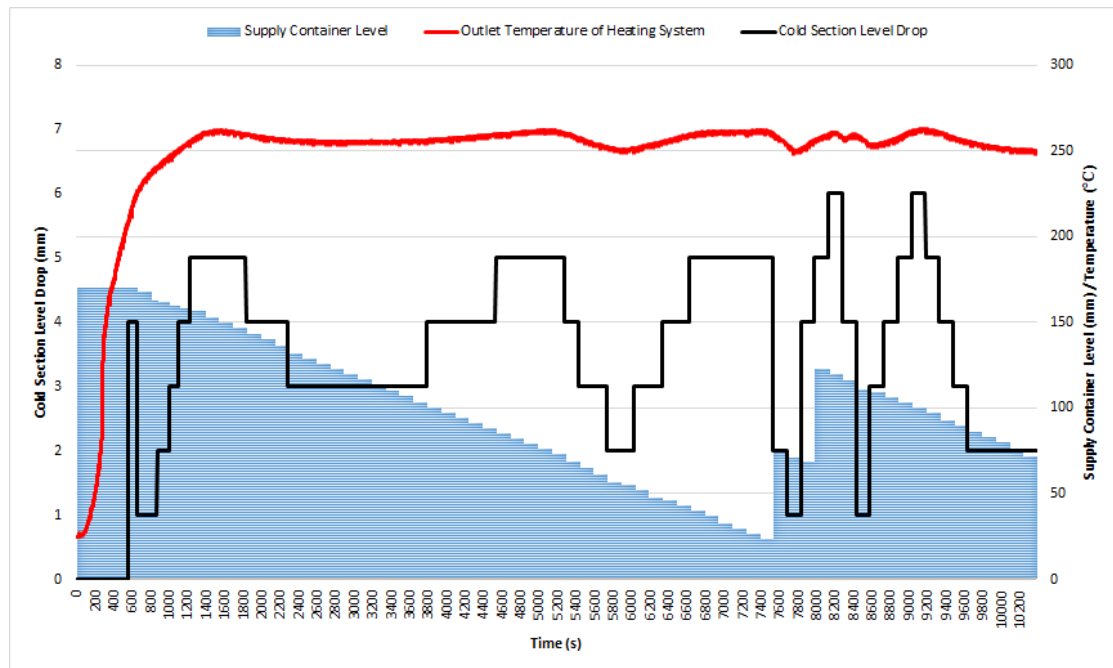


Figure 5.12: Correlation between supply container level, cold section level and output temperature

To get a better understanding of the correlation between the supply container level, cold section level and output temperature, they were logged when charging the heat storage. The output temperature was logged every second using a thermocouple, while the other two parameters were logged manually. Seven manual recordings were made during the first 1200 s, which includes the moment when the fill valve opened. After that, manual recordings were made every 150 s until the heat storage was fully charged. Recordings of the three parameters are plotted together in Figure 5.12. Cold section level drop refers to its deviation from the initial level where the fill valve is closed. Thus a larger value of this in the plot means a lower level in the cold section. The outlet of the supply container is 60 cm above the initial cold section level. Supply container level refers to how far it is from being empty. Although it may seem like much information to put into a single graph, it makes it easier to compare them. For instance, it can be seen that the output temperature graph follows a similar trend as the graph of the cold section level drop. This is in line with a previous discussion; the hot oil has to expand more when the cold section level is low, which results in a higher temperature. The decrease in the supply container level is nearly linear from the first output temperature peak up until around 7400 s. During this period, the fill valve kept the cold section level within a range of 3 mm. Although it oscillates slightly, it seems to be unaffected by the supply container level. The maximum and minimum output temperature recorded in the same period was 263°C and 249°C, respectively.

Around 7400 s and 8000 s, the supply container was filled with 3 litres of sunflower oil, and an increase of its level can be observed. This caused the cold section level to oscillate more rapidly and across a slightly wider range of 5 mm for the following 2000 s. However, it only stayed at these new outer points for a brief moment. The output temperature reacted accordingly and operated between 263°C and 248°C. In other words, refilling the supply tank during heating does indeed affect the fill valve, but the output temperature is still kept within a very similar range.



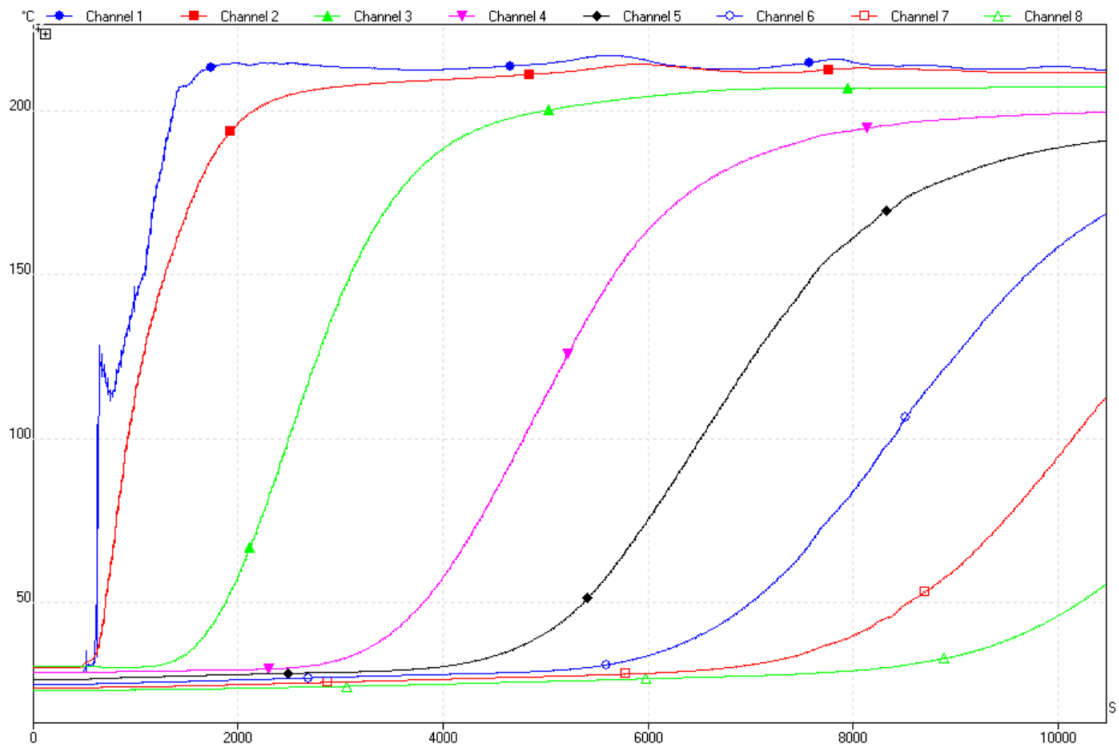


Figure 5.13: Temperature in the heat storage during charging

As soon as the temperature at the bottom of the heat storage, indicated by channel 8, becomes above 65°C, the heating system should be turned off. Figure 5.13 was recorded at the same time as Figure 5.12. The temperature in the upper part, indicated by channel 1 and 2, follows the output temperature of the heating system. Heat loss between the heating system and the heat storage cause the temperature to be reduced by around 40°C. Even though the temperature at the top is not constant, the layers below seem unaffected by the slight temperature oscillation, and a decent stratification is obtained.

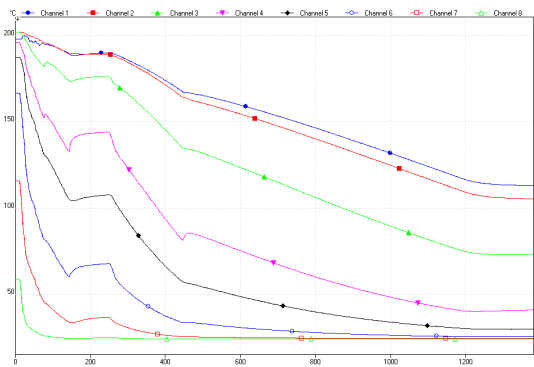


Figure 5.14: Heat storage reversal 14.05

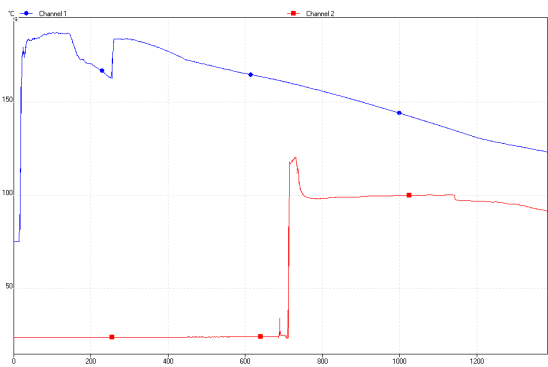
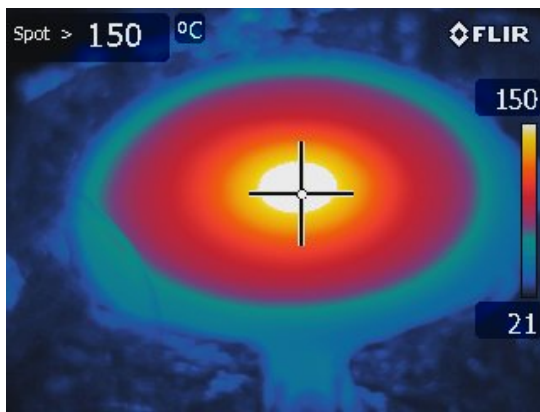
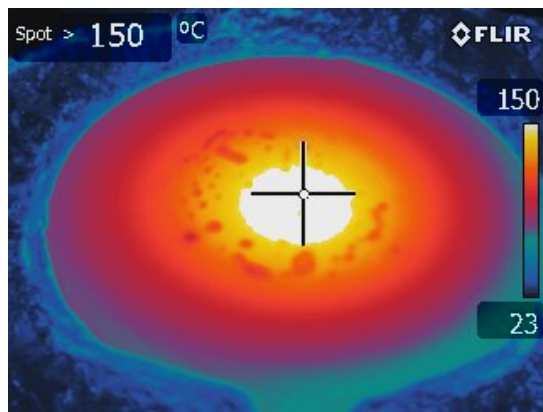


Figure 5.15: Application temperatures 14.05

The temperature in the heat storage, as well as the inlet and outlet of the cooking application, were recorded during reversal of the system. Figure 5.14 and 5.15 have the same starting point and show their temperatures. During the first 150 s, the valve that regulates the flow rate was set to deliver a high flow rate. This is indicated by a large temperature drop in the heat storage. Once outlet flow was observed it was shut, which is why the temperatures in upper part of the heat storage remain unchanged for the next 100 s. Figure 5.15 indicates that there is no flow out of the application at this point since the output temperature is unchanged. The reason was a connection error between the thermocouple and the computer, which was fixed when noticed in the middle of the test. Thereafter, it was attempted to obtain the mass flow rate calculated in Section 3.4.2. Since there was no way of knowing exactly how much a change in the ball valve opening affected the flow rate, an arbitrary opening was chosen. The heat storage temperature distribution was closely monitored, and at  $t \approx 450$  s it was decided that the temperatures were falling too fast. By reducing the opening of the valve slightly at this point, a more satisfying temperature drop was obtained, and it was kept for the remainder of the test. At  $t \approx 800$  s, the mass flow rate was found to be 0.0038 kg per second. This is equal to 49% of the mass flow rate the application was designed for.

Figure 5.16: Griddle at  $t \approx 60$  sFigure 5.17: Griddle at  $t \approx 300$  s

The IR photos in Figure 5.16 and 5.17 were taken moments before outlet flow was observed and before cooking, respectively. Although the griddle had not reached a uniform temperature, it was decided to attempt to fry a small pancake in the area near the centre where the temperatures were minimum 110°C. The spots seen in the middle of Figure 5.17 came from melted butter.

The pancake in Figure 5.18 was a lot smaller than an injera should be. However, it was clear that the temperature in the middle of the griddle was high enough to fry a pancake properly.

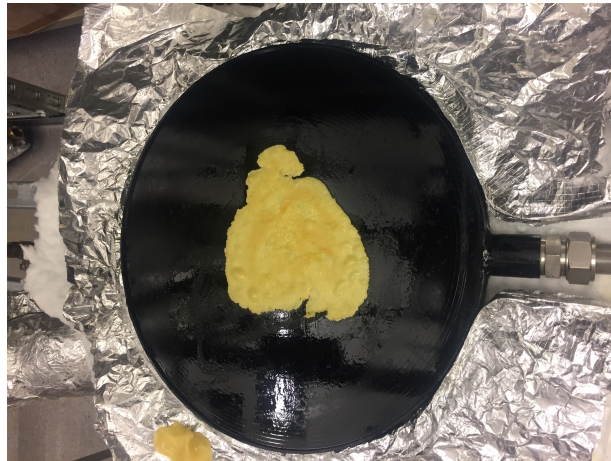
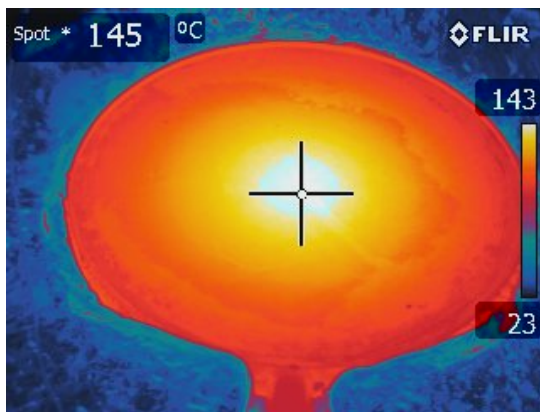
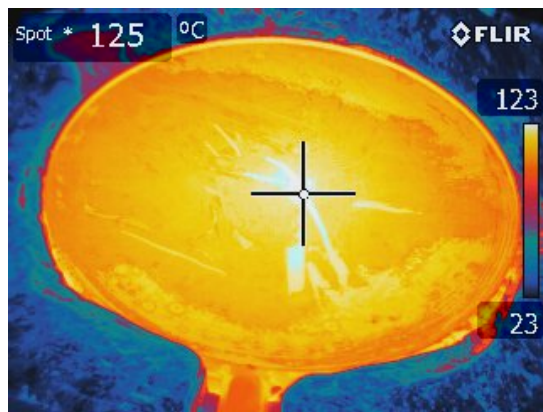


Figure 5.18: Pancake during frying

Figure 5.19: Griddle at  $t \approx 700$  sFigure 5.20: Griddle at  $t \approx 1300$  s

After the pancake was made, the temperature distribution of the griddle had evened out as shown in Figure 5.19. Estimations based on the temperatures given by the IR photo suggests a mean temperature of around  $120^{\circ}\text{C}$  and the edge temperature being slightly above  $100^{\circ}\text{C}$ . The photo in Figure 5.20 was taken before concluding the test and it shows that it is possible to obtain a temperature distribution which is very close to even. At average, the temperature is around  $120^{\circ}\text{C}$ . It should be noted that this is over 20 minutes after the first hot oil was let into the application, which is a lot longer than the simulations predicted. The temperature at the centre has also dropped during the period between the two photos, which is reasonable since the temperature in the heat storage was reduced. Besides, the temperature at the edge of the griddle will at some point have exceeded the temperature of the oil leaving since it is recorded to be  $90^{\circ}\text{C}$  at  $t \approx 1300$  s. As a result, heat will be transferred from some parts of the griddle to the oil and not the other way around. For obvious reasons, this should be avoided if possible.

## 5.7 Closed Cooking Application Test, 15.05.18

Even though the experiment in Section 5.6 was a success concerning making pancakes, it was observed that the temperature in the outer edges of the griddle was significantly lower than in the middle. The fact that the griddle was hotter in the centre was expected. Thus, it was desirable to examine how the temperature developed on the entire surface of the griddle as oil drained through the application. As this was the primary focus of the test, no cooking was performed during this experiment. Further, heating data from the system was not collected, but the rock bed was fully charged before the test began. In addition, for all temperatures stated in this section, except  $T=23^{\circ}\text{C}$ ,  $5^{\circ}\text{C}$  is added to the temperatures from the thermal camera. This is so that the calculated energy delivered from the griddle to the surroundings should be as correct as possible.

As mention in Section 5.6, a mass flow rate of 0.0038 kg per second was found reasonable considering the volume of the heat storage tank. Therefore, it was initially decided to continue with this flow for this entire test, and then follow the heat development on the pan surface. The mass flow rate was not measured to be identical, but the ball valve opening was identical.

Because of the volume of the pipes connecting the cooking application to the heat storage and the volume of the ducts inside the application, it would take approximately 7 minutes to fill the system with the given flow rate. Therefore, at  $t \approx 350$  s it was decided to increase the mass flow rate temporarily to initiate the heating process sooner. After  $t \approx 540$  s the oil started to exit the cooking application, and the ball valve controlling the mass flow rate was closed. These actions resulted in clear changes in the temperature both in the heat storage and in the cooking application. These changed can be studied in Figure 5.21 and 5.22, which shows the temperatures in the rock bed and cooking application, respectively.

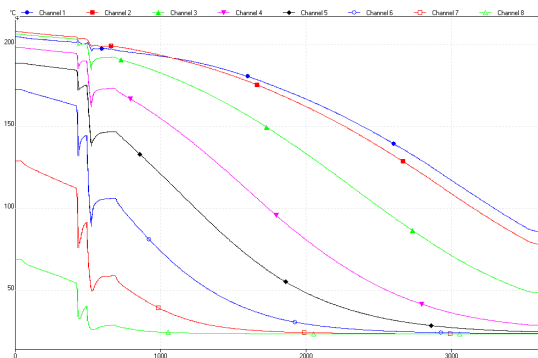


Figure 5.21: Heat storage reversal, 15.05

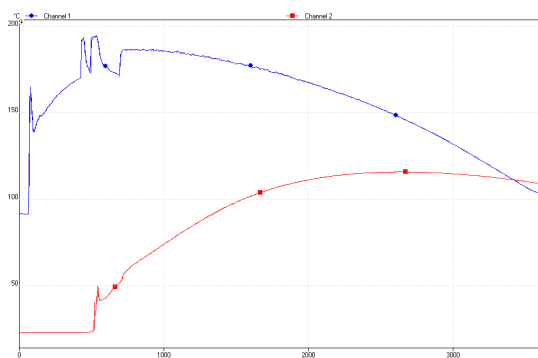


Figure 5.22: Application temperatures, 15.05

During the entire experiment, photos of the griddle were taken with a thermal camera. In Figure 5.23 the surface temperatures of the griddle are plotted for the centre and the periphery. After the increased mass flow rate was implemented, the temperature in the centre of the griddle increased rapidly. Before the ball valve was closed, the temperature reached  $155^{\circ}\text{C}$ . In the next 200 s, the temperature in the outer edges continue to rise while the temperature in the centre started to decline. After 750 s, the temperature in the centre had dropped to  $121^{\circ}\text{C}$ , and it was decided to open the ball valve again. For the rest of the experiment, the opening of the ball valve was set to the same position as initially decided. After  $t \approx 1550$  s the temperature in the centre peaked at  $152^{\circ}\text{C}$  before it slowly started to decline. As for the outer edges of the griddle, the temperature continued to rise until it peaked at  $120^{\circ}\text{C}$  after 2300 seconds. When the system

ran out of oil 3300 seconds after the experiment was initiated, the temperatures were 125 and 117°C at the centre and the outer edges, respectively. Further, the surface held a relatively high temperature for another 250 seconds before the experiment was ended.

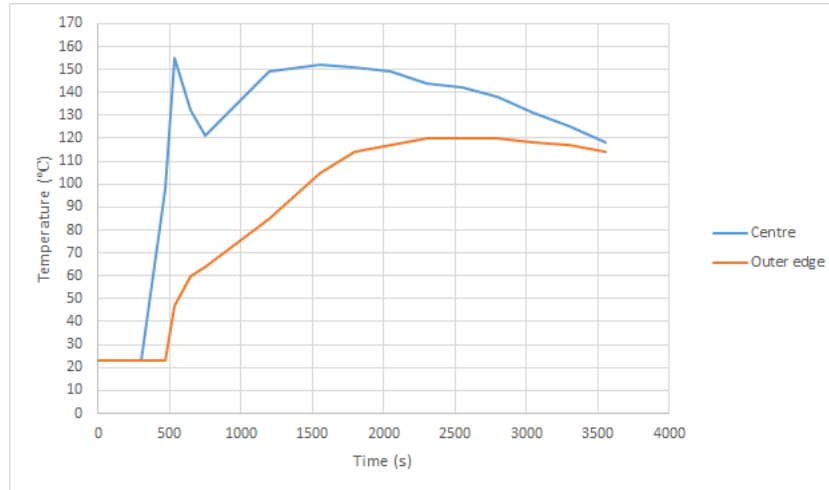


Figure 5.23: Temperature development on surface of griddle

Even though making injera would have lowered the surface temperature, it was satisfying to see that the entire griddle managed to obtain a temperature above 114 °C for nearly 30 minutes.

By obtaining the temperatures on the surface of the griddle, it is possible to calculate the heat transferred in the form of radiation and free convection from the griddle to the surroundings. For calculations, it is assumed that the surface temperature of the griddle is the mean value of the temperatures at the outer edges and the centre.

The most relevant heat transfer to calculate is when the surface temperature is hot enough to cook on. Therefore, the average mean temperature for the griddle between  $t = 1550$  s and  $t = 3300$  s is used as the surface temperature when calculating the energy released from the griddle. This time interval was chosen because this was when the mean temperature of the griddle was at least 120°C. The mean average temperature for this interval was 129°C. Further, it is assumed that the room temperature is 23°C.

Table 5.2 contains the temperatures needed to calculate the heat transfer from convection and radiation, as well as the surface area of the griddle.  $T_f$  comes from Equation 2.19.

| Property   | Value                |
|------------|----------------------|
| $T_\infty$ | 296 K                |
| $T_s$      | 402 K                |
| $T_f$      | 349 K                |
| $A_s$      | $0.1257 \text{ m}^2$ |

Table 5.2: Important temperatures and surface area of griddle

To calculate the heat transfer from radiation, Equation 2.25 is used, and the calculated value is shown in Table 5.3. The emissivity ( $\epsilon$ ) is found for anodised aluminium at 400 K[29].

| Property   | Value  |
|------------|--|
| $\sigma$   | $5.67 \cdot 10^{-8} \text{ W/m}^2 \text{ K}^4$ |
| $\epsilon$ | 0.76   |
| $q_{rad}$  | 99.9 W   |

Table 5.3: Heat transfer from radiation

In Table 5.4 the thermophysical properties for air at 349 K are presented. The values are retrieved by interpolating between 300 K and 350 K[29].

| Property | Value at 349 K                               |
|----------|--|
| $\rho$   | $0.9983 \text{ kg/m}^3$                      |
| $\mu$    | $207.7 \cdot 10^{-7} \text{ kg/m s}$         |
| $c_p$    | $1.009 \cdot 10^3 \text{ J/kg K}$            |
| $k$      | $29.9 \cdot 10^{-3} \text{ W/m}^2 \text{ K}$ |

Table 5.4: Thermophysical properties of air at 349 K

Table 5.5 display the calculated value for the heat transfer from convection, as well as other essential values. These values have been calculated using several equations in Section 2.6.1.

| Property   | Value                                |
|------------|--------------------------------------|
| $g$        | $9.81 \text{ m/s}^2$                 |
| $\beta$    | $2.865 \cdot 10^{-3} \text{ K}^{-1}$ |
| $x$        | 0.1 m                                |
| $Ra$       | $4.824 \cdot 10^6$                   |
| $C$        | 0.54                                 |
| $m$        | 0.25                                 |
| $Nu$       | 25.31                                |
| $\bar{h}$  | $7.568 \text{ W/m}^2 \text{ K}$      |
| $q_{conv}$ | 100.8 W                              |

Table 5.5: Heat transfer from convection

As seen from Table 5.3 and 5.5, the heat transfer from the plate is 99.9 W and 100.8 W from radiation and convection, respectively. This gives a total heat transfer of 200.7 W from the cooking surface of the griddle.

## 5.8 Closed Cooking Application Test, 16.05.18

Based on the results from the previous experiment griddle was finally ready for the real test; making injeras. As it is challenging to make the injera batter, as well as to fry the injera properly, external help was needed. Alem, a woman from Ethiopia, made the injera batter and contributed with her expertise during the test when baking injera flatbread.

Figure 5.24 displays the charging and discharging of the heat storage during the entire experiment. The rock bed was charged for approximately 2 hours and 15 minutes before the cooking started. Unfortunately, the heat storage was not fully charged at this time, but because of the external help, it was not possible to wait any longer. The thermocouple placed at the bottom of the rock bed, channel 8, showed that the temperature had just started to rise and only reached 27°C. For this reason, charging of the heat storage was continued parallel to the discharging to provide as much heated oil as possible.

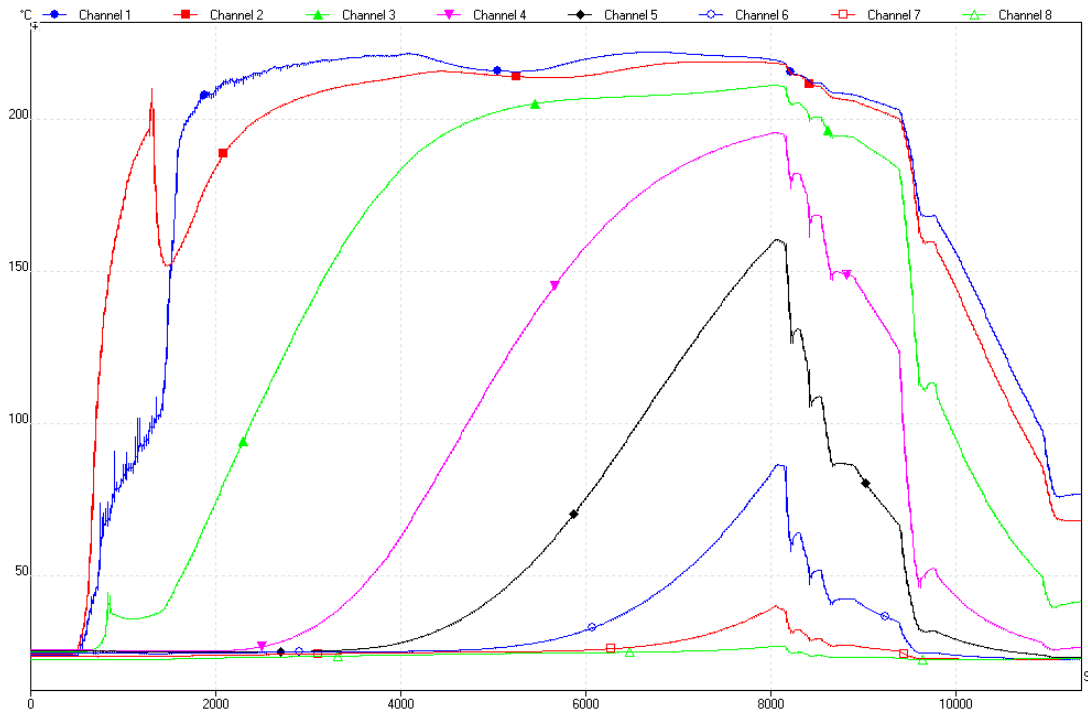


Figure 5.24: Charging and discharging of rock bed during test

From the beginning, the mass flow was set at a relatively high rate compared to the ball valve opening from the previous tests. This is evident in Figure 5.24, where the temperatures decrease quickly in the lower layers of the heat storage.

Unfortunately, no collection data was saved from the cooking application during the testing due to miss-click in the Pico program. However, the testers had an overview of the temperatures in and out of the cooking application continuously. Besides, a thermal camera was used to control the surface temperature of the griddle. When a circular area with an approximate radius of 12 cm reached a temperature of 110°C, the first round of injera batter was poured onto the griddle. The conclusion from the injera expert was that the surface was not hot enough.

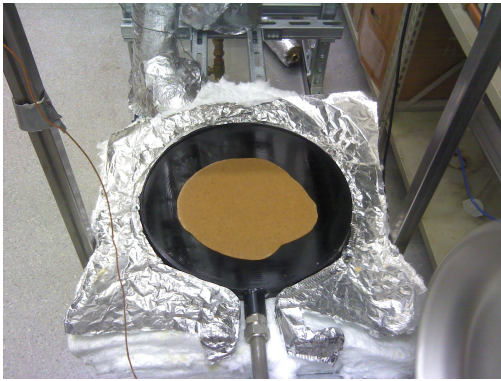


Figure 5.25: Injera during cooking

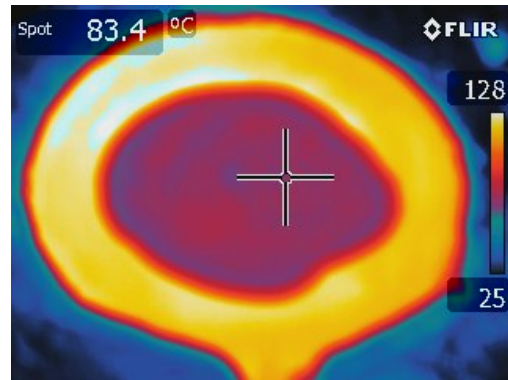


Figure 5.26: IR photo of injera

To achieve a higher surface temperature a lid, shown in Figure 5.27, was placed on top of the cooking application before and during the injeras were baked. By placing a lid on the griddle in between baking, the initial surface temperature would rise. The fact that the surface is adequately heated before the batter is poured on is a key. This is because the small craters that make the injera bread so airy are formed in the beginning. Because of the lid, it was never possible to make injera with a diameter of 40 cm because the bread had to be smaller than the lid. Figure 5.25 shows an injera bread during cooking. Figure 5.26 shows the same picture but through a thermal camera. Here, the surface temperature at the outer edges is as high as 128°C. 13°C higher than the maximum recorded temperature from the thermal camera in Section 5.7. This illustrates that the mass flow rate through the application was significantly higher.

In the end, six adequately cooked injeras were made during this experiment. Figure 5.28 shows a picture of one of the adequately baked injeras. As one can see, many small craters have been formed, which is the most important criterion for a successful injera bread.



Figure 5.27: Cooking application with lid



Figure 5.28: Picture of a successful injera bread



# Chapter 6

## Discussion

This chapter will evaluate individual components in the system and the performance of the system as one unit. It will also suggest what could have been done differently in order to achieve better results. The reliability of the fill valve is a key part which will be examined. The performance of the different cooking application designs will also be looked into, as they are essential to the final goal of cooking injera.

### 6.1 System Setup and Considerations for Upscaling

The heating system underwent considerable modifications during this thesis based on experiences from the project work. Being able to empty it more easily vastly reduced the time it took to test the fill valve. The improved insight due to the transparent pipe made it easier to calibrate the fill valve. This insight also increased the accuracy and convenience of level measurements and made it possible to reveal its correlation with the output temperature as shown in Section 5.6. Since the measurements were manual, they involve some uncertainties. A continuous and digital recording of the level would have provided better data, but the trend was clear. Ideally, the transparent pipe should have been longer so that the outlet of the "T" would be visible. However, that would require a different way of mounting it. This should be considered regardless, since removing it for the field trip showed that it was a comprehensive procedure. All of the Tec7 seals had to be broken, cleaned and then resealed when it was to be set up after the trip. It is possible that the "T" has to be removed due to damage or maintenance, and therefore, a better solution should be in place.

Even though the sunflower oil went through the system at high temperatures many times, no tests indicate that its function as a heat transfer fluid is affected. After a cycle was completed, the oil was poured into the cold storage container manually. The top of this container was more than 2 m above the floor and close to the roof. Occasionally, oil was spilt during the refilling process. A foot-operated hydraulic pump would reduce the spills and make it more convenient for the user to operate.

The heating element is placed in an insulated cylinder, which is open at the top. It was left open for two reasons; maintaining atmospheric pressure and providing insight during tests. The first reason is still essential, but the latter is no longer important since tests have shown that the concept is working.

If the fill valve malfunctions in a way that causes it to be fully open, the oil level would

increase rapidly. However, the diameter of the outlet pipe is large enough to drain more oil than the fill valve is able to supply. Therefore, the hot section cannot be flooded. The ventilation above the heating element, which is there to get rid of exhaust gases, also withdraws a significant amount of heat. For these reasons, the top should be isolated to reduce the heat loss by using a lid.

More of the energy from the heating element would then be used to heat the oil and the charging time of the storage would be reduced. The requirement of atmospheric pressure could be met by having a hole in the insulated lid. Several tests showed that there was a significant temperature difference between the oil when it was at the top of the hot section, in the supply pipe and at the top of the heat storage. A better solution should have been in place to reduce this heat loss. The lid mentioned above would have improved this issue, but the connection between the supply pipe and the heat storage should also have been better insulated. Higher temperatures in the heat storage would make it possible to obtain higher temperatures in the cooking application.

In Section 3.1 it was mentioned that the initial level in the heating system determines the outlet temperature because it decides how much the oil has to expand to reach the outlet. Using this assumption, Equation 3.1 shows that applying different effects to the heating element only affects the mass flow rate. In other words, the effect only changes the amount of oil delivered to the heat storage per unit of time. However, the tests in Section 5.1 and 5.2 showed that another factor has to be considered since the output temperature changed without the cold level changing. When changing the effect applied to the heating element, the temperature distribution in the hot section changes. At lower effects, temperatures closer to the bottom increase. This could be explained by the fact that the oil is moving slower through the system and along the heating element. Since a larger volume of oil is heated, a smaller average expansion is required to reach the outlet. As a result, the output temperature is reduced. This suspicion was discussed in the project work, and the thermocouples which were placed along the heating element made it possible to confirm.

If this heating system is connected directly to a PV system, different effects should be expected. For instance, cloudy weather would reduce the applied effect. The initial level can only be assumed to decide the output temperature if there is a uniform temperature distribution in the hot section. This would require the oil to be mixed. Since no automatic devices should be used in this system, a possible solution could be to place the inlet of the hot section at a higher position. The idea is that cold and dense oil would enter, sink towards the bottom of the hot section. As a result, a natural circulation would occur. Although it would probably not create a perfectly uniform temperature, it could reduce the change in output temperatures when the applied effect changes.

When charging the heat storage for the test in Section 5.4, the temperature in the hot section approached critically high values. This happened because the cold storage ran out of oil. Fortunately, no harm was done to people or equipment. The exact consequences of not intervening remain unknown, but this incident highlighted the need for a security measure in the heating system. The idea is that it should be a self-regulating system which only requires the user to fill it at the start of the day. Therefore, constant supervision of it should not be required. A level sensor that turns off the heating element once the cold storage was empty could be a solution. However, it would not be able to tell if the fill valve was clogged. A better solution would be to have a thermostat that turned off the heating element once a specific critical temperature is reached at the top of the hot section. A similar mechanism could also be used to turn off the heating element once the bottom temperature of the heat storage reaches its critical temperature.

The tests show that it takes nearly 3 hours to charge the heat storage fully when applying 500 W to the heating element. The test in Section 5.7 indicated that a fully charged rock bed resulted in a mean average surface temperature of 129°C for nearly 30 minutes using the closed cooking application. Also, the test in Section 5.8 showed that 5-6 injeras could be made, even though the rock bed was not fully charged. However, it should be noted that all of the cooking tests were conducted shortly after the heat storage was charged. Since one of the main purposes of this system is to enable cooking after nightfall by storing the oil for several hours, a decrease in cooking time should be expected. Reducing the heat loss throughout the system would increase the cooking time to some extent, but the energy saved would not be enough to justify adding another cooking application with the current heat storage. If this concept were to be used in a school or community house, multiple cooking applications would be needed. The current 2.5 m pipe that connects the heat storage and the cooking application causes a significant heat loss. If multiple cooking applications could be connected to a single pipe, the efficiency for each application would increase. It was discovered during tests that a higher mass flow rate resulted in a smaller temperature drop from the outlet of the rock bed to the inlet of the application. As the mass flow rate would have to be multiplied by the number of applications, the heat loss per application would decrease. By adding more cooking applications, more oil would have to be heated and stored. Depending on the power source available at the given site, the heating challenge can be solved either by applying more heating systems like the one in this report or fewer heating systems using a more powerful heating element. In the latter case, the fill valve would possibly have to be dimensioned otherwise. This is further discussed in Section 6.2. Regarding the heat storage challenge, it could be solved by simply increasing the heat storage volume. By increasing the storage tank, and obtaining a higher volume-surface-ratio, the heat losses per volume of storage would decrease. Another solution could be to connect several rock beds in series to increase the storage volume.

## 6.2 Fill Valves

In addition to resolving the three issues listed in Section 3.3, the fill valve had to be robust and easy to maintain. Although the aquarium fill valve was unlikely to resolve them, the design was worth testing. Since these types of fill valves are affordable and accessible, it would provide an easy solution to the most critical component in the heating system.

The custom-made fill valve met all of the criteria. Tests showed that it was able to keep the output temperature within a range of 15°C. This was an acceptable range in order to obtain stratification in the heat storage. However, the production process of the prototype was comprehensive. Therefore, it was dismantled instead of duplicated for the field trip. Large-scale production using the procedure described in Section 3.3.2 would not be recommended, but the concept was satisfactory for this system. More research should have been done in order to find a piston and a fitting T-shaped pipe. If this could be acquired at an affordable cost, the components which define the design would be in place. Since the sunflower oil is cold in this part of the heating system, the options for a floating device are countless.

Regarding upscaling of the system, a more powerful heating element will cause the mass flow rate to increase. From Figure 5.12, one can see that the largest level drop in the cold section was 6 mm during the heating period. Thus, the piston moves 6 mm from its closed position. As the outlet of the fill valve is 8 mm in diameter, this means that fill valve is nearly fully open when in this position. For the fill valve to be able to deliver a higher mass flow rate at the same pressure,

it would require a larger outlet hole. Although this has not been thoroughly investigated, nothing has indicated that it would not work if the fill valve were scaled up.

### 6.3 Open Cooking Application

The open cooking application was a solution consisting of parts that were easy to obtain, and that could be manufactured faster and without advanced machinery. However, it ended up being slightly more advanced than first expected, and it had to be produced by professional technicians at Trøndelag Isolasjon AS.

Unfortunately, the application did not fit perfectly with the 40 mm diameter paella pan it was originally designed for. This led to some disadvantages that most likely affected the performance of the cooking. The fact that the pan had to be cut so that it did not cover the entire opening of the cooking application led to substantial heat losses. Besides, the gap led to possibilities for contamination of the oil. If a substance like water entered, it would pose a potential danger for the user. As the pan did not rest on the edge of the application, nuts had to be used to ensure a certain distance between the two pans. These nuts were not mounted and could move freely. This led to a pan that was often out of level during tests. Further, a better solution for preventing the pan from floating on the oil should have been found. However, a more suitable solution than with a wrench and a pipe could have been implemented if the application had been constructed as planned.

The test in Section 5.5 showed that the surface of the pan reached temperatures high enough to cook the pancake in the centre, but it was not properly cooked at the edges. Therefore, the fact that the diameter of the cooking pan was only 34 cm did not have any influence. Looking back, using the thermal camera during the tests of the application should have been done to collect data on the temperature of the cooking surface.

The concept has potential and is far easier and cheaper to produce than the closed cooking application.

### 6.4 Closed Cooking Application

The closed cooking application was designed using a mass flow rate that was estimated to give a cooking time of 17 minutes given the available heat storage. The first test showed that this mass flow rate was too high, and caused the temperatures in the storage to drop too quickly. Therefore, a lower mass flow rate that was able to keep the griddle temperature above 110°C for nearly 30 minutes was found in the second test. As expected, the outlet temperature was reduced when the mass flow rate was lowered. The first couple of tests showed that during some periods, the temperature was lower at the outlet than in the griddle. To estimate the suitable cooking surface area when this occurred, the position in the channel where the oil and griddle temperatures were equal had to be determined. This was to be done by using the same procedure as in Section 3.4.2. As mentioned there, several cross sectional geometries for the channel were considered when designing the closed cooking applications for boiling and frying. Unfortunately, a wrong value of  $\bar{N}u_{duct,lam}$  was used in the final calculations. The value was for a square cross section from an earlier calculation, and it is significantly smaller than for the chosen rectangular cross section. Since  $q \propto \bar{N}u_{duct,lam}$ , changing it from 2.98 (square cross section) to 4.83 (rectangular cross section) means that  $q$  increases by 62%. A 126 W mismatch between Equation 2.14 and 3.1, the requirement for a physical solution, was accepted due to various uncertainties. However, a mismatch of 826 W could not have been accepted. This means

that the channels are longer than they should have been in order to obtain the desired 1000 W. By only changing the desired effect, it can be showed that the equations mentioned above are equal at 1972 W, thus nearly doubling the design mass flow rate. This means that the produced application was overdimensioned considering the size of the heat storage. It seems likely that this explains why it took a long time to increase the temperature towards the edge of the griddle.

Since it took a long time for the outer temperatures to increase, a pancake was cooked before a uniform temperature was obtained in the first test. The IR photo taken after cooking showed that the griddle temperature was nearly even. The first explanation that comes to mind is that the hot oil had been in the system for a longer period. On the other hand, it is possible that the pancake assisted the heat distribution by functioning as a lid. This effect was observed during all of the tests where anything was cooked.

A significant amount of heat is lost before the griddle is ready for cooking. To reduce heat loss from the griddle during the heat up period and during cooking, a lid should have been used. The only time a lid was used was when cooking during the final test. Alem pointed out that injera griddles usually have a lid which is attached by a hinge. This would make it easier to achieve the craters that characterise well-baked injeras, and should definitely be installed in future designs. Also, she suggested increasing the size of the griddle as it is smaller than a standard Ethiopian injera griddle. She believed that this would increase the chance of the product being accepted by the local communities. An additional benefit is that time can be saved since the size of the injera does not affect the cooking time.

## Chapter 7

# Conclusion

This report has shown that it is possible to create a self-regulating system that can store energy as heat, purely driven by gravity and the physical property changes of sunflower oil. The sub-systems that have been examined were intended to be produced using simple tools. However, it was found valuable to investigate concepts which required more advanced tools as well. This was because it was challenging to find components which satisfied the performance requirements that were set. Also, it was believed that it would be easier to find simpler components if a concept had been proven to work.

For the heating system, it was difficult to find a simple fill valve which resolved the issues that were discovered during the project work. By creating a fill valve that was independent of the inlet pressure, it was possible to maintain a relatively stable cold section level which only varied by 6 mm. When a constant effect of 500 W was applied to the heating element, the fill valve was able to maintain its output temperature within the range of 248-263°C for nearly three hours. That proved to be acceptable for the heat storage to obtain stratification. When the effect was changed, it had a significant impact on the output temperature. However, since the effect did not affect the cold level, the fill valve concept can be considered useful. On the other hand, it revealed a weakness of the heating system, since a constant effect cannot be expected if it is powered directly by a PV system.

The concept of the open cooking application should not be shelved based on the relatively poor test results. They were affected by the fact that the design had some flaws and that it was not produced as intended. It is possible that the concept can be used for standard frying purposes. However, if the goal is to make injera, the closed cooking application design is more promising. Since the design is based on an injera griddle, it is more likely to be accepted due to traditional reasons. Using the available heat storage, it was shown that the temperature of the griddle could be kept over the required cooking temperature, 110°C, for nearly 30 minutes. Since the heat storage had only been charged for about three hours, this was a satisfactory result.

The overall impression of the system is that it is a viable concept for utilising excess energy from solar systems. However, since it was the first prototype, there is a lot of room for improvements. A few small modifications, such as better insulation in the heating section or attaching a lid to the cooking application, would significantly improve the performance of the system. Ways to simplify some of the components and their production process should also be investigated.

## 7.1 Recommendations for Further Work

Numerous improvements for this system have been discussed in this report. However, a few of them can be considered more important than others. This section will present the improvements which are believed to make the most impact, as well as suggesting other areas that may be useful to investigate.

It has been pointed out that the closed cooking application was produced based on wrong calculations. Nevertheless, it worked to some extent. A new griddle should be produced with a shorter spiral so that the outer temperatures would increase faster. In addition, the diameter should be increased to 50 cm and a lid has to be attached. These alterations would make it more suitable for cooking injera, according to the feedback from Alem.

The temperature of the residual oil from any cooking application used in this system will be over 100°C. When a satisfying design has been found, it could be worth investigating how to utilise this energy. An idea could be to use it in a heat exchanger for heating water.

Before the heating system can transition from being a prototype to be used in a complete solar energy system, several things need to be addressed. First of all, it requires a security measurement which will turn off the heating element if the temperatures are getting critically high. Also, a way to make a PV panel direct its power to the system once its battery is fully charged needs to be in place. How much its output effect is changing during the day should be researched. If this is found to be significant, a solution for the change in output temperature must be found. It is worth looking into if the explanation of a changing temperature distribution in the hot section is the main reason for the change in output temperature.

Both the systems which were built during this project were clunky. There are a lot of open containers, and the size of the system needs to be reduced. The best option is probably to place the different subsystems closer to each other, and in a circle instead of a line. If the requirement of being purely driven by gravity is still essential, it is unlikely that the height can be significantly reduced. A more compact and enclosed system would reduce heat loss and make it safer.

# Bibliography

- [1] International Energy Agency, “Energy access outlook 2017 from poverty to prosperity,” Tech. Rep., 2017, p. 114.
- [2] Lighting Africa, “The off-grid lighting market in sub-saharan africa: Market research synthesis report,” Tech. Rep., 2011, pp. 17–26.
- [3] World Health Organization, *Household air pollution and health?* <http://www.who.int/mediacentre/factsheets/fs292/en/>, Retrieved: 11.11.17.
- [4] Norwegian Agency for Development Cooperation, *Fire lysparer gir en ny hverdag*, <http://www.norad.no/en/aktuelt/filmer/fire-lysparer-gir-ny-hverdag/>, Retrieved: 11.11.17.
- [5] A. A. Mas’ud, A. V. Wirba, F. Muhammad-Sukki, R. Albarracın, S. H. Abu-Bakar, A. B. Munir, and N. A. Bani, “A review on the recent progress made on solar photovoltaic in selected countries of sub-saharan africa,” *Renewable and sustainable energy reviews*, vol. 62, pp. 441–452, 2016.
- [6] E. A. Rehfuss, E. Puzzolo, D. Stanistreet, D. Pope, and N. G. Bruce, “Enablers and barriers to large-scale uptake of improved solid fuel stoves: A systematic review,” *Environmental health perspectives*, vol. 122, no. 2, p. 120, 2014.
- [7] O. S. Sjøgren and A. B. Steen, “Solar heat storage in oil based rock bed,” Dept. Energy and Process Engineering, Norwegian University of Science and Technology, Tech. Rep., 2017, Project work 9th semester.
- [8] R. Muthusivagami, R. Velraj, and R. Sethumadhavan, “Solar cookers with and without thermal storage—a review,” *Renewable and Sustainable Energy Reviews*, vol. 14, no. 2, pp. 691–701, 2010.
- [9] E. Cuce and P. M. Cuce, “A comprehensive review on solar cookers,” *Applied Energy*, vol. 102, pp. 1399–1421, 2013.
- [10] S. Srinivasan, Tinnokesh, and Siddharth, “Residential solar cooker with enhanced heat supply,” *International Journal of Scientific and Research Publications*, vol. 3, 10 2013.
- [11] N. Nahar, “Performance and testing of a hot box storage solar cooker,” *Energy Conversion and Management*, vol. 44, no. 8, pp. 1323–1331, 2003.
- [12] K. Schwarzer and M. E. V. Da Silva, “Solar cooking system with or without heat storage for families and institutions,” *Solar Energy*, vol. 75, no. 1, pp. 35–41, 2003.
- [13] A. Balzar, P. Stumpf, S. Eckhoff, H. Ackermann, and M. Grupp, “A solar cooker using vacuum-tube collectors with integrated heat pipes,” *Solar Energy*, vol. 58, no. 1-3, pp. 63–68, 1996.



## BIBLIOGRAPHY

---

- [14] A. Gil, M. Medrano, I. Martorell, A. Lázaro, P. Dolado, B. Zalba, and L. F. Cabeza, “State of the art on high temperature thermal energy storage for power generation. part 1—concepts, materials and modellization,” *Renewable and Sustainable Energy Reviews*, vol. 14, no. 1, pp. 31–55, 2010.
- [15] N. Nallusamy, S. Sampath, and R. Velraj, “Experimental investigation on a combined sensible and latent heat storage system integrated with constant/varying (solar) heat sources,” *Renewable Energy*, vol. 32, no. 7, pp. 1206–1227, 2007.
- [16] H. Garg, S. Mullick, and A. Bhargava, “Sensible heat storage,” in *Solar Thermal Energy Storage*, Springer, 1985, pp. 1–153.
- [17] O. E. Ataer, “Storage of thermal energy,” *Energy Storage Systems-Volume I*, pp. 97–111, 2009.
- [18] G. Faninger, “Sensible heat storage,” *Sustainable Solar Housing*, vol. 2, p. 215, 2007.
- [19] R. Skahjem and S. F. Duley, “Oil based solar concentrator with heat storage,” Master’s thesis, NTNU, 2016.
- [20] S. Sharma, D. Buddhi, R. Sawhney, and A. Sharma, “Design, development and performance evaluation of a latent heat storage unit for evening cooking in a solar cooker,” *Energy Conversion and Management*, vol. 41, no. 14, pp. 1497–1508, 2000.
- [21] D. Aydin, S. P. Casey, and S. Riffat, “The latest advancements on thermochemical heat storage systems,” *Renewable and Sustainable Energy Reviews*, vol. 41, pp. 356–367, 2015.
- [22] S. Tescari, G. Lantin, M. Lange, S. Breuer, C. Agrafiotis, M. Roeb, and C. Sattler, “Numerical model to design a thermochemical storage system for solar power plant,” *Energy Procedia*, vol. 75, pp. 2137–2143, 2015.
- [23] Store norske leksikon, 2015, *Ohms lov*, [https://snl.no/Ohms\\_lov](https://snl.no/Ohms_lov), Retrieved: 21.05.18.
- [24] Engineering ToolBox, 2003, *Electrical formulas*, [https://www.engineeringtoolbox.com/electrical-formulas-d\\_455.html](https://www.engineeringtoolbox.com/electrical-formulas-d_455.html), Retrieved: 21.05.18.
- [25] O. Fasina and Z. Colley, “Viscosity and specific heat of vegetable oils as a function of temperature: 35 c to 180 c,” *International Journal of Food Properties*, vol. 11, no. 4, pp. 738–746, 2008.
- [26] B. Esteban, J.-R. Riba, G. Baquero, A. Rius, and R. Puig, “Temperature dependence of density and viscosity of vegetable oils,” *Biomass and bioenergy*, vol. 42, pp. 164–171, 2012.
- [27] Die Deutschen Versicherer, *Container handbook*, [http://www.containerhandbuch.de/chb\\_e/scha/index.html](http://www.containerhandbuch.de/chb_e/scha/index.html), Retrieved: 21.11.17.
- [28] E. Næss, *Laminar flow in conduits, lecture notes in course tep07*, NTNU 2017.
- [29] T. L. Bergman, F. P. Incropera, D. P. DeWitt, and A. S. Lavine, *Fundamentals of heat and mass transfer*. John Wiley & Sons, 2011.
- [30] J. Holman, *Heat transfer, 10th edition*, 2010.
- [31] Autodesk, Inc., *Autodesk Inventor®*, [www.autodesk.com/products/inventor/overview](http://www.autodesk.com/products/inventor/overview), Retrieved: 23.05.18.
- [32] Relekta AS, *Tec7*, [http://www.tec7.no/Admin/Public/DWSDownload.aspx?File=Files%2fFiler%2fTekniskNovatech%2fTec7\\_info\\_N0.pdf](http://www.tec7.no/Admin/Public/DWSDownload.aspx?File=Files%2fFiler%2fTekniskNovatech%2fTec7_info_N0.pdf), Retrieved: 03.05.18.
- [33] Pico Technology, *Thermocouple Data Logger*, <https://www.picotech.com/data-logger/tc-08/thermocouple-data-logger>, Retrieved: 19.11.17.

## BIBLIOGRAPHY

---

- [34] ebalta Kunststoff GmbH, *ebazell 260*, <https://www.ebalta.de/rs/datasheet/en/502.pdf>, Retrieved: 10.05.18.
- [35] O. S. Sjøgren and A. B. Steen, “Mechanical temperature control of oil based heat storage,” Dept. Energy and Process Engineering, Norwegian University of Science and Technology, Tech. Rep., 2018, Masters Thesis.
- [36] WASS Electronics Inc., *FAQ: What temperature should I use to cook injera?* <http://www.wasselectronics.com/faqs/>, Retrieved: 17.11.17.
- [37] A. H. Tesfay, M. B. Kahsay, and O. J. Nydal, “Design and development of solar thermal injera baking: Steam based direct baking,” 2014.
- [38] GLAVA AS, *PYROGEL® XT-E*, <https://www.glava.no/teknisk-isolering/produkter/aerogel/pyrogel/pyrogel-xt-e/>, Retrieved: 30.05.18.
- [39] COMSOL AB, Stockholm, Sweden, *COMSOL Multiphysics® v. 5.3*. [www.comsol.com](http://www.comsol.com), Retrieved: 23.05.18.
- [40] E. E. G. Rojas, J. S. Coimbra, and J. Telis-Romero, “Thermophysical properties of cotton, canola, sunflower and soybean oils as a function of temperature,” *International journal of food properties*, vol. 16, no. 7, pp. 1620–1629, 2013.
- [41] Murray Bourne, *Length of an Archimedean Spiral*, <https://www.intmath.com/blog/mathematics/length-of-an-archimedean-spiral-6595>, Retrieved: 04.02.18.
- [42] Autodesk, Inc., *Autodesk Fusion 360™*, [www.autodesk.com/products/fusion-360/overview](http://www.autodesk.com/products/fusion-360/overview), Retrieved: 23.05.18.
- [43] Kalpamart, *Singh Water Heating Rod*, <https://kalpamart.com/shop/electrical-equipments/singh-water-heating-rod/>, Retrieved: 10.05.18.

# Appendices

## Appendix A

# Laminar Flow in Conduits

This appendix includes the formulas, definitions and constants used to calculate the pressure loss in the system.

# LAMINAR FLOW IN CONDUITS

## PRESSURE DROP IN THE INLET REGION

The total pressured drop in a pipe/conduit of length  $x$  can be calculated from:

$$\Delta p = (4 \cdot c_{f,app}) \cdot \frac{x}{D_h} \cdot \left( \frac{\rho \cdot V^2}{2} \right) \quad [Pa]$$

where  $c_{f,app}$  is the length-averaged apparent friction coefficient, including both viscous friction and flow acceleration.

An empirical expression for the apparent friction coefficient, which is generally within  $\pm 2\%$  of the numerical solution of the full Navier-Stokes equation for several channel geometries is:

$$(c_{f,app} \cdot Re) = \frac{3.44}{\sqrt{\zeta}} + \frac{c_{f,p} \cdot Re + \frac{K_\infty}{4 \cdot \zeta} - \frac{3.44}{\sqrt{\zeta}}}{1 + \frac{c}{\zeta^2}}$$

Here,

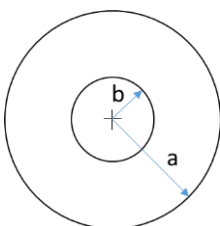
$$\zeta = \frac{x/D_h}{Re} ; Re = \frac{\rho \cdot V \cdot D_h}{\mu} ; D_h = 4 \cdot \frac{\text{Flow Area}}{\text{Wetted Perimeter}}$$

The coefficients  $K_\infty, c$  and  $(c_{f,p} \cdot Re)$  are listed for for several geometries (circular tubes and annuli, rectangular and triangular ducts) in Table 1:

**Table 1**

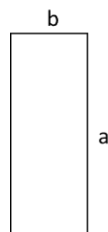
| $b/a$                             | $C_{f,p} Re$ | $K_\infty$ | $c$      |
|-----------------------------------|--------------|------------|----------|
| <b>Pipe or Concentric Annulus</b> |              |            |          |
| 0.0                               | 16.00        | 1.25       | 0.000212 |
| 0.05                              | 21.57        | 0.830      | 0.000050 |
| 0.10                              | 22.34        | 0.784      | 0.000043 |
| 0.50                              | 23.81        | 0.688      | 0.000032 |
| 0.75                              | 23.97        | 0.678      | 0.000030 |
| 1.00                              | 24.00        | 0.674      | 0.000029 |
| <b>Rectangular Duct</b>           |              |            |          |
| 1.00                              | 14.23        | 1.43       | 0.00029  |
| 0.50                              | 15.55        | 1.28       | 0.00021  |
| 0.20                              | 19.07        | 0.931      | 0.000076 |
| 0.00                              | 24.00        | 0.674      | 0.000029 |
| <b>Equilateral Triangle</b>       |              |            |          |
| —                                 | 13.33        | 1.69       | 0.00053  |

Annulus:



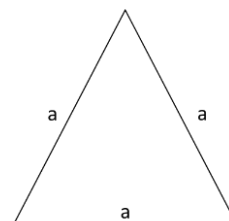
$$D_h = 2 \cdot (a - b)$$

Rectangular duct:



$$D_h = 2 \cdot \frac{a \cdot b}{a + b}$$

Triangular duct:



$$D_h = \frac{\sqrt{3}}{4} \cdot a^2$$

## Appendix B

# Risk Assessment Report

This appendix includes the most important pages of the risk assessment report.

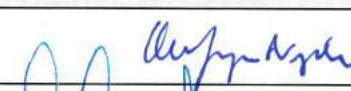

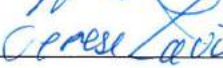
# Risk Assessment Report

## Oil based Heat Storage Rig

|                            |  |
|----------------------------|--|
| Prosjektnavn               | Solar heat storage in oil based rock bed |
| Apparatur                  | Oil based heat storage rig               |
| Enhet                      | NTNU                                     |
| Apparaturansvarlig         | Ole Jørgen Nydal                         |
| Prosjektleder              | Ole Jørgen Nydal                         |
| HMS-koordinator            | Morten Grønli                            |
| HMS-ansvarlig (linjeleder) | Therese Løvås                            |
| Plassering                 | EPT-TermiskLab                           |
| Romnummer                  | C082                                     |
| Risikovurdering utført av  | Oskar Stadaas Sjøgren                    |

### Approval:

|   |           |
|---|-----------|
| Apparatur kort (UNIT CARD) valid for:                 | 12 months |
| Forsøk pågår kort (EXPERIMENT IN PROGRESS) valid for: | 12 months |

| Rolle                      | Navn             | Dato       | Signatur  |
|----------------------------|------------------|------------|---|
| Prosjektleder              | Ole Jørgen Nydal | 5/12/2017  |  |
| HMS koordinator            | Morten Grønli    | 23/10-2017 |  |
| HMS ansvarlig (linjeleder) | Therese Løvås    | 25/10-2017 |  |

## TABLE OF CONTENTS

|     |   |   |
|-----|---|---|
| 1   | INTRODUCTION .....  | 1 |
| 2   | ORGANISATION .....  | 1 |
| 3   | RISK MANAGEMENT IN THE PROJECT .....  | 1 |
| 4   | DESCRIPTIONS OF EXPERIMENTAL SETUP .....  | 2 |
| 5   | EVACUATION FROM THE EXPERIMENTAL AREA.....  | 2 |
| 6   | WARNING.....  | 3 |
| 6.1 | Before experiments.....   | 3 |
| 6.2 | Non-conformance .....   | 3 |
| 7   | ASSESSMENT OF TECHNICAL SAFETY .....  | 4 |
| 7.1 | HAZOP.....  | 4 |
| 7.2 | Flammable, reactive and pressurized substances and gas.....                       | 4 |
| 7.3 | Pressurized equipment.....  | 4 |
| 7.4 | Effects on the environment (emissions, noise, temperature, vibration, smell)..... | 4 |
| 7.5 | Radiation.....  | 4 |
| 7.6 | Chemicals.....  | 4 |
| 7.7 | Electricity safety (deviations from the norms/standards) .....                    | 5 |
| 8   | ASSESSMENT OF OPERATIONAL SAFETY .....  | 5 |
| 8.1 | Procedure HAZOP.....  | 5 |
| 8.2 | Operation procedure and emergency shutdown procedure .....                        | 5 |
| 8.3 | Training of operators.....  | 5 |
| 8.4 | Technical modifications.....  | 6 |
| 8.5 | Personal protective equipment .....   | 6 |
| 8.6 | General Safety.....   | 6 |
| 8.7 | Safety equipment .....  | 6 |
| 8.8 | Special predations .....  | 6 |
| 9   | QUANTIFYING OF RISK - RISK MATRIX.....  | 6 |
| 10  | REGULATIONS AND GUIDELINES.....   | 8 |
| 11  | DOCUMENTATION.....  | 8 |



## 1 INTRODUCTION

The setup consists of a small pipe system, including a heating element, connected to a heat storage. The heat storage is composed of a large aluminium cylinder filled with rocks. The heating element is insulated and out inside an aluminium cylinder. There is hot oil flowing from a cold reservoir into the heating component. From there it is directed into the rock bed, which is initially filled with cold oil. The cold oil is forced out by the added hot oil and is directed into a cold reservoir. The maximum temperature for the experiment will be around 220°C. The flow in this system is driven by gravitational forces. There is a valve between the rock bed and the cold reservoir to ensure atmospheric pressure.

The purpose of the experiment is to test the stratification of hot oil and see if the gravitational forces can be used as a driving force for this system.

The experimental rig is located at the cellar floor, room C082, in Varmeteknisk Lab.

## 2 ORGANISATION

| Rolle                       |                  |
|-----------------------------|------------------|
| Prosjektleder               | Ole Jørgen Nydal |
| Apparaturansvarlig          | Ole Jørgen Nydal |
| Romansvarlig                | Paul Svendsen    |
| HMS koordinator             | Morten Grønli    |
| HMS ansvarlig (linjeleder): | Therese Løvås    |

## 3 RISK MANAGEMENT IN THE PROJECT

| Hovedaktiviteter risikostyring  | Nødvendige tiltak, dokumentasjon   | DATE       |
|---|--|------------|
| Prosjekt initiering   | Prosjekt initiering mal  | 21.08.2017 |
| Veiledningsmøte<br>Guidance Meeting                                     | Skjema for Veiledningsmøte med pre-risikovurdering                                   | 28.08.2017 |
| Innledende risikovurdering<br>Initial Assessment                        | Fareidentifikasjon – HAZID<br>Skjema grovanalyse                                     |            |
| Vurdering av teknisk sikkerhet<br>Evaluation of technical security      | Prosess-HAZOP<br>Tekniske dokumentasjoner  |            |
| Vurdering av operasjonell sikkerhet<br>Evaluation of operational safety | Prosedyre-HAZOP<br>Opplæringsplan for operatører                                     |            |
| Sluttvurdering, kvalitetssikring<br>Final assessment, quality assurance | Uavhengig kontroll<br>Utstedelse av apparaturkort<br>Utstedelse av forsøk pågår kort |            |

## 4 DESCRIPTIONS OF EXPERIMENTAL SETUP

The rig consists of the following components (see figure below):

1. Cold oil reservoirs
2. Float ball
3. Heating tube
4. Heating element
5. Output valve for hot oil when system is reversed
6. Rock bed (heat storage)
7. Draining valve
8. Pressure valve
9. Thermocouple wires connected to a Piko Logger



The shutdown of the system is simple and is done by unplugging the power supply to the heating element in the heat tube. If required, the oil can be drained from the system by using the valve below the rock bed. The hot oil shall never exceed the bottom of the rock bed.

## 5 EVACUATION FROM THE EXPERIMENTAL AREA

Evacuate at signal from the alarm system or local gas alarms with its own local alert with sound and light outside the room in question, see 6.2

Evacuation from the rigging area takes place through the marked emergency exits to the assembly point, (corner of Old Chemistry Kjelhuset or parking 1a-b.)

### **Action on rig before evacuation:**

*Turn off the power supply of the electrical heater by unplugging it.*

## 6 WARNING

### 6.1 Before experiments

Send an e-mail with information about the planned experiment to:

[iept-experiments@ivt.ntnu.no](mailto:iept-experiments@ivt.ntnu.no)

The e-mail must include the following information:

- Name of responsible person:
- Experimental setup/rig:
- Start Experiments: (date and time)
- Stop Experiments: (date and time)

You must get the approval back from the laboratory management before start up. All running experiments are notified in the activity calendar for the lab to be sure they are coordinated with other activity.

### 6.2 Non-conformance

#### FIRE

If you are NOT able to extinguish the fire, activate the nearest fire alarm and evacuate area. Be then available for fire brigade and building caretaker to detect fire place.

If possible, notify:

| NTNU                            | SINTEF                              |
|---------------------------------|-------------------------------------|
| Morten Grønli, Mob: 918 97 515  | Linda Helander, Mob: +47 406 48 621 |
| Terese Løvås: Mob: 918 97 209   | Petter Røkke, Mob: 901 20 221       |
| NTNU – SINTEF Beredskapstelefon | 800 80 388                          |

#### GAS ALARM

If a gas alarm occurs, close gas bottles immediately and ventilate the area. If the level of the gas concentration does not decrease within a reasonable time, activate the fire alarm and evacuate the lab. Designated personnel or fire department checks the leak to determine whether it is possible to seal the leak and ventilate the area in a responsible manner.

#### PERSONAL INJURY

- First aid kit in the fire / first aid stations
- Shout for help
- Start life-saving first aid
- **CALL 113** if there is any doubt whether there is a serious injury

#### OTHER NON-CONFORMANCE (AVVIK)

##### **NTNU:**

You will find the reporting form for non-conformance on:

<https://innsida.ntnu.no/wiki/-/wiki/Norsk/Melde+avvik>

##### **SINTEF:**

Synergi

## 7 ASSESSMENT OF TECHNICAL SAFETY

### 7.1 HAZOP

The experiment set up is divided into the following nodes:

|        |   |
|--------|---|
| Node 1 | Testing the oil stratification in the storage |
|--------|---|

**Attachments, Form:** Hazop\_mal

**Conclusion:** No real dangers. Avoid touching potential hot surfaces (storage, pipes, heat tube).

### 7.2 Flammable, reactive and pressurized substances and gas

Are any flammable, reactive and pressurized substances and gases in use?

|    |  |
|----|--|
| NO |  |
|----|--|

**Attachments:** EX zones?

**Conclusion:** No real dangers.

### 7.3 Pressurized equipment

Is any pressurized equipment in use?

|    |  |
|----|--|
| NO |  |
|----|--|

**Attachments:** Certificate for pressurized equipment (see Attachment to Risk Assessment)

**Conclusion:** No real dangers. No attachment necessary

### 7.4 Effects on the environment (emissions, noise, temperature, vibration, smell)

|    |  |
|----|--|
| NO |  |
|----|--|

**Attachments:** No attachment necessary.

**Conclusion:** The experiment shall not generate emission of smoke, gas, odour, etc when operated properly. Still, there should be used a ventilation channel over the rock bed "just in case". The oil should be stored safe in an own container and considered as special waste when the experiments are done.

### 7.5 Radiation

*See Chapter 13 "Guide to the report template".*

|    |  |
|----|--|
| NO |  |
|----|--|

**Attachments:** No attachment necessary

**Conclusion:** No real dangers. No attachment necessary.

### 7.6 Chemicals

|     |                        |
|-----|------------------------|
| YES | Duratherm 630 heat oil |
|-----|------------------------|

**Attachments:** MSDS

**Conclusion:** The oil used is a high heat transfer oil but it is not dangerous for health, you can smell it and touch it like the common oil we use in our houses. Of course, you must not use it like an edible product.

### 7.7 Electricity safety (deviations from the norms/standards)

|           |  |
|-----------|--|
| <b>NO</b> |  |
|-----------|--|

**Attachments:** No attachment necessary.

**Conclusion:** No real dangers.

## 8 ASSESSMENT OF OPERATIONAL SAFETY

Ensure that the procedures cover all identified risk factors that must be taken care of. Ensure that the operators and technical performance have sufficient expertise.

### 8.1 Procedure HAZOP

The method is a procedure to identify causes and sources of danger to operational problems.

Procedure:

- 1) Put a board in the bottom of the structure to avoid spills of hot oil.
- 2) Tested all the system connections using water to check for leaks.
- 3) Ensure the heater is working and we can control it using the thermostat.
- 4) Insulated some of the pipes where necessary.
- 5) Use thermal camera in addition to thermocouples to see if we get a thermal front in the rock bed.

**Attachments:** HAZOP\_MAL\_Proseedyre

**Conclusion:** The procedure is safe, only needs avoid the contact with the hot elements during the heating of the oil.

### 8.2 Operation procedure and emergency shutdown procedure

The operating procedure is a checklist that must be filled out for each experiment.

Emergency procedure should attempt to set the experiment set up in a harmless state by unforeseen events.

**Attachments:** Procedure for running experiments

**Emergency shutdown procedure:** Pull out the plug connected to the heat element box (no power means no heat)

### 8.3 Training of operators

A Document showing training plan for operators

- *What are the requirements for the training of operators?*
- *What it takes to be an independent operator*
- *Job Description for operators*

**Attachments:** Training program for operators

#### 8.4 Technical modifications

No technical modifications needed during the experiment that produce risk. Only possible addition of rock-bed to the main storage, that means full the storage with little rocks, this does not become in a dangerous situation.

**Conclusion:** No dangerous/important modifications during the experiment.

#### 8.5 Personal protective equipment

Eye protection should be used in the rig zone. Gloves should be used when handling the tubes as some of them can be hot.

**Conclusion:** Plastic glasses and gloves is the only special equipment needed to protect.

#### 8.6 General Safety

Warning signs must be close the hot elements.  
An operator must be controlling the rig.

**Conclusion:** Signs and monitoring by operator.

#### 8.7 Safety equipment

No need for any special safety equipment except warning signs, gloves and plastic glasses.

#### 8.8 Special predations

One operator must be in the rig zone during tests to make sure the temperature is within safe range and there is no major leaks.

### 9 QUANTIFYING OF RISK - RISK MATRIX

See Chapter 13 "Guide to the report template".

The risk matrix will provide visualization and an overview of activity risks so that management and users get the most complete picture of risk factors.

| IDnr | Aktivitet-hendelse                    | Frekv-Sans | Kons | RV |
|------|---------------------------------------|------------|------|----|
| 1    | People getting burned on heat element | 2          | C    | C2 |
| 3    | Oil leakage                           | 1          | B    | B1 |
|      |                                       |            |      |    |

**Conclusion:** We consider the risk to people, environment and economic very small. The aim of the risk assessment is to achieve avoid all the risk related with the possible burns.

|                     |               |                    |           |           |           |           |
|---------------------|---------------|--------------------|-----------|-----------|-----------|-----------|
| <b>CONSEQUENCES</b> | Catastrophic  | <b>E1</b>          | <b>E2</b> | <b>E3</b> | <b>E4</b> | <b>E5</b> |
|                     | Major         | <b>D1</b>          | <b>D2</b> | <b>D3</b> | <b>D4</b> | <b>D5</b> |
|                     | Moderate      | <b>C1</b>          | <b>C2</b> | <b>C3</b> | <b>C4</b> | <b>C5</b> |
|                     | Minor         | <b>B1</b>          | <b>B2</b> | <b>B3</b> | <b>B4</b> | <b>B5</b> |
|                     | Insignificant | <b>A1</b>          | <b>A2</b> | <b>A3</b> | <b>A4</b> | <b>A5</b> |
|                     |               | Rare               | Unlikely  | Possible  | Likely    | Almost    |
|                     |               | <b>PROBABILITY</b> |           |           |           |           |

Table 8. Risk's Matrix

Table 9. The principle of the acceptance criterion. Explanation of the colors used in the matrix

| COLOUR | DESCRIPTION  |
|--------|--|
| Red    | Unacceptable risk Action has to be taken to reduce risk      |
| Yellow | Assessment area. Actions has to be considered                |
| Green  | Acceptable risk. Action can be taken based on other criteria |

## ATTACHMENT E: PROCEDURE FOR RUNNING EXPERIMENTS

|   |             |                         |
|---|-------------|-------------------------|
| <b>Prosjekt</b><br>Solar heat storage in oil based rock bed | <b>Dato</b> | <b>Signatur</b>         |
| <b>Apparatur</b><br>Oil based heat storage rig              |             |                         |
| <b>Prosjektleder</b><br>Ole Jørgen Nydal                    | 23/10/17    | <i>Ole Jørgen Nydal</i> |

|  | <b>Conditions for the experiment:</b>  | <b>Completed</b>   |
|--|--|--------------------|
|  | Experiments should be run in normal working hours, 08:00-16:00 during winter time and 08.00-15.00 during summer time.  |                    |
|  | One person must always be present while running experiments, and should be approved as an experimental leader.   |                    |
|  | Be sure that everyone taking part of the experiment is wearing the necessary protecting equipment and is aware of the shut down procedure and escape routes. |                    |
|  | <b>Preparations</b>  | <b>Carried out</b> |
|  | Post the "Experiment in progress" sign.  |                    |
|  | Be sure that the ventilation in the room is working  |                    |
|  | <b>Start of Experiment</b>   | <b>Carried out</b> |
|  | Plug wire from heating element into electrical output  |                    |
|  |  |                    |
|  | <b>During the experiment</b>   |                    |
|  | Control of temperature   |                    |
|  |  |                    |
|  | <b>End of experiment</b>   |                    |
|  | Unplug wire from heating element   |                    |
|  |  |                    |
|  | Remove all obstructions/barriers/signs around the experiment.  |                    |
|  | Tidy up and return all tools and equipment.  |                    |
|  | Tidy and cleanup work areas.   |                    |
|  | Return equipment and systems back to their normal operation settings (fire alarm)  |                    |
|  | <b>To reflect on before the next experiment and experience useful for others</b>   |                    |
|  | Was the experiment completed as planned and on scheduled in professional terms?  |                    |
|  | Was the competence which was needed for security and completion of the experiment available to you?  |                    |
|  | Do you have any information/ knowledge from the experiment that you should document and share with fellow colleagues?  |                    |



**Operator(s):**

| Navn                  | Dato      | Signatur                     |
|-----------------------|-----------|------------------------------|
| Christian Bogsnes     | 23/10 -17 | <i>Christian Bogsnes</i>     |
| Even Ersdal Hansen    | 23/10 -17 | <i>Even E. Hansen</i>        |
| Alexander Bjåen Steen | 23/10 -17 | <i>Alexander B. Steen</i>    |
| Oskar Stadaas Sjøgren | 23/10 -17 | <i>Oskar Stadaas Sjøgren</i> |

**ATTACHMENT F: TRAINING OF OPERATORS**

|   |             |                         |
|---|-------------|-------------------------|
| <b>Prosjekt</b><br>Solar heat storage in oil based rock bed | <b>Dato</b> | <b>Signatur</b>         |
| <b>Apparatur</b><br>Oil based heat storage rig              |             |                         |
| <b>Prosjektleder</b><br>Ole Jørgen Nydal                    | 23/10/17    | <i>Ole Jørgen Nydal</i> |

|  |  |
|--|--|
| <b>Knowledge about EPT LAB in general</b>  |  |
| Lab  |  |
| <ul style="list-style-type: none"> <li>• Access</li> <li>• routines and rules</li> <li>• working hour</li> </ul> |  |
| Knowledge about the evacuation procedures.   |  |
| Activity calendar for the Lab  |  |
| Early warning, <a href="mailto:iept-experiments@ivt.ntnu.no">iept-experiments@ivt.ntnu.no</a>                    |  |
| <b>Knowledge about the experiments</b>   |  |
| Procedures for the experiments   |  |
| Emergency shutdown.  |  |
| Nearest fire and first aid station.  |  |
|  |  |

I hereby declare that I have read and understood the regulatory requirements has received appropriate training to run this experiment and are aware of my personal responsibility by working in EPT laboratories.

**Operator(s):**

| Navn                  | Dato     | Signatur                     |
|-----------------------|----------|------------------------------|
| Christian Bogsnes     | 23/10-17 | <i>Christian Bogsnes</i>     |
| Even Ersdal Hansen    | 23/10-17 | <i>Even E. Hansen</i>        |
| Alexander Bjåen Steen | 23/10-17 | <i>Alexander B. Steen</i>    |
| Oskar Stadaas Sjøgren | 23/10-17 | <i>Oskar Stadaas Sjøgren</i> |

## APPARATURKORT / UNITCARD

**Dette kortet SKAL henges godt synlig på apparaturen!**  
***This card MUST be posted on a visible place on the unit!***

|  |  |
|--|--|
| <b>Apparatur (Unit)</b><br>Oil based heat storage rig  |  |
| <b>Prosjektleder (Project Leader)</b><br>Ole Jørgen Nydal  | <b>Telefon mobil/privat (Phone no. mobile/private)</b><br>+47 97715994 |
| <b>Apparaturansvarlig (Unit Responsible)</b><br>Ole Jørgen Nydal   | <b>Telefon mobil/privat (Phone no. mobile/private)</b><br>+47 97715994 |
| <b>Sikkerhetsrisikoer (Safety hazards)</b><br>Hot surfaces<br>Heated oil   |  |
| <b>Sikkerhetsregler (Safety rules)</b><br>Use safety gloves and goggles<br>Do not touch the rig without approval of the operator |  |
| <b>Nødstop prosedyre (Emergency shutdown)</b><br>Unplug the heating element.   |  |

**Her finner du (Here you will find):**

|                                      |              |
|--------------------------------------|--------------|
| <b>Prosedyrer (Procedures)</b>       | HSE handbook |
| <b>Bruksanvisning (Users manual)</b> | HSE handbook |

**Nærmeste (Nearest)**

|  |  |
|--|--|
| <b>Brannslukningsapparat (fire extinguisher)</b> |  |
| <b>Førstehjelpsskap (first aid cabinet)</b>      |  |

NTNU  
 Institutt for energi og prosessteknikk

SINTEF Energi  
 Avdeling energiprosesser

Dato

Dato

Signert

Signert

## FORSØK PÅGÅR / EXPERIMENT IN PROGRESS

**Dette kortet SKAL henges opp før forsøk kan starte!**  
***This card MUST be posted on the unit before the experiment startup!***

|  |  |
|--|--|
| <b>Apparatur (Unit)</b><br>Oil based heat storage rig  |  |
| <b>Prosjektleder (Project Leader)</b><br>Ole Jørgen Nydal  | <b>Telefon mobil/privat (Phone no. mobile/private)</b><br>+47 97715994   |
| <b>Apparaturansvarlig (Unit Responsible)</b><br>Ole Jørgen Nydal   | <b>Telefon mobil/privat (Phone no. mobile/private)</b><br>+47 97715994   |
| <b>Godkjente operatører (Approved Operators)</b><br>Paul Svendsen<br>Even Ersdal Hansen<br>Christian Bogsnes<br>Alexander Bjåen Steen<br>Oskar Stadaas Sjøgren   | <b>Telefon mobil/privat (Phone no. mobile/private)</b><br>+47 91897987<br>+47 91574645<br>+47 91790717<br>+47 99301245<br>+47 92653327 |
| <b>Prosjekt (Project)</b><br>Solar heat storage in oil based rock bed  |  |
| <b>Forsøkestid / Experimental time (start - stop)</b>  |  |
| <b>Kort beskrivelse av forsøket og relaterte farer (Short description of the experiment and related hazards)</b> <ul style="list-style-type: none"> <li>• Hot circulating oil (through insulated pipes and heat storage).</li> <li>• Do not touch the surfaces to avoid scald risk.</li> <li>• Be careful with the electric cable from the heating element and thermocouples.</li> </ul> |  |

**NTNU**  
**Institutt for energi og prosessteknikk**

**SINTEF Energi**  
**Avdeling energiprosesser**

**Dato**

---

**Dato**

---

**Signert**

---

**Signert**

---